2012

Promoting Mitochondrial Biogenesis with the SIRTI Activator SRT1720 to Improve Mitochondrial and Renal Function after Acute Kidney Injury

Jason Allen Funk
Medical University of South Carolina

Promoting Mitochondrial Biogenesis with the SIRT1 Activator SRT1720 to Improve Mitochondrial and Renal Function after Acute Kidney Injury

By

Jason Allen Funk

A dissertation submitted to the faculty of the Medical University of South Carolina
in partial fulfillment of the requirements for the degree of
Doctor of Philosophy in the College of Graduate Studies.

Program in Pharmaceutical and Biomedical Sciences

2012

Approved by:

Chairman, Advisory Committee

ACKNOWLEDGEMENTS

TABLE OF CONTENTS

Chapter 2: SRT1720 INDUCES MITOCHONDRIAL BIOGENESIS AND RESCUES MITOCHONDRIAL FUNCTION AFTER OXIDANT INJURY IN RENAL PROXIMAL TUBULE CELLS

Chapter 3: PERSISTENT DISRUPTION OF MITOCHONDRIAL HOMEOSTASIS AFTER ACUTE KIDNEY INJURY

ABSTRACT

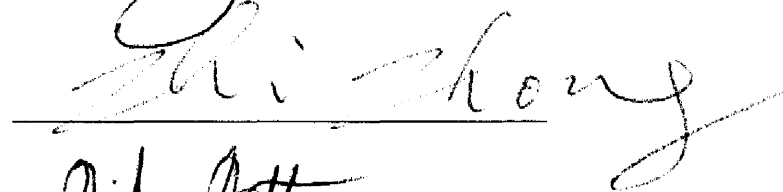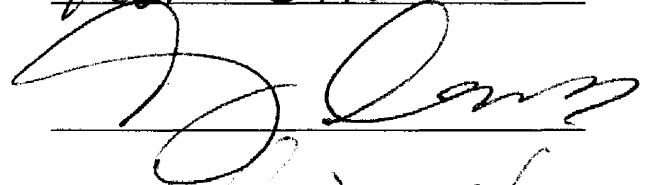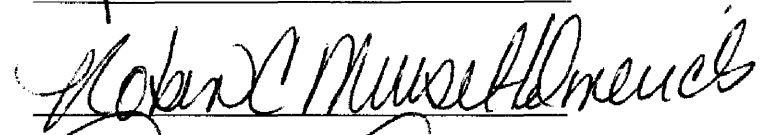JASON ALLEN FUNK. Promoting Mitochondrial Biogenesis with the SIRT1 Activator SRT1720 to Improve Mitochondrial and Renal Function after Acute Kidney Injury (Under the direction of Dr. Rick G. Schnellmann)
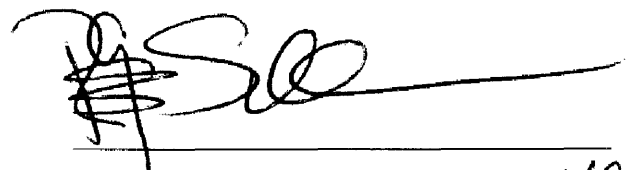
Mitochondrial dysfunction is a primary pathological consequence of acute kidney injury (AKI). Induction of mitochondrial biogenesis via the nuclear coactivator of transcription PPARγ-coactivator-1α (PGC-1α), the master regulator of mitochondrial biogenesis, rescues mitochondrial function in renal cells after oxidant injury. The primary goal of this project was to evaluate the recovery of mitochondrial function after *in vivo* AKI, and to determine the influence of mitochondrial biogenesis during the repair process.

Deacetylation of PGC-1α by the class III HDAC SIRT1 produces a more active form of the protein and stimulates mitochondrial biogenesis. The potent SIRT1 activator SRT1720 induced deacetylation of PGC-1α, increased mitochondrial proteins, and elevated mitochondrial respiration and total cellular ATP levels in primary renal proximal tubule cell (RPTC) cultures. The effects of SRT1720 occurred in a SIRT1-dependent manner and exposure of SRT1720 following oxidant injury to RPTC expedited recovery of mitochondrial and cellular functions.

Acute kidney injury (AKI), either by ischemia-reperfusion (I/R) or glycerol-induced myoglobinuric injury, produced persistent proximal tubule damage even in the face of recovered glomerular filtration. Tubule pathology was determined histologically, by the continued presence of dilated, flattened tubules, and the loss of Na^+,K^+-ATPase

expression. The persistent tubule injury was associated with sustained loss of mitochondrial protein expression, alterations in fusion/fission proteins, and elevated mitochondrial biogenesis proteins.

Treating with SRT1720 after I/R injury in rats induced PGC-1α deacetylation and restored mitochondrial protein expression and function by 144h after reperfusion, but not at 72h. Restoration of mitochondrial function was associated with attenuated kidney injury molecule-1 (Kim-1), recovery of Na^+,K^+-ATPase expression and localization, and normalized vimentin expression. The results suggested that recovery of mitochondrial function correlates with faster recovery of a normal, differentiated, polarized proximal tubule epithelium.

Taken together, we have demonstrated that mitochondrial biogenesis is an essential component of renal cell repair following AKI, and by promoting faster recovery of mitochondrial function, we can expedite recovery of the differentiated tubule epithelium with basolateral-apical polarity. These discoveries may ultimately point towards new therapeutic techniques that can be further examined as potential interventions to treat AKI and other disorders associated with sustained mitochondrial dysfunction.

Chapter 1:

Acute kidney injury and mitochondrial biogenesis

RENAL ANATOMY

Overview

The primary functions of the kidney are to regulate body fluid volume, electrolyte balance, and excretion of waste products such as urea, ammonia, and xenobiotics in the bloodstream. The kidney also secretes hormones (e.g. renin) which, along with maintaining fluid volume, help regulate blood pressure. The kidney is comprised of three distinct zones, from the outer most region designated the renal cortex, to the renal medulla (divided into the outer medulla, further segmented into the outer stripe and inner stripe, and the inner medulla), to the inner most region designated as the renal papilla.

The nephron

The nephron is the functional unit of the kidney and is responsible for urine formation by maintaining fluid and solute balance through a series of filtration, secretion, and reabsorption mechanisms. The nephron consists of a vascular element, the glomerulus, and a tubular component (further segmented into the proximal tubule, the loop of Henle, and the distal tubule and collecting duct). Each of these components is discussed in further detail below.

Renal vasculature. The glomerulus is supplied with blood via the afferent arterioles, and it exits through the efferent arterioles. The afferent and efferent arterioles are able to regulate blood flow and capillary pressure within the glomerulus, which respond to nervous system innervation, angiotensin II, vasopressin, endothelin, adenosine, and norepinephrine. After exiting the glomeruli via the efferent arterioles, blood is then routed to either the peritubular network, supplying the cortical tubules, or to the vasa recta, a capillary loop supplying the medullary regions. The cortical region receives the highest proportion of blood flow entering the kidney at approximately 90%. In comparison, the renal medulla receives only 6-10% of renal blood flow, and the papilla approximately 1-2%.

Glomerulus. Plasma components must first pass through the glomerular filtration barrier, which entails passing through the capillary endothelium, the basement membrane, and the epithelial cells of Bowman's capsule. The glomerulus allows a large fraction of fluid to be filtered, but acts as a size- and charge-specific barrier to particles in the blood (37). In general small molecules (<60kD) are freely filtered, whereas larger molecules are restricted due to the size of pores created by podocytes, the epithelium of the glomerulus. Polyanionic molecules are generally restricted from passing through with the glomerular filtrate, due to an electrostatic repulsion generated by the anionic nature of the glomerular basement membrane. Therefore, size and charge, as well as shape of a molecule determine whether it will pass through with the glomerular filtrate. Glomerular filtration rate (GFR), which is dependent on differences in capillary pressures as described in the vasculature section above, is a measure of the functional capacity of

the kidney. Normal GFR in humans is approximately 180 ml/min; however as discussed in more detail below, almost all of this fluid is reabsorbed in the tubules.

Proximal Tubule. The proximal tubule is segmented into the S1, S2, and S3 regions of the tubule. The three segments have distinct characteristics, such as distinguishable differences in brush border morphology, as well as mitochondrial and lysosomal numbers. The majority of renal reabsorption occurs within the proximal tubule, where approximately 75-90% of H_2O, and 65% Na^+, as well as Cl^-, Ca^{2+}, PO_4, and HCO_3^- filtered by the glomerulus are reabsorbed in this tubular section. Additionally, the proximal tubule is the primary site for reabsorption of glucose, carbohydrates, amino acids, and small peptides. Aside from morphological differences, segments of the proximal tubule can also be distinguished by distinct physiological properties characterized by differences in reabsorption capacity of specific solutes at each segment. The S1 segment is the primary site of HCO_3^-, low molecular weight proteins, amino acids, and glucose. Organic anion secretion occurs primarily at the S2 segment, and cation secretion at the S1/S2 segments. Glutathione (GSH) transport primarily occurs at the S3 segment. Metabolic differences and enzyme localization are distinguishing characteristics which influence the physiological distinctions among the S1, S2, and S3 segments.

Loop of Henle, distal tubule, and collecting duct. The loop of Henle consists of the thin descending and ascending limbs and the thick ascending limb. The majority of the Na^+, K^+, and water that is not reabsorbed at the proximal tubule are reabsorbed at this site of

the tubular network. Approximately 25% of Na$^+$ is reabsorbed at the loop of Henle. The thick ascending limb requires a lot of energy provided by the Na$^+$, K$^+$-ATPase to actively transport ions across the membrane. This dependence on metabolic activity for the Na$^+$, K$^+$-ATPase in the absence of adequate blood supply makes this segment particularly susceptible to ischemic injury. The distal tubule and collecting duct is where the final solute reabsorption and fluid balancing takes place in urine production.

ACUTE KIDNEY INJURY

Acute kidney injury definition

Acute kidney injury (AKI) is defined as an abrupt reduction in renal function associated with decreased urine output and an accumulation of serum waste products, namely urea and creatinine (243). Classically, the term acute renal failure (ARF) was used to describe a sudden decline in glomerular filtration rate (GFR). More recently, however, AKI has replaced ARF to encompass the entire spectrum of renal injury that occurs, including a decline in glomerular filtration as well as the less severe challenges to the kidney which lead to clinically relevant changes in renal function. By current standards, this would be reflected by an increase in serum creatinine of 0.3 mg/dL. The term kidney failure has since been reserved for a situation in which functional decline has persisted, and renal replacement therapy is considered a last alternative. More specifically, classification systems have been introduced to better stratify the injury, based upon changes in serum creatinine or GFR, and changes in urine output. The Acute Dialysis Quality Initiative (ADQI) and the Acute Kidney Injury Network (AKIN) introduced the stratification systems defined as Risk, Injury, Failure, Loss, and End-stage kidney disease (RIFLE

criteria) and the AKIN classification system illustrated in Fig 1 below. Briefly, the RIFLE criteria define Risk as a 1.5-fold increase in SCr or 25% decrease in GFR, Injury as a 2-fold increase in SCr or 50% reduction in GFR, Failure as a 3-fold increase in SCr or a 75% reduction in GFR. Additionally, loss of urine output over progressively longer periods of time can be used to stratify the injury as well, as detailed in Fig 1-1. Loss of kidney function is determined when there is persistent renal failure for greater than four weeks, and end-stage renal disease is the final step before renal replacement therapy is initiated. The AKIN classification system stratifies AKI in three distinct stages with similar criteria outlined above in the RIFLE description. Classification of the injury has allowed for better comparison across clinical studies covering diverse populations and severities, as well as better prognostic measures to be taken as outcome severity correlates with stage of AKI (159).
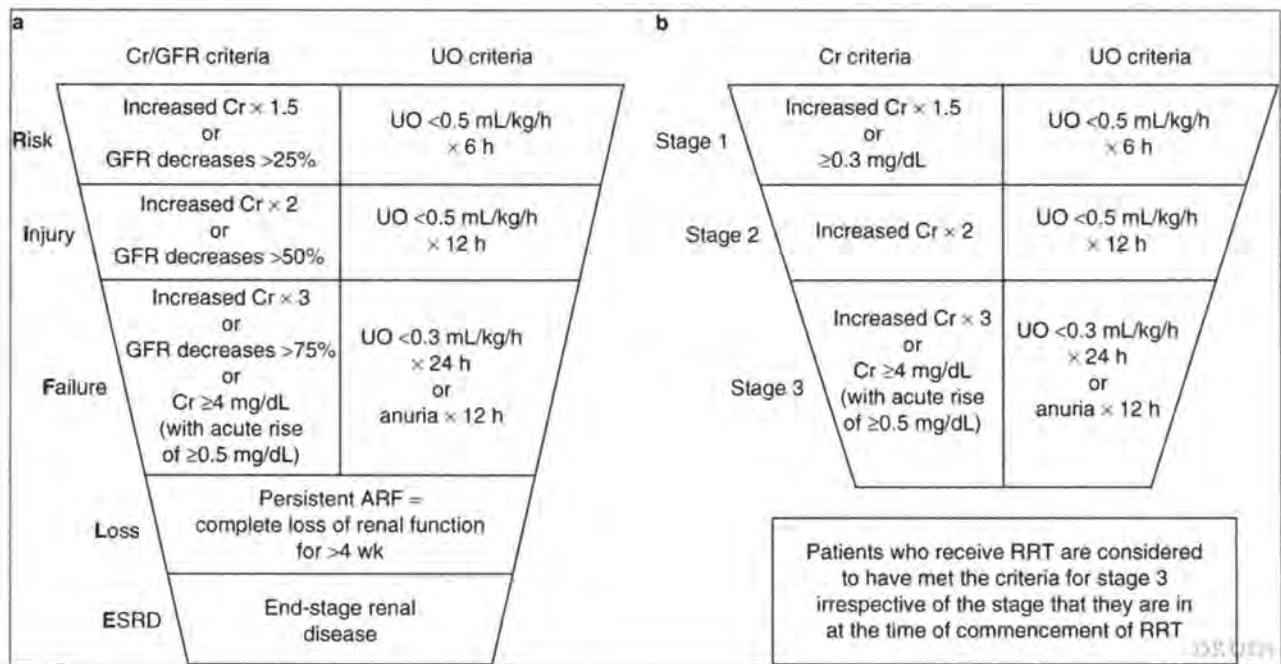
Fig. 1-1 (a) Risk, Injury, Failure, Loss of renal function and End-stage kidney disease (RIFLE) and (b) Acute Kidney Injury Network (AKIN) classifications for acute kidney injury (adapted from Bellomo et al. and Mehta et al., with permission from BioMed Central). ARF = acute renal failure; Cr = creatinine; GFR = glomerular filtration rate; RRT = renal replacement therapy; UO = urine output (159).

AKI incidence, mortality, and cost

In hospitalized patient populations, incidence of AKI has been estimated at 5-7% (194), and this number can be as high as 25% in critically ill patients (74, 165). Mortality rates vary depending on severity of injury and populations studied; however in ICU patients it is estimated at 50-80% (165, 212, 243, 273). Additionally, in the U.S. medical expenses associated with treatment of AKI have been estimated to exceed $8 billion per year (87, 116). Reliable statistics are difficult to find on the demographics of AKI populations, due in part to the varying degrees of injury that are seen clinically, as well as the influence that certain populations studied skew the numbers, and the inherent nature of the injury associated with underlying and/or secondary complications. Stratifying the injury and evaluating the additional consequences attributed to a specific degree of injury may help clarify the overall impact on healthcare of AKI. In such a study, it was determined that even a moderate, although clinically-relevant, increase in serum creatinine of 0.3 – 0.4 mg/dl resulted in a 70% increase in risk of death, an increased length of hospital stay of 3.5 days, and an added $9000 in total costs (54). When more robust changes in SCr were examined, these numbers were greatly inflated. Figure 1-2 depicts two of the graphs from this study which demonstrate the exponential increase in mortality risk and added cost associated with progressively elevated SCr levels. Apparent in these graphs is that even moderate changes (which constituted the majority of cases observed) resulted in elevated risk of death and cost and more robust elevations resulted in marked increases in these adverse outcomes (Fig 1-2). The results of this study again highlight the important contribution that classification systems such as the RIFLE criteria and the AKIN system have had in order to correlate varying degrees of injury with adverse outcomes, the

significant impact on patient recovery and cost from even minor renal dysfunction, and a

platform to better compare data across clinical studies with diverse populations and

injuries.
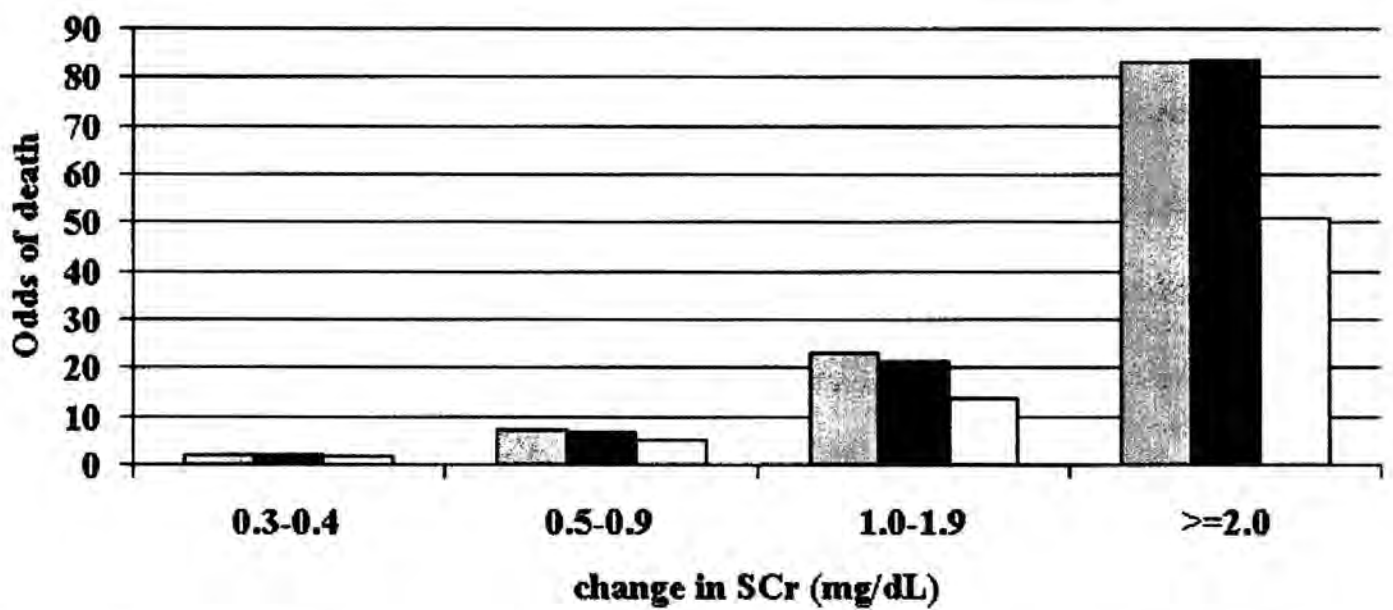
Fig 1-2a. Mortality associated with change in serum creatinine. Green bars are unadjusted, blue bars are age and gender adjusted, and gray bars are multivariable adjusted. Multivariable analyses adjusted for age, gender, diagnosis-related group (DRG) weight, chronic kidney disease (CKD) status, and ICD-9-CM codes for respiratory, gastrointestinal, malignant, and infectious diseases; $n = 1564, 885, 246$, and 105 for change in SCr 0.3 to 0.4, 0.5 to 0.9, 1.0 to 1.9, and ≥ 2.0 mg/dl.
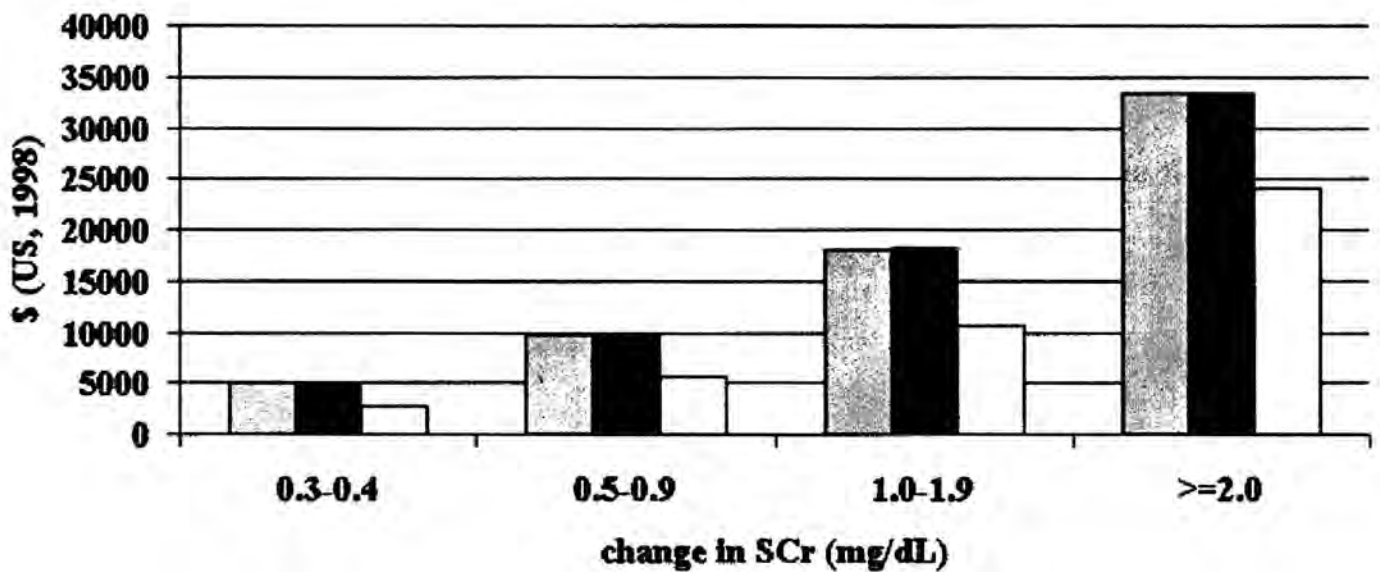
Fig 1-2b. Mean hospital costs associated with changes in SCr. Green bars are unadjusted, blue bars are age and gender adjusted, and gray bars are multivariable adjusted. Multivariable analyses adjusted for age, gender, DRG weight, and ICD-9-CM codes for cardiovascular, respiratory, malignant, and infectious diseases; $n = 1564, 885, 246$, and 105 for change in SCr 0.3 to 0.4, 0.5 to 0.9, 1.0 to 1.9, and ≥ 2.0 mg/dl (54).

Pre-renal, intrinsic, and post-renal AKI

AKI can be further classified into subcategories describing initiation of injury: prerenal, renal (or intrinsic), and postrenal AKI. Prerenal azotemia, which account for 55-60% of AKI cases, describes conditions in which there is precipitous loss of blood flow to the kidney (e.g. hypoperfusion), commonly observed in cases of septic shock or vascular disease/injury. The loss of renal blood flow often leads to direct renal cell injury (primarily within the proximal tubule), which overlaps intrinsic injury and often leads to confusion when attempting to differentially diagnose these two classifications of renal injury. Intrinsic AKI develops when there is direct damage to components of the nephron (e.g. the glomerulus, tubules, vasculature, etc). Most commonly, intrinsic AKI is observed with acute tubular necrosis from nephrotoxic or ischemic injury. Intrinsic AKI accounts for 35-40% of cases observed, and when examined together, pre-renal causes with ischemic ATN account for approximately 75% of AKI cases (194). Post-renal injury may be observed when there is obstruction of urine outflow within the urinary tract can lead to increased pressure within the kidney and reduced GFR.

Causes of AKI

The majority of AKI cases can be attributed to septic shock, major surgery, cardiogenic shock, hypovolemia, and drug/toxicant exposure. A recent study identified septic shock associated with 47.5% of AKI cases examined in an ICU patient cohort. A number of drugs have been linked to AKI, including aminoglycoside antibiotics, anticancer agents, radio contrast media, and NSAIDs. Gentamicin, which is used for the treatment of gram negative bacteria, has a high rate of nephrotoxicity associated with its use. As high as

30% of patients treated for more than 7 days with gentamicin develop symptoms of AKI (174). Cisplatin is used in the treatment of a number of cancers, but it has a high rate of nephrotoxicity associated with its use, and thus cisplatin therapies must be monitored closely. Cisplatin-induced AKI results from direct tubule toxicity due to mitochondrial dysfunction, ROS production, inflammation, and ATP depletion (5, 45, 148). Radiocontrast media are commonly used clinically, such as in cardiac catheterization, but is a frequent cause of AKI in the hospital (41). In patients with certain cardiovascular or pre-existing kidney disorders, incidence of AKI from radiocontrast media can be as high as 50% (6). Nephrotoxicity is associated with direct tubule toxicity, as well as reduced blood flow to the kidney and GFR (82). Acetaminophen is a widely used analgesic, but in high doses is known to cause liver and kidney injury. Acetaminophen toxicity is associated with acute tubular necrosis due to increased oxidative stress and lipid peroxidation, as well as GSH depletion (1, 21).

Pathophysiology of ischemia/reperfusion (I/R) AKI

Renal ischemia/reperfusion (I/R) is a common cause of AKI. An ischemic insult occurs when there is reduced blood flow to the kidney and may occur after drug or toxicant exposure, vascular diseases, sepsis, or blood volume depletion and hypotension (29, 273). The pathophysiology of ischemic AKI is comprised of both microvascular and tubular components. The microvascular injury is characterized by increased vasoconstriction and decreased vasodilation, endothelial and smooth muscle cell damage, and leukocyte infiltration (29, 59, 252). The tubular component consists of cytoskeletal breakdown, loss of cell polarity, cell death, desquamation of viable and nonviable cells, and tubular

11

obstruction (28-29). These components are discussed in further detail in the following sections.

Spatial/temporal pattern of I/R injury. During initiation of injury, the effects of disrupted perfusion and ATP depletion are most widely felt, primarily in the PT. After post-ischemic reperfusion, the extension phase is characterized by both recovery and further injury, as ATP is restored but injury to the vascular endothelium results in persistent localized ischemia which further progresses the injury. The injury during this phase occurs mostly commonly in the S3 segment of PT and medullary thick ascending limb (MTAL) at the cortico-medullary border (187). This is primarily due to the network of microvessels in the region and the oxygen demands of the tubules located in the outer stripe of the outer medulla (101, 286). Finally, during the maintenance phase, there is again a combination of both recovery and injury mechanisms. Local ischemia may have subsided, however the effects of inflammation and cellular responses to apoptotic stimuli leads to continued cell injury/death.

Vascular injury in I/R. The microvascular injury that occurs primarily in the glomerulus and medulla consists of structural damage to the endothelial cells and the vascular smooth muscle cells. The vessels experience persistent constriction due to the combined effects of increased reactivity to vasoconstrictors (endothelin, adenosine, angiotensin II, thromboxane A2, and sympathetic nerve activity) as well as a decreased reactivity to vasodilators (nitric oxide, PGE2, acetylcholine, bradykinin) (59). The microvascular architecture within the kidney leads to differential reperfusion in the post-ischemic

12

kidney, which may help explain why certain zones are more affected during the extension phase of the injury. In the post-ischemic kidney, there is a reduction in blood flow to the outer medulla compared to the cortical capillaries (286).

Lethal tubular injury in I/R. Both necrosis and apoptosis appear to have a role in the pathology of ischemic AKI. The extent of each may depend on the severity of the injury and the region of the nephron affected. Severe ATP depletion during ischemic phase can lead to necrotic cell death, most commonly seen in the proximal tubule, and may occur via opening of a plasma membrane "death channel" early in the injury process (78). ATP depletion may also lead to disrupted ion balance (28), and generalized protein dephosphorylation, disruption, and aggregation (28, 153, 262). Persistent localized ischemia, primarily within the outer medullary region, leads to a more extensive necrotic response in the affected areas.

Apoptosis undoubtedly occurs during ischemic injury, as demonstrated in both animal models (147, 235) as well as human AKI (44, 206, 244). However, the influence on observed organ dysfunction is still controversial as it has been estimated that only 3-5% of tubule cells undergo apoptosis, which questions the contribution of this form of cell death. Additionally, the majority of apoptosis occurs in the more susceptible distal tubule, whereas the bulk of viable and non-viable cell loss occurs in the proximal tubule segments. Finally ATP, which is required for the apoptotic program, is severely depleted early during the ischemic episode. The influence of apoptosis in ischemic AKI appears to increase over time after injury as expression of pro-apoptotic proteins, such as bax,

bad, bak, and caspases, increase in response to a number of pathological mechanisms, including DNA damage, ROS production, ceramide production, and inflammation (98, 146, 260).

Sub-lethal tubular injury in I/R. There is substantial loss of cytoskeletal integrity and cell polarity during ischemic injury, which results in mislocalization of membrane proteins and adhesion molecules. The actin network is disrupted early after onset of ischemia due to several cell processes altered during ischemic injury which can affect cytoskeletal components and cytoskeleton-membrane interactions. One, ATP is dramatically reduced during ischemia, and ATP is required for polymerization/depolymerization of actin and tubulin, and for actin-myosin interactions (19-20). Two, Ca^{2+} is elevated after ischemia. Ca^{2+} modulates actin-myosin interactions, microtubule formation, as well as actin-binding proteins (3, 298). Additionally, Ca^{2+} activation of calpains may affect degradation of actin and actin-binding proteins, as well as integral membrane proteins (e.g. laminin, fibronectin), membrane associated proteins (e.g. ankyrin, α-actinin), and cross linking proteins (e.g. villin, fimbrin) (63, 108, 197). Third, degradation of phospholipids which interact with cytoskeletal proteins, such as diacylglycerol and palmitic acid to α-actinin, may also be altered during ischemic injury (197). Finally, abnormal production of ROS, which have been shown to cross link actin and actin-binding proteins, may disrupt cytoskeleton in response to ischemia (181, 274).

Cytoskeletal disruption and loss of polarity leads to significant functional consequences, including the loss of the apical brush border and redistribution of membrane proteins,

including the Na^+, K^+-ATPase and cell adhesion molecules. Apical microvilli are lost

during ischemia, and are either shed into the tubular lumen and excreted or internalized

into the cell (95-96, 285). This results in a substantial reduction in membrane surface

area, a functional necessity of the apical membrane for efficient reabsorption.

Redistribution of membrane proteins, which are localized to specific sides of the

polarized proximal tubule epithelial cell, occurs early during ischemia and happens

concurrently with disruption of the actin cytoskeleton. This phenomenon is best

exemplified by the delocalization of the Na^+, K^+-ATPase from the basolateral membrane.

Under normal physiologic conditions, Na^+ enters the cell actively and passively through

transport proteins on the apical membrane. Na^+ is then shuttled out of the cell against its

electrochemical gradient via the Na^+, K^+-ATPase on the basolateral membrane and is

coupled to ATP utilization, providing the gradient needed for uptake of a variety of

solutes and water reabsorption through apical membrane proteins. Redistribution of the

Na^+, K^+-ATPase from the basolateral membrane to the apical disrupts proximal tubule

Na^+ reabsorption, as apical transport of Na^+ establishes a futile cycle where Na^+ is both

absorbed and subsequently transported back out of the cell at the apical membrane (184,

186, 256). Tubule epithelial cells are attached to the extra cellular matrix (ECM) by

integrin adhesion molecules and to each other by junctional complexes and adherens

complexes. Cells become detached from the basement membrane and from adjacent cells

during ischemic injury due, in part, to the delocalization and disruption of adhesion

complexes (100). This process leads to sloughing of both viable and non-viable cells in

to the tubular lumen, along with detached microvilli and glycoproteins, such as

fibronectin (324). The clinical manifestation is observed by the presence of tubular casts, which further obstruct luminal flow, and also appear in the urine of AKI patients (100).

Tubule epithelial repair: de-differentiation/proliferation/re-differentiation. The renal tubule epithelium has a unique capacity to fully recover after acute ischemic or toxic injury. Normal recovery after AKI is essential due to the increased risk of progression to CKD and ESRD (136). Following AKI, there is a robust elevation in renal cell turnover, which is in contrast to the normally slow turnover rate under normal circumstances (193). The increase in cell turnover is a consequence of significant cell death after injury as well as elevated proliferation to replace these cells, most prominently seen in the S3 segment of the proximal tubule in the necrotic outer stripe of the outer medulla. The source of progenitor cells after injury has been an intense area of study in which there is still not a definitive answer. It has been proposed that the new cells may originate from either bone marrow stromal cells, a resident renal progenitor population, or from surviving attached epithelial cells. Several studies have demonstrated that bone marrow derived cells, such as hematopoietic stem cells (HSCs) and mesenchymal stem cells (MSCs), directly replace epithelial cells after injury (143, 167). Administration of exogenous MSCs following injury promotes restoration of normal epithelium and accelerates the recovery of renal function, suggesting that MSCs may indeed play an important role in renal regeneration (69, 126-127, 245, 257); however, subsequent studies contradicted this assessment and instead suggested that the bone marrow derived cells have a more supportive role in the repair process (79, 127-128). More recent studies examining whether an intrarenal stem cell population or resident epithelial cells were the source of proliferating cells in the

16

tubular epithelium suggest that the surviving tubular cells proliferate after injury (128).

After injury with epithelial cell loss, surviving cells de-differentiate, migrate, proliferate,

and re-differentiate to repopulate the denuded tubular epithelium (273). The process is

illustrated in Fig 1-3, and discussed in more detail below.

The signaling network activated after injury is a complex cascade which stimulates the

normally quiescent tubules to initiate a vigorous mitogenic response. Initially, surviving

tubular cells transition from mature, polarized cells to a less differentiated phenotype

(115). Undifferentiated, proliferating cells express developmental markers such as the

proliferation marker PCNA and the intermediate filament vimentin, indicating a switch

from epithelial to mesenchymal phenotype (302). Epithelial to mesenchymal transition

(EMT) is dependent on activation of the EGF receptor (322). At this time, de-

differentiated cells do not retain apical-basal polarity. This is highlighted by the

mislocalization of specific proteins, namely the Na^+,K^+-ATPase, from the basolateral

membrane (201-202, 204). Following migration and proliferation, the surviving cells re-

differentiate to restore the normal polarized tubular epithelium. When the EGF receptor

is turned off following dedifferentiation, mesenchymal RPTC redifferentiate and

repolarize as evidenced by reductions in vimentin expression, return of cortical actin

structure and the basolateral localization of the Na^+,K^+-ATPase (115).
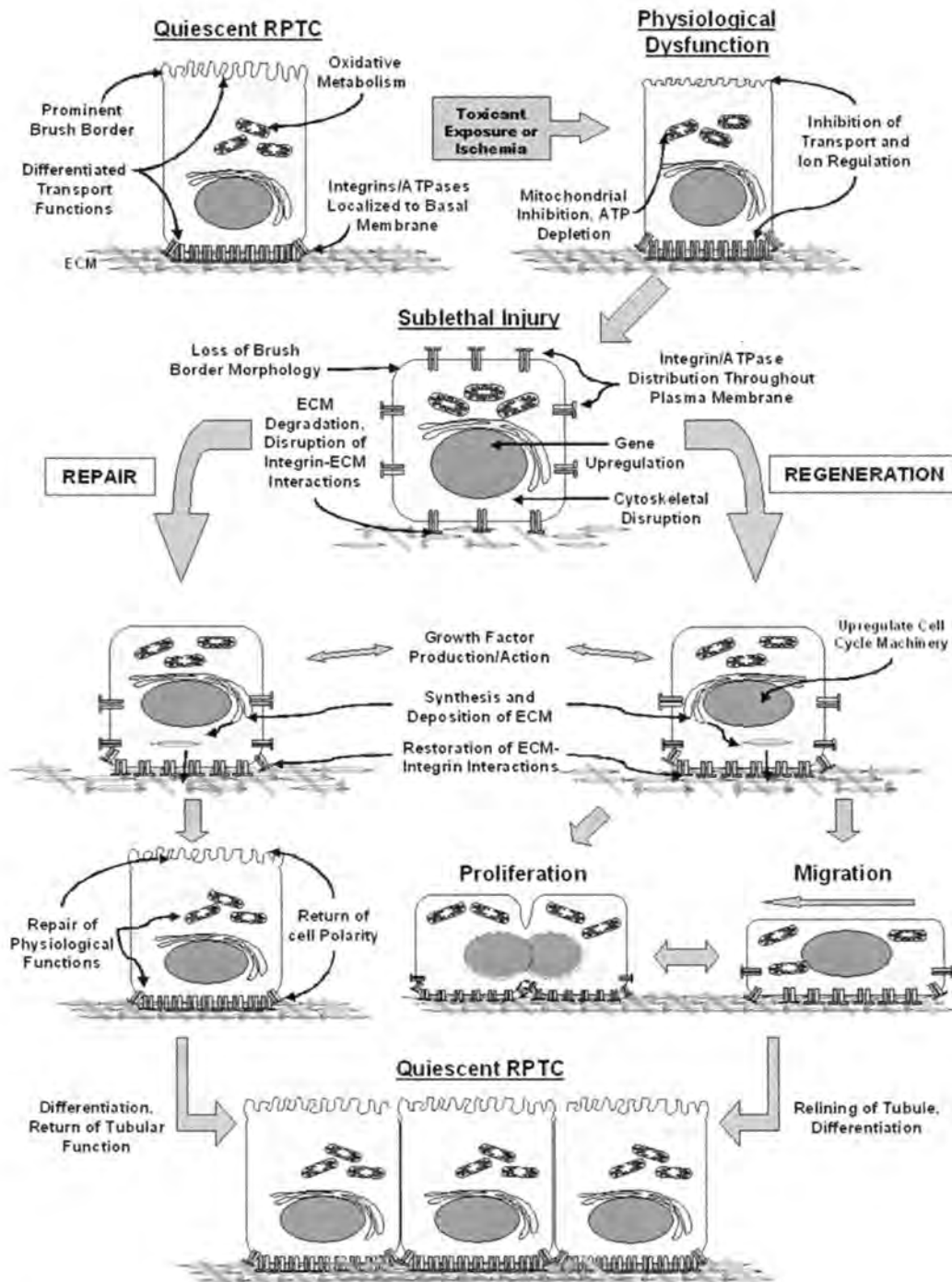
Fig 1-3. Repair and regeneration of RPTC following acute sublethal toxicant injury. Sublethally injured RPTC either repair physiological functions and restore normal tubular function or dedifferentiate, migrate, and/or proliferate to replace lost cells, then differentiate and resume normal function. The processes of repair and regeneration work in concert to ensure relining of the damaged nephron and restoration of renal function. (203)

18

Abnormal repair and progression to ESRD. Ideal recovery after AKI would result in complete repair of the tubular epithelium as described in the previous section. Frequently, however, due to a number of factors, there is abnormal recovery which results in incomplete repair of the kidney. Factors such as microvascular damage and persistent hypoxia, chronic tubulointerestitial inflammation, as well as fibroblast proliferation and excess extracellular matrix deposition can lead to postischemic fibrosis and incomplete tubular repair. A fundamental difference exists which may ultimately determine whether injured tubules undergo repair versus fibrotic responses during recovery; however, the mechanisms governing this molecular switch are still unclear. There is some debate on the source of myofibroblasts present in injured tubules. Evidence suggests that epithelial cells undergo transition to a mesenchymal phenotype (EMT), and may be a primary mechanism of fibrosis; however, contrasting data has pointed to perivascular fibroblasts in the generation of myofibroblasts (128-129, 137, 157, 320-321).

Myoglobinuric AKI

Rhabdomyolysis is a condition in which heme proteins, released in the form of myoglobin from muscle cells or hemoglobin from erythrocytes, produce secondary organ toxicity, predominantly AKI (36, 195). Although the mechanism of myoglobinuric-induced AKI is not entirely known, a number of factors including ischemic injury resulting from vasoconstriction and blood volume depletion as blood pools at the site of muscle injury, direct tubule toxicity from iron influx and hydroxyl radical formation, and tubular obstruction contribute to the disease process (36, 215-216).

Mechanisms of myoglobinuric kidney injury. Renal vasoconstriction is an essential component to the progression of myoglobinuric AKI. The importance of this factor is underscored by the fact that volume expansion or early renal vasodilator therapy can significantly attenuate injury to the kidney (Dubrow, et al., Acute Renal Failure, 1988, p279). There are several mechanisms which lead to renal vasoconstriction in rhabdomyolysis, including fluid third spacing and intravascular volume depletion, endotoxin cytokine release after muscle injury, and inhibition of endogenous vasodilators. Muscle necrosis leads to significant third spacing, where as much as 18 liters of fluid may extravascate into injured limbs, leading to dramatic intravascular volume depletion (22). Volume repletion early in the injury process can ameliorate clinical symptoms of kidney injury validates the influence of fluid loss on the injury (22, 225, 231). Endotoxin release following severe muscle injury can also lead to renal vasoconstriction (11, 200, 250, 311-312), and the pathological role of endotoxin release has been supported by studies demonstrating that endotoxin tolerance prevents heme-protein induced renal damage (200, 250).

Heme protein cytotoxicity. Besides the effects on renal vasoconstriction, there is also evidence that the heme-protein myoglobin is directly toxic to the proximal tubule epithelial cells. There is evidence that an adverse heme protein-ischemic interaction occurs within the proximal tubule, without hemodynamic effects. It is suspected that porphyrin iron ring present in hemoglobin and myoglobin mediates its toxic effects (61).

Oxidant stress. Using ^{59}Fe labeled hemoglobin, Bunn, et al., showed that the proximal

tubules epithelium reabsorbs the Fe after it is readily filtered (42-43). When the amount

of hemoglobin is tolerable for the proximal tubule to handle, the porphyrin ring is

catabolized and the released iron is transferred to ferritin (42-43). However, when excess

hemoglobin is present, and reabsorption capacity is surpassed, significant intraluminal

free iron release is observed (42-43, 315).

As a transition metal, iron readily accepts and donates electrons, facilitating the

production of free radicals (8, 66, 113-114, 183). The influence of free radicals on cell

and tissue damage is well characterized in both renal and extrarenal injuries (88, 142,

210, 248, 292, 296). Iron-mediated oxidant stress has been described in many systems as

a pathological mechanism leading to tissue damage (88, 142, 296), and iron chelators

have been shown to be protective in these models. A role for free iron in the nephrotoxic

response to hemoglobin and myoglobin was conclusively demonstrated when it was

shown that the iron chelator DFO and hydroxyl radical scavengers attenuated kidney

injury in an i.v. hemoglobin-induced nephrotoxicity model, a glycerol-mediated AKI

model, and a combined ischemic/hemoglobinuric AKI model (107, 211, 249). Protection

of organ function was associated with a reduction in lipid peroxidation. Subsequently, it

was demonstrated that there is a dramatic increase in H_2O_2 production in rat kidneys in a

myohemoglobinuric injury model (107). This observation, in addition to the protection

with iron chelators and hydroxyl radical scavengers, confirms the role that free iron and

radical production contribute to the injury process.

Preventing and treating myohemoglobinuric AKI. Intravascular volume depletion is a primary factor in the development of renal failure following myohemoglobinuria. There is evidence that immediate and vigorous volume replacement therapy early after onset of clinical rhabdomyolysis offers significant protection from AKI. Retrospective analyses on crush syndrome patients indicated that those patients who were given i.v. saline immediately after injury did not develop AKI, whereas patients who did not receive fluid replacement for up to six hours after injury developed AKI (22, 225, 231). A second benefit of volume replacement therapy is that glomerular filtration rate (GFR) is increased and flushes out intraluminal heme proteins, thus preventing heme protein cast formation and proximal tubule heme uptake. Mannitol infusion has also proven effective at mitigating injury in experimental myohemoglobinuric AKI (313-314). Mannitol is a proximal tubule acting diuretic, and thus induces excretion of heme proteins and reduces proximal tubule reabsorption. It is also a potent renal vasodilator, which increases renal perfusion and lessening effects of ischemic injury and heme protein injury. Finally, neutralizing the toxicity of heme protein may be an effective measure to limit renal injury under myohemoglobinuric conditions. The most promising candidates in this strategy is the use of iron chelators, such as DFO, or antioxidants, such as glutathione, to limit cytotoxicity (2, 211, 249, 314, 316).

Animal models of AKI

The use of animal models to study AKI is an essential practice that has led to our understanding of many of the pathological processes involved in development of kidney injury and/or failure described in the previous sections. There are obvious limitations

inherent with any model employed with the purpose to simulate a type of disease or injury observed clinically in humans; however, there are several acute renal failure models which have proven reliable systems to study mechanisms of kidney injury and recovery which sufficiently mimic human disorders.

I/R model of AKI. I/R injury can be simulated in a number of animals, but is most commonly performed in mice and rats. Experimentally, this can be accomplished by clamping and obstructing blood flow to either one or both kidneys (clamping of the renal artery or the renal pedicle) for a specified amount of time followed by reperfusion for typically 24h. In rats, it has been reported that a 60m clamping of both kidneys followed by 24h reperfusion resulted in development of acute renal failure (23). Unilateral clamping for 45-60m followed by 24h reperfusion has also been reported to sufficiently induce kidney injury (71, 166). These procedures have also been used in mouse models, although the ischemia time in mice in generally less than used in rat models (261). Experimental I/R results in acute tubular necrosis of renal epithelial cells primarily located within the region bordering the cortex and outer medulla (122). Apoptotic cell death may also be present after the initial insult, and pathologically I/R injury is characterized by dilated tubules with flattened epithelial cells and cast formations obstructing the tubular lumen (122).

Glycerol-induced myoglobinuric AKI model. Myoglobinuric AKI was discussed in section 2.6, and as mentioned, it is generally the result of a muscle injury due to trauma, exertion, drugs/toxins, disease and/or virus (283). Experimentally, myoglobinuric AKI is

most often simulated by administering an intramuscular (i.m.) injection of 50% glycerol (v/v in water) at a dose of 8-10 ml/kg body weight equally distributed between the two hind limbs of a rat (238). Because of the influence of intravascular volume depletion on manifestation of the AKI in this type of injury, rats are generally dehydrated for 12-24h prior to glycerol injection (237). Similar to what is observed in cases of rhabdomyolysis in humans, glycerol-induced AKI results in myoglobinuria, acute tubular necrosis, and alterations in renal hemodynamics (145, 303).

AKI Biomarkers

Several new biomarkers have emerged in the last 10 years as a result of more emphasis placed on the need to identify new markers that are able to detect earlier or milder kidney injury, as well as markers that differentially diagnose the site of injury, and provide better diagnostic information. Fig 1-4 highlights some of the more promising biomarkers to emerge, and the advantage they represent when compared to more traditional markers, such as serum creatinine. Some of these are discussed in the following sections.

Creatinine. Serum creatinine is a standard measurement that has been used extensively to diagnose AKI. Creatinine can be measured in the urine, and by using mathematical approaches, creatinine clearance can be estimated. However, there are several limitations to the use of creatinine as a marker of kidney function. Serum creatinine concentrations can vary greatly within age groups, muscle mass, and hydration status. Therefore, baseline creatinine measurements for individuals are important to establish changes due to reduced kidney function. Changes in creatinine may not be detectable until significant

kidney function is already lost, which makes it a poor biomarker for detection of early renal injury.

Blood urea nitrogen. BUN is another marker which has been used extensively as a diagnostic tool for AKI. However, like creatinine measurements, BUN levels can be affected by factors outside of strictly renal influence.

KIM-1. Kidney injury molecule-1 (KIM-1 in humans, Kim-1 in rodents) is a cell membrane glycoprotein which has a short intracellular domain, a transmembrane domain, and a large extracellular domain. It was identified using a PCR-based technique to identify genes up-regulated after ischemia/reperfusion in the rat (131). KIM-1 has many properties which make it an ideal biomarker, such as the absence of its expression in the normal kidney; its robust elevation after injury and its presence in the apical membrane of proximal tubules; its expression is maintained until complete cell recovery; rapid cleavage of its ectodomain and excretion into the urine; and the relative stability of the cleaved domain in urine samples at room temperature. In pre-clinical studies, Kim-1 has proven to be a specific and early predictor of tubule damage scored by histopathology when compared to other AKI biomarkers (including BUN and SCr) after exposure to a panel of toxicants (281). KIM-1 has also shown to be an effective clinical predictor of AKI in post-operative populations which have undergone cardiac surgery (117), in renal transplant patients (263), in patients with congestive heart failure (72), and in patients with nondiabetic chronic kidney disease with proteinuria (291).

NGAL. NGAL is a 25 kDa protein originally discovered in neutrophils, which forms a barrel-shaped structure with a hydrophobic region that binds small, lipophilic molecules, such as the iron-binding siderophores. NGAL is expressed at very low levels in human tissue, but is dramatically up-regulated in injured kidney epithelial cells – NGAL is also elevated in colon, liver, and lung after injury. NGAL has proven to be an effective early indicator of AKI, as it is among the fastest up-regulated genes in the post-ischemic kidney, and is detectable in urine within 2 hours of reperfusion (260). It has also proven an effective prognostic indicator for clinical outcomes, including dialysis and mortality (110).

Biomarkers

Normal epithelium → (Ischemia/reperfusion, Toxicity) → Damage → Cell death (Necrosis, Apoptosis) → ↓GFR

Potential urinary biomarkers for early diagnosis of AKI

NAG · NGAL
β_2M · CYR-61
α_1M · IL-18
RBP · OPN
Cystatin C · FABP
KIM-1 · NHE3
Clusterin · Fetuin A
Microalbumin

Delayed biomarkers for kidney injury

↑ Serum creatinine
↑ Blood urea nitrogen
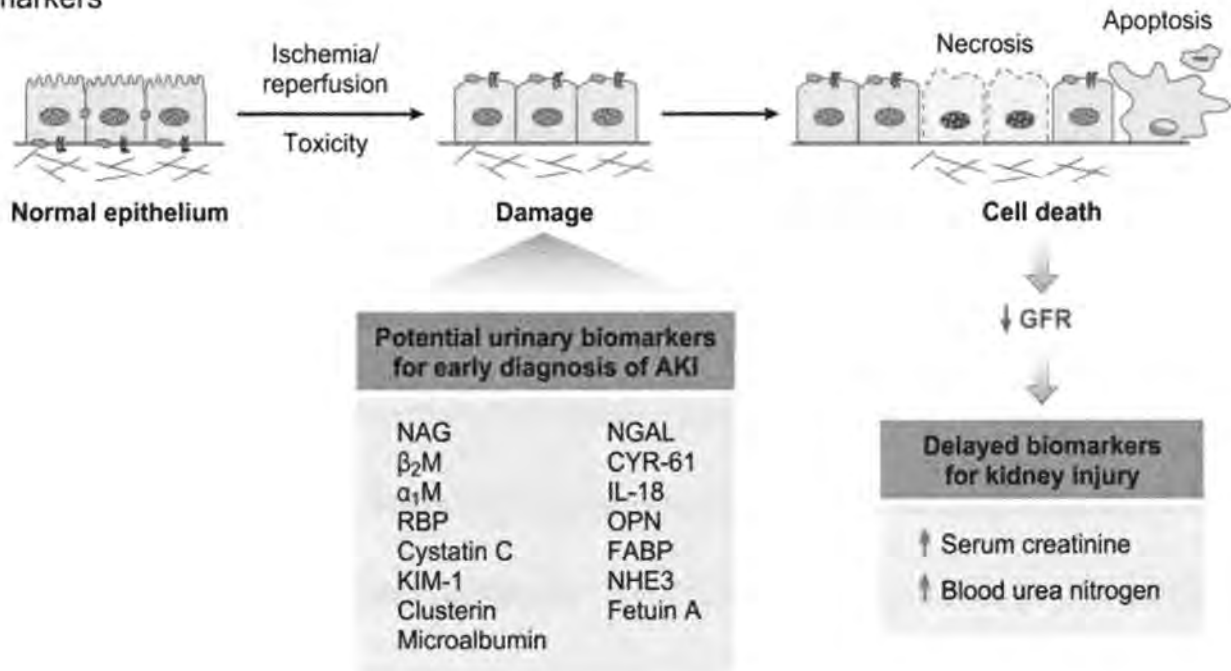
Fig 1-4. Biomarkers of AKI: Traditionally used markers, such as blood urea nitrogen (BUN) and creatinine (CR), are insensitive, nonspecific, and do not adequately differentiate between the different stages of AKI. A delay in diagnosis prevents timely patient management decisions, including administration of putative therapeutic agents. Urinary biomarkers of AKI will facilitate earlier diagnosis and specific preventative and therapeutic strategies, ultimately resulting in fewer complications and improved outcomes (280).

Pharmacological treatment of AKI

Pharmacological approaches. As a preventative measure, numerous pharmacological agents have been tested in patients at risk for AKI. Targets which have been investigated include agents which promote natriuresis, increase renal blood flow, or inhibit inflammation and oxidative stress. Therapies which have been attempted but have been proven ineffective include, 1) vasoactive drugs: dopamine (163), fenoldopam (258), and theophylline (156), 2) anti-inflammatory or antioxidant drugs: dexamethasone (171), N-acetylcysteine (109), and 3) loop diuretics (163, 253). Drugs which have shown some promise in various studies, but still require further investigation include, 1) anti-inflammatory/antioxidant drugs: sodium bicarbonate (111) and statins (309), 2) growth factor erythropoietin (254), and 3) vasoactive drugs: natriuretic peptides (191), fenoldopam (190), nitroprusside sodium (149), and clonidine (158). Although a number of interventions have been examined, there are currently no drugs available which have demonstrated conclusive evidence for improved renal protection or recovery. The complexity of the injury certainly has a role in the failures of many pharmacological interventions attempted, but it may also be attributed to multiple pathological mechanisms occurring simultaneously, or optimization of dosing protocols after injury. Currently, no pharmacological intervention has proven consistently successful to reverse established AKI with improved outcomes. Improved biomarkers for earlier diagnosis of AKI will certainly help improve efficacy of pharmacological intervention. Also, recognition of the multi-faceted nature of the injury, with a potential need for a multi-targeted therapeutic approach may also improve outcome in AKI intervention studies.

MITOCHONDRIAL DYSFUNCTION

Mitochondrial dysfunction in disease and aging

Reduced mitochondrial biogenesis and function have been observed in diseases

characterized by metabolic deficiencies, such as obesity and diabetes (226, 232, 246).

Insulin resistance is associated with mitochondrial dysfunction; however, it is not

completely clear whether insulin resistance is the result of mitochondrial impairment or if

changes in mitochondrial function are the result of insulin resistance (53). There is a

strong positive correlation between high fat content and reduced PGC-1α in obese

subjects, mice, and adipocytes treated with high glucose (226, 246). Reduced

mitochondrial DNA and proteins has been observed in adipocytes from diabetic mouse

models(55, 232). Additionally, both PGC-1α and PGC-1β are considerably reduced in

skeletal muscle from diabetic patients (213). Consistent with these findings, reductions

in PGC-1α responsive genes involved in oxidative phosphorylation have also been

observed in skeletal muscle of diabetic patients compared to healthy individuals (188).

Insulin resistance and high glucose and fat exposure also alter mitochondrial morphology,

including smaller mitochondria and condensed cristae (92). The altered morphology is

associated with decreased expression of the mitochondrial fusion protein Mfn1, and

increased expression of fission protein Drp1. Reduced Mfn2 has also been reported in

skeletal muscle taken from type 2 diabetic patients (9-10, 92). This is consistent with the

observations of small mitochondrial size and elevated fragmentation in diabetic patients

(150, 277).

During the normal aging process, there is also reduced mitochondrial biogenesis, with decreased expression of mitochondrial genes in skeletal muscle, adipose tissue, kidney, brain, and heart (170, 173, 177, 318). In addition to reduced mitochondrial biogenesis, there is a general decrease in mitochondrial turnover (269-271). This combination may result in an accumulation of damaged and/or dysfunctional mitochondria.

Mitochondrial Toxicants

A number of xenobiotics that produce cell and tissue dysfunction elicit their toxic effects by targeting the mitochondria, either directly or indirectly. In fact, since 1960 there have been 44 drugs withdrawn from the market which have demonstrated mitochondrial dysfunction, and there are another 384 labeled with black box warnings, which show higher than normal mitochondrial toxicity (81). Mitochondrial toxicants may function by inhibiting complexes of the electron transport chain (ETC), obstructing electron flow, disrupting ATP synthesis, altering Ca^{2+} homeostasis, or disrupting mitochondrial membrane integrity (293). For example, complex I of the ETC is a common target of toxicants, such as the compound 1-methyl-4-phenylpyridinium (MPP^+), which is used in animal models of Parkinson's disease (13, 141). Other commonly used ETC toxicants in the study of mitochondrial toxicity/function include rotenone, antimycin, cyanide, and oligomycin (120-121, 175). As a primary site of oxidant and free radical generation, due to the ETC chain, toxicants containing transition metals or structures capable of redox cycling can exert mitochondrial toxicity by facilitating the excessive production of damaging oxidized agents (293). One such example is the chemotherapeutic drug

doxorubicin, which induces generation of ROS and increased lipid oxidation, resulting in reduced integrity of the mitochondrial membrane (102-103).

Mitochondrial dysfunction in AKI

Mitochondrial damage is a major contributor to the lethal and sublethal tubular cell injury observed in the disease progression of AKI (86, 112, 139-140, 297). Increased production of ROS and NO, formed prominently within the mitochondria, as well as compromised antioxidant mechanisms following ischemic periods make the mitochondria particularly susceptible (215-216, 249, 317). Additionally, elevations in intracellular and mitochondrial Ca^{2+} and Fe^{3+} may contribute to the central role of the mitochondria in the disease process (65, 140). Subsequent disruption of mitochondrial respiratory complexes, membrane depolarization, ATP depletion, lipid peroxidation, membrane permeabilization and release of apoptotic proteins contribute to mitochondrial and cellular injury (28-29, 36, 112). Depolarization with high amplitude swelling can be visualized in mitochondria following hypoxia/reoxygenation (297). This is shown in Fig 1-5 below (Fig 1-5D, arrowhead).

The dynamic nature of mitochondria lends to dramatic alterations in structural integrity and population following acute toxic challenge. Mitochondrial fragmentation has been observed in models of AKI, and this process contributes to the resulting injury (39). Additionally, it has been reported that inhibiting mitochondrial fragmentation using a dominant-negative to Drp1 prevents the morphological changes to mitochondria, as well as the release of apoptotic proteins, and attenuates measurable injury in a mouse I/R

model (39). However, the role of mitochondrial fission and fusion following initial

injury and during the recovery and maintenance phase is still not completely understood.
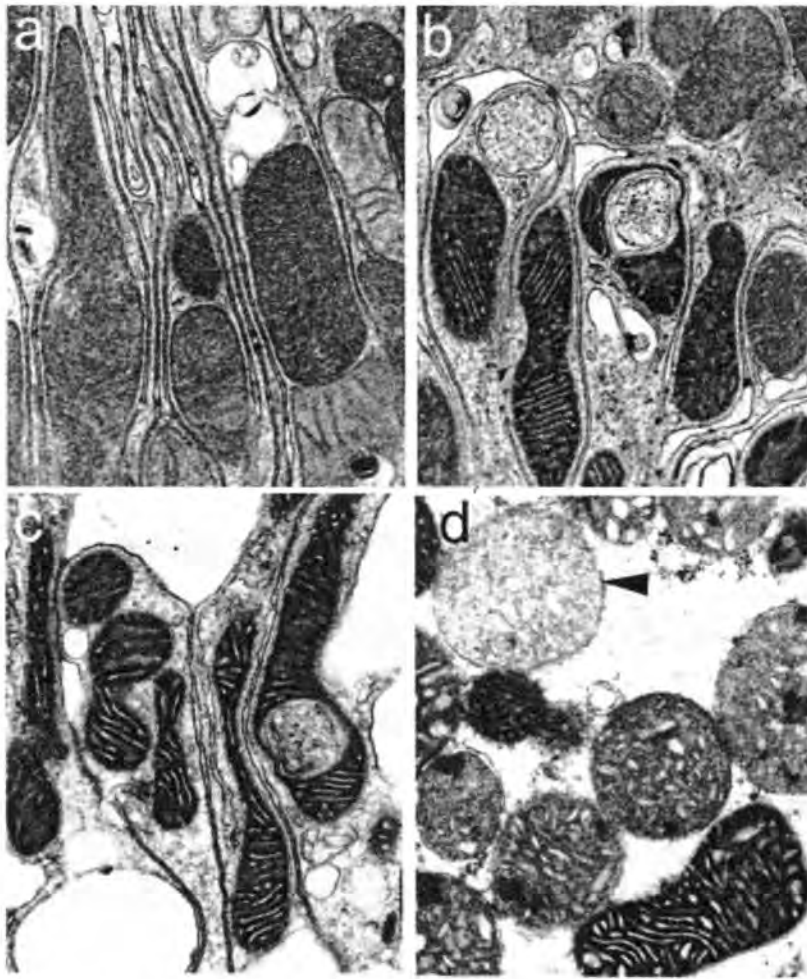
Fig 1-5. Mitochondrial ultrastructural changes. (*a*) Control. (*b*) Sixty-minute hypoxia. (*c* and *d*) Sixty-minute hypoxia followed by 60-min reoxygenation. Arrowhead, mitochondrion with high-amplitude swelling. (×24,100.) (297)

33

MITOCHONDRIAL BIOGENESIS

Definition of mitochondrial biogenesis

Mitochondrial biogenesis is the growth and division of pre-existing mitochondria, whether that occurs during the cell cycle or from normal mitochondrial turnover (7). The term biogenesis can be interpreted several different ways, and therefore in an attempt to describe mitochondrial biogenesis, it has been classified into three categories: 1) de novo synthesis of the organelle from precursor units, 2) formation from other membranous structures, and 3) growth and division of pre-existing mitochondria (198). The majority of evidence supports option 3 as the typical method of mitochondrial biogenesis. Mitochondrial biogenesis occurs under basal conditions and is an adaptive response initiated by cells to maintain energy demands or heat expenditure following injury, cold exposure, or caloric restriction (217, 310). A primary regulator of mitochondrial biogenesis is the nuclear transcriptional coactivator peroxisome proliferator-activated receptor coactivator-1α (PGC-1α). Through induction of uncoupling proteins (UCP-2), nuclear respiratory factors (NRF1/2), and as a coactivator of the promoter region of mitochondrial transcription factors Tfam, TFB1M, and TFB2M, PGC-1α has significant influence on mitochondrial function (97, 168, 217, 219, 308).

Transcriptional regulation of mitochondrial biogenesis

Nuclear Transcription Factors

NRF-1. Nuclear respiratory factor-1 (NRF-1) binding sites were first discovered in the cytochrome c promoter region (83). Since its discovery within the cytochrome *c* promoter, specific NRF-1 binding sites within the promoters of numerous mitochondrial

respiratory genes have been identified (52, 83), including the majority of nuclear-encoded

subunits of the respiratory chain (151, 240-241). NRF-1 also has a role in coordinating

expression of mitochondrial-encoded respiratory genes. Mitochondrial transcription

factor A (Tfam) and transcription factor B1 and B2 (TFB1M and TFB2M) contain NRF-

1 binding sites within their respective promoters. Reviewed more extensively later,

mitochondrial transcription factors regulate expression and replication of the

mitochondrial genome. TOM20 and TOM70, subunits of the transport of outer

membrane complex, as well as COX17, an assembly factor for cytochrome oxidase, are

also activated by NRF-1 (25, 264). Signals that increase mitochondrial biogenesis, such

as exercise-induced Ca2+ and AMPK pathways, also elevate NRF-1 expression,

highlighting its role in energy dependent adaptation (18, 24-25). It should be noted,

however, that the same effects of exercise on NRF-1 expression observed in rodent

models has not yet been reported in humans.

NRF-2. Nuclear respiratory factor 2, also known as GA-binding protein, was discovered

via a cis-acting domain within the promoter of subunit IV of cytochrome c oxidase

(COXIV) (239). In addition to COXIV, NRF-2 has been linked to several other COX

subunits, as knockdown results in diminished expression of all nuclear-encoded COX

genes (207). Outside of COX expression, NRF-2 has been shown to regulate expression

of respiratory genes such as the mitochondrial transcription factors Tfam and TFB1M and

TFB2M (97, 289).

ERRs. The estrogen-related receptor (ERR) family consists of ERRα, ERRβ, and ERRγ members. The ERRs are sequentially similar to the estrogen receptor and share similar DNA-binding and ligand-binding domains (94), but are not activated by estrogens or estrogen-like molecules (104). Similar to the other transcription factors discussed in this section, the transcriptional activity of the ERRs is regulated by physical interactions with coactivators such as the PGC-1 family and SRC, and corepressors such as RIP140 (94, 287), and this is particularly exemplified by the activity of ERRα, which seems to only be active when associated with PGC-1 coactivators (130, 144, 242). ERRs bind to ERR response elements within the promoter region of transcriptional targets, regulating transcription of genes associated with fatty acid oxidation, oxidative-phosphorylation, the tricarboxylic acid (TCA) cycle, and mitochondrial import and dynamics (94, 288). ERR response elements are enriched in regulatory domains of PGC-1α and mitochondrial genes, and are often associated with NRF sites as well (80, 189, 242, 255). Additionally, similar to PGC-1α expression, ERR distribution demonstrates a positive correlation with tissues that are highly metabolic (94, 189, 242). Knockdown studies have demonstrated that ERRα expression is required for exogenous PGC-1α-induced mitochondrial biogenesis and respiratory control (189, 242).

PPARs. The peroxisome proliferator-activated receptors (PPARα, PPARγ, and PPARδ) are a family of nuclear receptors that primarily regulate lipid metabolism. PPARα and PPARδ regulate lipid metabolism, and PPARγ is a primary regulator of lipid synthesis and storage. Similar to the NRFs and ERRs, PPARs associate with PGC-1 coactivators to enhance transcription of target genes (217, 284, 295). Although not as ubiquitous as

the NRFs or ERRs, PPARs (specifically PPARγ and PPARδ) have a role in mitochondrial biogenesis in specific cell types. Adipose tissues, which are not particularly enriched with mitochondria, respond to PPARγ agonists, such as pioglitazone, and PPAR ligands to increase mitochondrial biogenesis (55, 232, 301). Additionally, PGC-1α contains a PPAR response element in its promoter region, which, as a PPARγ coactivator, enables PGC-1α to enhance its own transcription (124). Indeed, PGC-1α expression is elevated in studies examining PPAR ligands, suggesting that PPAR activation also indirectly activates mitochondrial biogenesis via up-regulation of PGC-1α (232, 301). In skeletal muscle, activation of PPARδ stimulates mitochondrial biogenesis, and enhances lipid metabolism and fatty acid oxidation (265). Similar to PPARγ activation, the role of PPARδ may be an indirect role on mitochondrial biogenesis by increasing PGC-1 expression instead of direct induction of mitochondrial genes, such as those involved in oxidative phosphorylation (14, 124, 265).

PGC-1α and the nuclear coactivators

As outlined in the previous section, there are several diverse classes of transcription factors which control expression of a variety of activities associated with mitochondrial biogenesis. This observation prompted the hypothesis that there was a common molecule coordinating the activities of these transcription factors, which was confirmed with the discovery of the PGC-1 transcriptional coactivators (217).

PGC-1α. Peroxisome proliferator activated receptor γ (PPAR) coactivator-1α was discovered as an interacting partner with PPARγ regulating adaptive thermogenesis upon

cold exposure in brown adipose tissue (217). Several studies have demonstrated essential

LXXLL motifs adjacent to the activation domain for coactivating function of PGC-1α. In

addition to PPARγ, PGC-1α associates with several other nuclear hormone receptors,

including the NRFs and ERRs. PGC-1α associates with the NRFs and trans-activates

genes involved in mitochondrial respiration (236). Additionally, PGC-1α increases Tfam

and TFB mRNA by targeting NRF recognition sites within the promoters of these genes

(73). PGC-1α also induces expression of respiratory genes via conserved ERR and NRF2

recognition sites located within promoter regions of genes encoding cytochrome c and

ATP synthase β (143, 190).

PGC-1α is highly expressed in metabolic tissues, and its expression and activity are

regulated by a network of receptors, including the nuclear hormone receptors thyroid

hormone and PPARγ (217, 306); signaling pathways, such as the MAPK and CaMK

pathways (12, 307); and post-translational phosphorylation, methylation, and acetylation

modifications (12, 62, 218, 272). Additionally, PGC-1α transcription is regulated by the

activity of signaling molecules and transcription factors such as protein kinase B,

forkhead transcription factor, and myocyte enhancer factor-2 (MEF-2) (68, 70).

Mitochondrial transcription factors

Tfam. Tfam is a nuclear-encoded, mitochondrial transcription factor that is up-regulated

and then translocated to the mitochondria when there is a mitochondrial biogenesis

signal. It is involved in the transcription and replication of the mitochondrial genome,

binding to a common site on the promoters of the two strands of the mitochondrial genome.

Other components of mitochondrial biogenesis

Protein Import. Because only 13 of the 1000+ proteins which comprise an intact mitochondrion are actually encoded within the mitochondrion, the vast majority of mitochondrial proteins must be imported into the organelle and assembled after being synthesized exogenously. Nuclear-encoded transcripts are translated in the cytosol containing specific mitochondrial targeting sequences directing the precursor proteins to appropriate sites within mitochondria where they undergo further processing and folding to create the mature protein. The proteins are transported across the mitochondrial membranes via the translocase of the outer membrane (TOM) complex and the translocase of inner membrane (TIM) complex, and are then subjected to further cleavage and folding by mitochondrial proteases and chaperones.

Physiological states that induce mitochondrial biogenesis

Activation of the network of genes associated with mitochondrial biogenesis accompanies a diverse set of signaling pathways initiated in response to various physiological stimuli when there is an increased energetic demand or a need for increased efficiency. Outlined in Fig 1-6 below and described in the next section, endurance exercise training in muscle cells, cold exposure in brown adipose tissue, and caloric restriction all activate pathways which lead to enhanced PGC-1α expression and/or activity and mitochondrial biogenesis. Additionally, as documented in numerous studies

examining cell/tissue injury, specifically those that target the mitochondria, biogenic

pathways are up-regulated after injurious stimuli, including damage to renal cells.

Endurance exercise: muscle

β-AR → ↑cAMP → PKA → CRTC / CREB → ↑ PGC-1α

↑Ca²⁺ → Cn, CAMK, CAMKKβ
CAMK → p38 → ↑ PGC-1α

Neuregulin

↑AMP:ATP → AMPK → ↑ PGC-1α, GABP

Exposure to cold: BAT

Adenylyl cyclase, SNS, β-AR

↑cAMP → PKA → ATF2, p38 → ↑ PGC-1α

Caloric restriction: muscle

Adiponectin, ↑AMP:ATP

↑SIRT1, AMPK → ↑ PGC-1α

Alt. activation: macrophage

IL-4, IL-13, IL-4R, IL-13R → STAT6 → ↑PPAR → ↑ PGC-1β
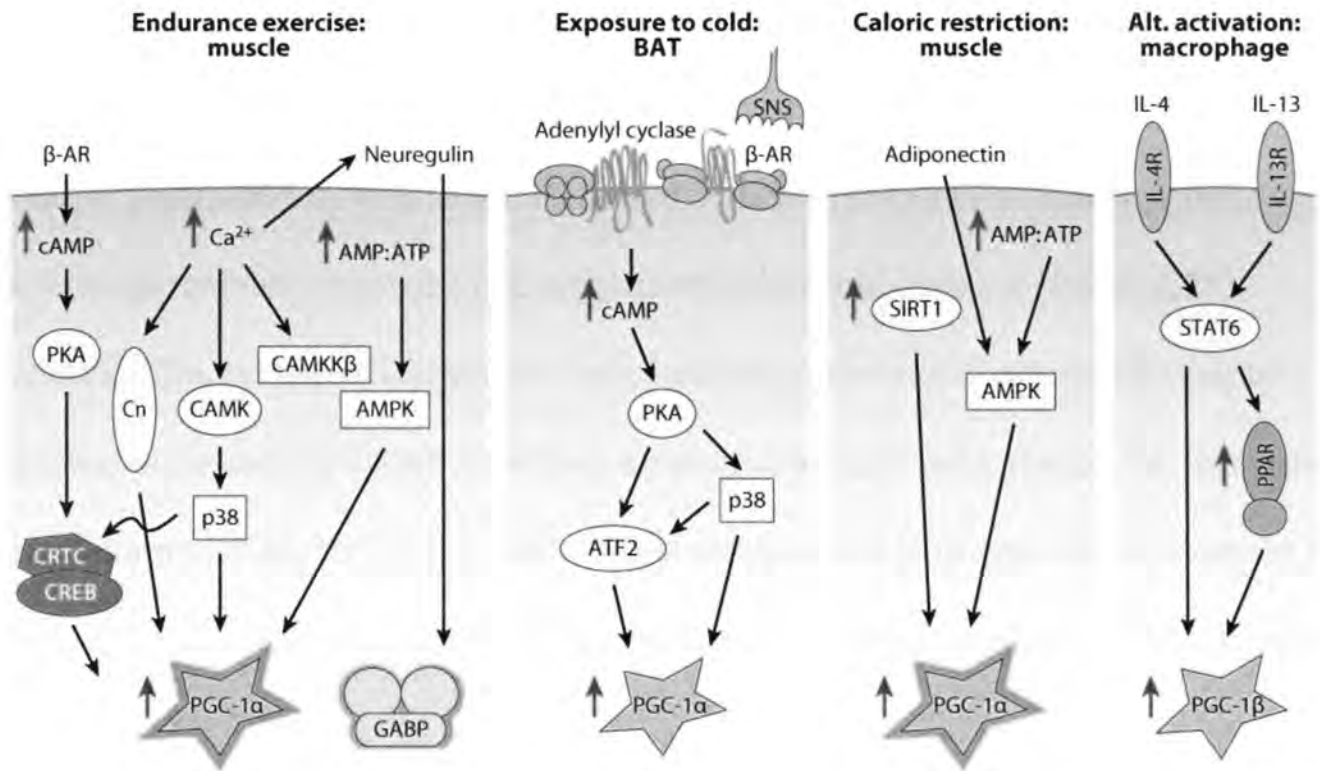
Fig 1-6. Diverse physiological signals regulate mitochondrial biogenesis in a tissue-specific manner. Shown are signaling pathways that induce mitochondrial biogenesis in skeletal muscle in response to endurance exercise or caloric restriction, in BAT in response to cold exposure, and in macrophages in response to signals promoting alternative activation. The signals enhance activity (*orange outlines*) and/or expression (*upward blue vertical arrows*) of transcriptional regulators PGC-1α, GABP, or PGC-1β (123).

Exercise. Physical activity induces an energetic demand that can induce a mitochondrial biogenic response, particularly within skeletal muscle. Increased cytosolic Ca^{2+} due to muscle contraction as well as stimulation of AMPK in response to energy deficit can lead to a transcriptional response to up-regulate mitochondrial gene expression (228). Additionally, sympathetic nervous system stimulation results in adrenergic receptor activation, increasing cAMP signaling. Even after a single bout of exercise, increased expression of PGC-1α, NRF-1, ERRα, and mitochondrial genes have been observed (51, 176, 214, 228, 234), and repeated bouts result in measurable increases in mitochondrial numbers (56, 228).

Cold exposure. PGC-1α is induced upon cold exposure via sympathetic nervous system activity and adrenergic receptor stimulation, which in rodents occurs primarily in brown adipose tissue (BAT), resulting in elevated cAMP and subsequently activation of protein kinase A, p38 MAPK, and CREB. Cold exposure also induces a state of adaptive thermogenesis by inducing PGC-1α to stimulate uncoupling proteins (Ucp1), which generate heat by manipulating the mitochondrial proton gradient (50, 217, 219).

Caloric restriction. Mitochondrial biogenesis under a restricted diet has been well studied and the two primary mediators of the response have been AMPK and SIRT1 (57, 172, 199). Additionally, activation of endothelial nitric oxide synthase (eNOS) has been implicated in the biogenic response in caloric restriction models. The demand for more efficient energetic utilization is likely the catalyst for the effects of CR on mitochondria,

and activation of each of these factors results in regulation of PGC-1α activity and expression (34, 93, 138).

*Mitochondrial biogenesis in renal cell injury.* Previous work from our lab has demonstrated that severe mitochondrial dysfunction occurs within at least 24h after acute oxidant exposure to primary renal proximal tubule cells (RPTC), represented by dramatic reductions in ATP levels and mitochondrial oxygen consumption (205, 220). Nowak, et al., showed that these functional parameters spontaneously recovered over the course of approximately 6 days (205). Rasbach, et al., further clarified this recovery with the discovery that PGC-1α was robustly up-regulated in response to mitochondrial injury via a Src-EGFR-p38 MAPK signaling pathway (220). Fig 1-7 below illustrates the induction of PGC-1α protein 24h after TBHP exposure. The elevated expression is maintained for 72h after exposure. Concurrently, basal and FCCP-uncouple oxygen consumption recover from maximal injury at 24h until full recovery by 6 days after exposure (Fig 1-7). Recovery of other mitochondrial and cellular functions, including cellular ATP levels, ouabain-sensitive respiration, glucose uptake follow similar patterns and also recover during this period of elevated PGC-1α (205).

A.

PGC-1α →
Actin →
Day: 0 1 2 3 4 5 6

B.
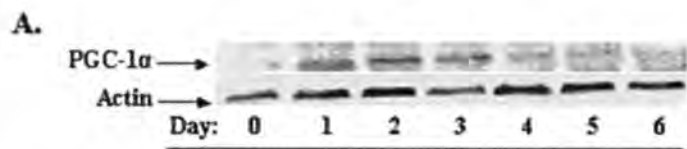
PGC-1α Expresssion During RPTC Recovery
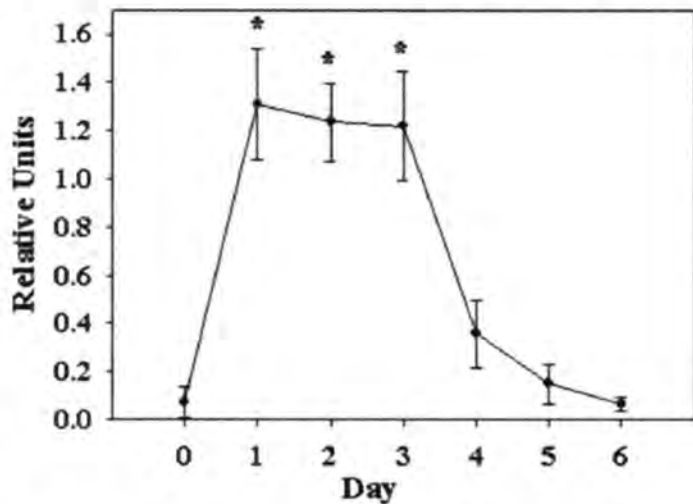
C.

Basal Respiration

D.
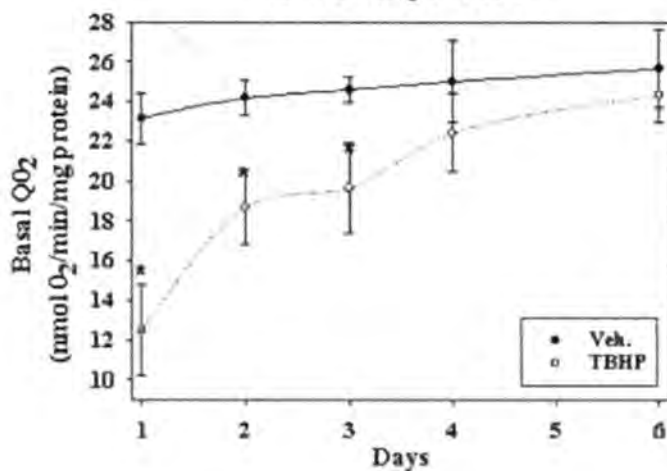
Uncoupled Respiration
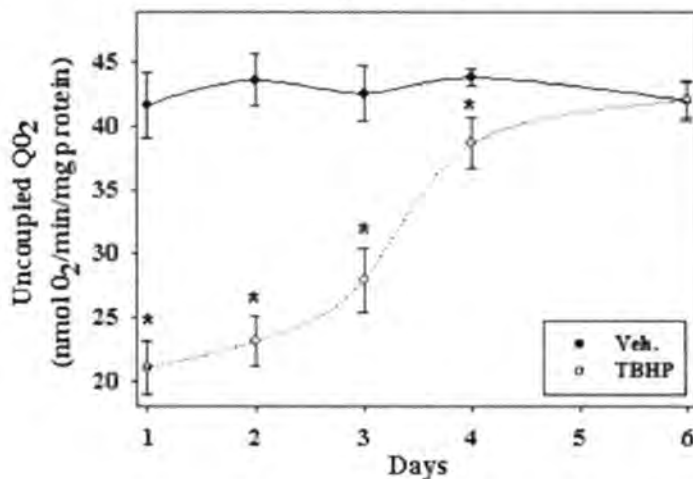
Figure 1-7. Induction of PGC-1α protein (A,B) correlates with recovery of basal (C) and uncoupled (D) respiration after oxidant injury in RPTC (220).

44

Further support for the role of PGC-1α in the recovery of mitochondrial function following acute oxidant injury was demonstrated when PGC-1α was overexpressed following oxidant injury (221). In cells overexpressing PGC-1α after injury, recovery of mitochondrial proteins, ATP, and mitochondrial respiration occurred within 24h after overexpression (Fig 1-8). Illustrated in Fig 1-8 below, the mitochondrial proteins ATP synthase β and NDUFB8 were significantly reduced after TBHP exposure, but were nearly fully recovered in cells forced to over-express PGC-1α (Fig 1-8A). Additionally, as expected mitochondrial functional markers, including total cellular ATP (Fig 1-8B), basal respiration (Fig 1-8C) and uncoupled respiration (Fig 1-8D) were significantly reduced following oxidant injury, but were fully recovered in cell overexpressing PGC-1α.
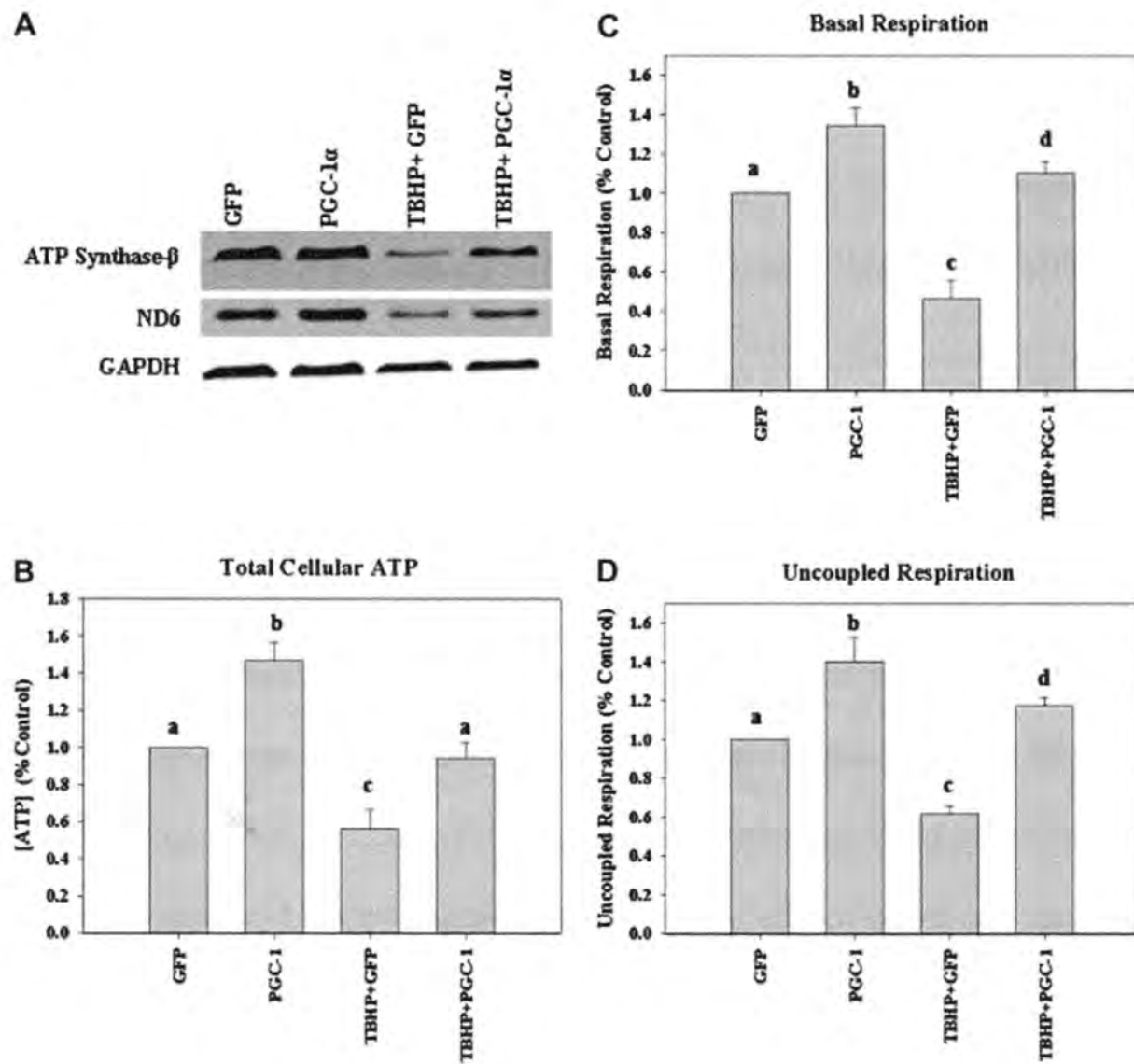
Figure 1-8. Overexpression of PGC-1α after oxidant injury restored mitochondrial protein expression (A), as well as total cellular ATP (B) and basal (C) and uncoupled (D) oxygen consumption in RPTC exposed to *tert*butyl-hydroperoxide (221).

SIRT1 and AMPK regulation of PGC-1α

In addition to transcriptional control of PGC-1α, it is also subject to a number of post-translational modifications. Under energetic crises, primary responders for maintaining energy and nutrient homeostasis are AMP-activated kinase (AMPK) and SIRT1.

AMPK. AMPK is a Ser/Thr kinase, which upon activation stimulates a series of signaling pathways which promote ATP production and inhibit energy-expending processes. AMPK is able to influence metabolic activities in both the short term, by directly phosphorylating metabolic enzymes, as well as more long-lasting effects by altering gene expression profiles to accommodate changes in metabolic status. AMPK monitors cellular energy levels, inducing ATP synthesis and inhibiting ATP expenditure when ATP levels are low (118), by regulating expression of mitochondrial and metabolic genes via direct phosphorylation of PGC-1α (138).

SIRT1. SIRT1 is a nuclear protein that is also activated in response to energy depletion, and promotes induction of genes that regulate metabolic adaptation to low energy levels. As a member of a conserved family of NAD^+-dependent deacetylase enzymes known as the *sirtuins*, SIRT1 is one of seven mammalian orthologs of the silent information regulator 2 (Sir2), a yeast protein that has been shown to regulate gene silencing and lifespan (133). Upon activation, SIRT1 catalyzes a lysine deacetylation reaction, which hydrolyzes NAD+ in the process (267), resulting in a de-acetylated protein target, nicotinamide, and O-acetyl-ADP ribose (35, 266). Targets of SIRT1 deacetylation include transcription factors, coregulators of transcription, and histones (84).

SIRT1, and the yeast protein Sir2, has been proposed as a link between the effects of caloric restriction and lifespan extension (105-106, 169, 230, 276). Consistent with these findings are the reports that treatment with the SIRT1 activator resveratrol also extended lifespan in a number of organisms (125, 304). In mammals the link between SIRT1 and lifespan extension is a little less clear. It has been documented that caloric restriction modulates lifespan in mammals, including primates (162, 233), and SIRT1 is activated in caloric restriction models (58). Additionally, SIRT1 overexpression in mice mimics several characteristics found under calorie restriction, including increased metabolic activity and leanness, and reduced cholesterol, insulin, and fasted glucose levels (33). Fig 1-9 illustrates some of the known key regulatory factors which control SIRT1 function, as well as the biological effects of increased SIRT1 activity.
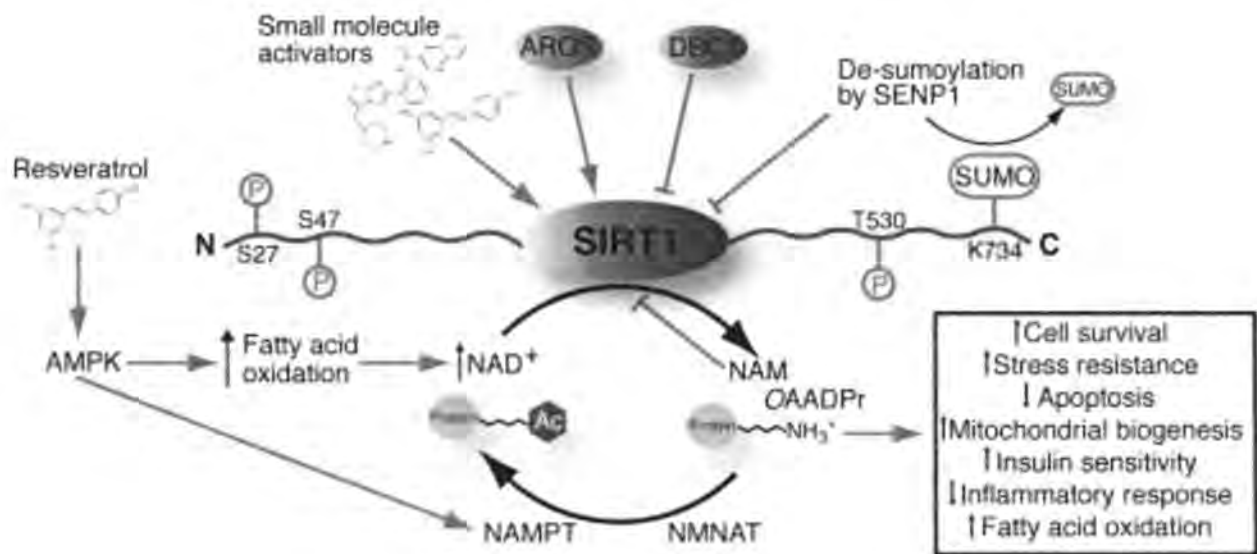
Fig 1-9. Potential regulatory pathways of SIRT1 that could be exploited to increase SIRT1-mediated deacetylation. Phosphorylation, sumoylation, AMPK, small molecules, increased NAD^+ levels and AROS binding are purposed activators (depicted in green). Nicotinamide, DBC1 binding, and de-sumoylation are purposed inhibitory pathways that could be regulated to increase SIRT1 activity (depicted in red). AMPK: AMP-activated kinase, AROS: Active regulator of SIRT1, DBC1: Deleted in breast cancer-1, NAM: Nicotinamide, NAMPT: Nicotinamide phosphoribosyltransferase, NMANT: Nicotinamide mononucleotide adenylyltransferase, *O*AADPr: *O*-Acetyl-ADP-ribose, SENP1: Sentrin specific protease 1, SUMO: Small ubiquitin-like modifier. (77)

One of the primary targets of SIRT1 deacetylation is the transcriptional co-activator PGC-1α. SIRT1 catalyzes the deacetylation and activation of PGC-1α in both *in vitro* and *in vivo* systems (196, 229), which may contribute to a protective role in metabolic regulation and resistance to oxidative stress (32, 125). Additionally, mutation of the acetylation sites on PGC-1α to an arginine, mimicking the deacetylated state, enhances PGC-1α transcriptional activity (229), supporting SIRT1 deacetylation as a positive influence on PGC-1α activity. Conversely, the acetyltransferases Steroid Receptor Coactivator 3 (SRC-3) and General Control Nonderepressible 5 (GCN5) have been shown to acetylate PGC-1α and repress its activity (62). Under states of high-fat feeding, SRC-3 and GCN5 are elevated and SIRT1 expression is decreased, leading to hyperacetylation of PGC-1α (62). In contrast, under fasting conditions or caloric restriction, SIRT1 is elevated and SRC-3 and GCN5 are reduced, which results in deacetylated PGC-1α.

Rather than exclusive mechanisms of adaptation, recent evidence points to concurrent regulation and convergent mechanisms induced by AMPK and SIRT1 in response to changes in cellular energy levels and redox states, with a primary target of both pathways converging on PGC-1α (48).

Pharmacological activators of mitochondrial biogenesis

SIRT1 activators. A widely recognized SIRT1 activator is the compound resveratrol found primarily in the skins of grapes. Resveratrol is a natural antioxidant and phytoestrogenic compound, and has been shown to increase SIRT1 activity when

examined by in vitro activation assays (16, 125). The interaction of resveratrol with SIRT1 is allosteric, and increases SIRT1 affinity for its target substrate as well as NAD+ (125). Additionally, resveratrol treatment has been shown to have effects on lifespan extenstion, mimicking caloric restriction-mediated Sir2 activation (125, 169). Recently, there has been a lot of controversy about the actual intracellular target of resveratrol, and some reports suggest that it may not be a direct activator of SIRT1 (208). The structures of proposed SIRT1 activators, including resveratrol, are shown in Fig 1-10 below.

Our lab demonstrated that a number of isoflavone-derived molecules were able to increase SIRT1 activity (either by increasing expression or activity of SIRT1), and induce mitochondrial biogenesis in primary RPTC (223). Daidzein, formononetin, 3-(2',4'-dichlorophenyl)-7-hydroxy-4H-chromen-4-one (DCHC) and 7-hydoroxy-4H-chomen-4-one (7-C) increased activation of SIRT1 in an *in vitro* fluorescence-based deactylation assay. Daidzein, formononetin, genistein, biochanin A,4',7-dimethoxyisoflavone (4',7-D), and5,7,4'-trimethoxyisoflavone (5,7,4'-T) increased SIRT1 expression in RPTC. RPTC exposed to the compounds had increased mitochondrial protein expression (including the OXPHOS proteins ATP synthase β and NDUFB8), as well as elevated mitochondrial respiration rates and cellular ATP levels (223).

SRT1720, a potent SIRT1 activator. SRT1720 was first reported as a SIRT1 activator in a high-throughput *in vitro* fluorescence polarization screen (178). Along with two other compounds identified in the screen, SRT1720 was found to activate SIRT1 over 1000-fold more potently than resveratrol, and exposure of this compound led to deacetylation

of SIRT1 target proteins in both cells and animals (85, 178). The structure of SRT1720 is depicted in Fig 1-10. It should be noted that although it has been characterized as a potent SIRT1 activator in vitro, and exposure induces deacetylation of SIRT1-target proteins, the true direct target of SRT1720 has been controversial (208). In genetic and diet-induced obese and diabetic rodents, 4- to 10-weeks of SRT1720 treatment improves insulin sensitivity and reduces plasma glucose levels while enhancing skeletal muscle mitochondrial activity (178). Additionally, C2C12 cells treated with SRT1720 express elevated citrate synthase activity and ATP levels, suggesting induction of mitochondrial biogenesis upon exposure (251). Recently, it was reported that SRT1720 treatment in obese mice extends both mean and maximum lifespan (180). In addition to increased lifespan, SRT1720 also had positive effects on health benefits such as reduced liver steatosis, increased insulin sensitivity, enhanced locomoter activity, and reduced markers of inflammation. Using conditional knockouts, Minor, et al., also demonstrated that the effects of SRT1720 were dependent on SIRT1 and PGC-1α (180).

SIRT1 activators

Resveratrol

Quercetin

Piceatannol

Isonicotinamide

SRT1720

SRT1460

SRT2183
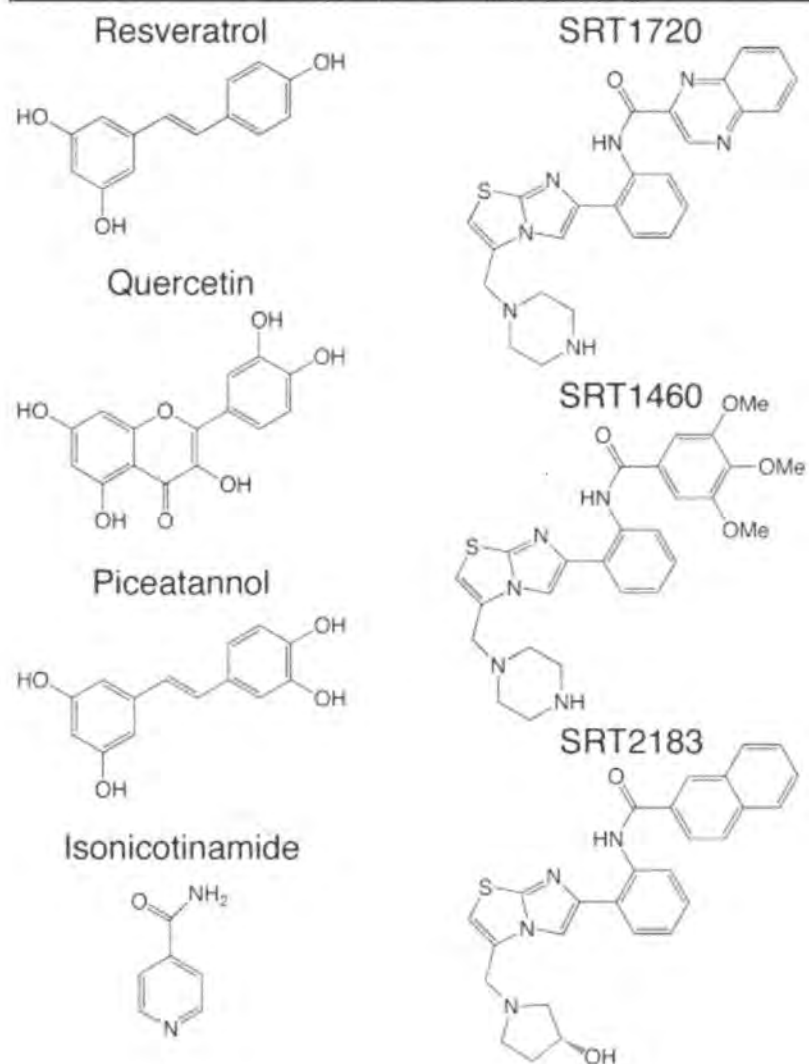
Fig 1-10. Structure of proposed SIRT1 activators (77).

Assessing mitochondrial biogenesis

Fluorescent Microscopy. Fluorescent microscopy is a commonly used method to evaluate mitochondrial abundance and health. Potentiometric dyes such as TMRM, Rhodamine 123, and JC-1 are sequestered within the mitochondrial membrane based on the membrane potential of polarized mitochondria. Therefore, these dyes are excellent tools for evaluating mitochondrial health because visualization is dependent on respiring, polarized mitochondria in cells in culture or in living tissue (via intravital microscopy); however, the potentiometric dyes are not ideal for examining mitochondrial abundance because they may not detect all mitochondria present. Dyes such as Mito-tracker, which fluoresces upon entering the mitochondria, and 10-n-nonyl-acridine orange, which binds to cardiolipin in the inner membrane, are thought to be less dependent on mitochondrial membrane potential; however, studies in yeast have shown that this may not always be accurate (99).

Mitochondrial DNA (mtDNA) content. As previously described, mitochondria have their own genome set which typically ranges from approximately 2 to 10 copies per mitochondrion. Despite the lack of a true 1:1 ratio for mtDNA:mitochondria, the measure of mtDNA should be proportional to the number of mitochondria. Determination of mitochondrial DNA content can be done by traditional Southern blot techniques, or by more commonly applied PCR-based assays. In such cases, primers are designed against a region of the mitochondrial genome, such as a coding region (e.g. NADH dehydrogenase subunit 1) or a non-coding region (e.g. the mitochondrial D-loop),

to measure the content of mtDNA and are normalized to a marker of total genomic DNA (26).

Examining components of biogenic machinery. As detailed previously in this section, there are several key components of the mitochondrial biogenic process which are universally enhanced to coordinate the nuclear and mitochondrial transcriptional activities involved. NRF1 and NRF2 are transcription factors involved in regulating nuclear transcriptional activities. Tfam is a mitochondrial transcription factor which regulates mtDNA transcription and replication. PGC-1α is a nuclear coactivator of transcription which associates with a number of transcription factors which regulate mitochondrial gene expression (such as the NRFs), coordinating the cell's response to external stimuli with a mitochondrial gene profile to increase abundance. Up-regulation of these factors can be detected by conventional methonds (e.g. PCR, western analysis, etc.) when mitochondrial biogenesis is turned on. One concern with examining components of the biogenic process, however, is that these factors may only be transiently up-regulated, so determining the optimal time of examination is essential.

Mitochondrial respiratory complexes. An indirect measure of mitochondrial content is to evaluate transcript or protein expression of subunits of the mitochondrial respiratory chain. Greater numbers of mitochondria should equate to elevated expression of OxPhos complexes. There are both nuclear-encoded and mitochondrial-encoded subunits which comprise the NADH dehydrogenase (complex I), cytochrome *c* oxidase (complex IV), and ATP synthase (complex V), and antibodies are available which recognize a number

55

of the subunits within these complexes. Additionally, mRNA expression of the subunits can also be examined, although as discussed previously in the biogenic machinery section, some of these genes may only be transiently up-regulated.

Evaluating mitochondrial function. Finally, a relatively quick way to evaluate mitochondrial biogenesis is by examining functional output. High throughput assays can be developed using the Seahorse Extracellular Flux to measure maximal oxygen consumption rates (uncoupled respiration) to evaluate mitochondrial biogenesis and toxicity (17). We have also demonstrated that intracellular ATP levels can correlate with increased mitochondrial numbers (221, 223). Of course, either of these measurements may only mean that the mitochondria are functioning more efficiently in one sample set versus another, so these types of measurements would generally need to be used in combination with one or more of the methods described above.

Chapter 2:

SRT1720 Induces Mitochondrial Biogenesis and Rescues Mitochondrial Function After Oxidant Injury in Renal Proximal Tubule Cells

ABSTRACT

Mitochondrial biogenesis occurs under basal conditions and is an adaptive response initiated by cells to maintain energetic demands and metabolic homeostasis following injuries targeting mitochondrial function. Identifying pharmacological agents that stimulate mitochondrial biogenesis is a critical step in the development of new therapeutics for the treatment of these injuries and to test the hypothesis that these agents will expedite recovery of cell and organ function following acute organ injuries. In this study, we examined the effects of SRT1720 on mitochondrial biogenesis and function in primary cultures of renal proximal tubule cells (RPTC). We also tested the ability of this compound to restore mitochondrial functions following oxidant-induced RPTC injury. SRT1720 (3-10 μM) induced mitochondrial biogenesis in RPTC within 24 hrs as determined by elevations in mitochondrial DNA copy number, increased expression of the mitochondrial proteins NDUFB8 and ATP synthase β, and elevated mitochondrial respiration rates and ATP levels. Induction of mitochondrial biogenesis was dependent on SIRT1 deacetylase activity, correlated with deacetylated nuclear PGC-1α, and occurred in the absence of AMP-dependent kinase (AMPK) activation. Finally, SRT1720 treatment accelerated recovery of mitochondrial functions following acute oxidant injury. This study demonstrates that SRT1720 can induce mitochondrial

biogenesis through SIRT1 activity and deacetylated PGC-1α, but not AMPK, in RPTC within 24 hrs following oxidant injury. The results support further study of mitochondrial biogenesis as a repair process and a pharmacological target in acute organ injuries and disorders plagued by mitochondrial impairment.

INTRODUCTION

Mitochondrial dysfunction is a primary pathological consequence of ischemic or toxic insults. In ischemic acute kidney injury (AKI), de-energization of the mitochondria and persistent energy depletion may hinder critical energy-dependent repair mechanisms and lead to irreversible cell injury, limiting restoration of organ function (86, 297). As such, there is therapeutic potential for agents that promote mitochondrial function to treat injuries characterized by mitochondrial impairment.

Mitochondrial biogenesis occurs under basal conditions and is an adaptive response initiated by cells to maintain energy demands or heat expenditure following injury, cold exposure, or caloric restriction (217, 310). A primary regulator of mitochondrial biogenesis is the nuclear transcriptional coactivator peroxisome proliferator-activated receptor coactivator-1α (PGC-1α). Through induction of uncoupling proteins (UCP-2), nuclear respiratory factors (NRF1/2), and as a coactivator of the promoter region of mitochondrial transcription factors Tfam, TFB1M, and TFB2M, PGC-1α has significant influence on mitochondrial function (97, 168, 217, 219, 308).

PGC-1α is highly expressed in metabolic tissues, and its expression and activity are regulated by a network of receptors, including the nuclear hormone receptors thyroid hormone and PPARγ (217, 306); signaling pathways, such as the MAPK and CaMK pathways (12, 307); and post-translational phosphorylation, methylation, and acetylation modifications (12, 62, 218, 272). Additionally, PGC-1α transcription is regulated by the

activity of signaling molecules and transcription factors such as protein kinase B, forkhead transcription factor, and myocyte enhancer factor-2 (MEF-2) (68, 70).

Under energetic crises, primary responders for maintaining energy and nutrient homeostasis are AMP-activated kinase (AMPK) and SIRT1. Rather than exclusive mechanisms of adaptation, recent evidence points to concurrent regulation and convergent mechanisms induced by AMPK and SIRT1 in response to changes in cellular energy levels and redox states, with a primary target of both pathways converging on PGC-1α (48). AMPK monitors cellular energy levels, inducing ATP synthesis and inhibiting ATP expenditure when ATP levels are low (118), by regulating expression of mitochondrial and metabolic genes via direct phosphorylation of PGC-1α (138). SIRT1 is a nuclear protein that is also activated in response to energy depletion, and promotes induction of genes that regulate metabolic adaptation to low energy levels. As a member of a conserved family of NAD^+-dependent deacetylase enzymes known as the *sirtuins*, SIRT1 monitors cellular energy levels and becomes active in response to elevated $NAD^+/NADH$ ratios (161). SIRT1 catalyzes the deacetylation and activation of PGC-1α in both *in vitro* and *in vivo* systems (196, 229), which may contribute to a protective role in metabolic regulation and resistance to oxidative stress (32, 125)

A number of small molecules have been reported, such as resveratrol and isoflavone-derived compounds (125, 223), to induce mitochondrial biogenesis in RPTC. SRT1720 was reported to be a SIRT1 activator, and exposure of this compound led to deacetylation of SIRT1 target proteins in both cells and animals (85, 178). In genetic and diet-induced

obese and diabetic rodents, 4- to 10-weeks of SRT1720 treatment improves insulin sensitivity and reduces plasma glucose levels while enhancing skeletal muscle mitochondrial activity (178). Additionally, C2C12 cells treated with SRT1720 express elevated citrate synthase activity and ATP levels, suggesting induction of mitochondrial biogenesis (251). However, the acute effects of this compound in primary cultures of renal proximal tubule cells, which better mimic the metabolic properties of cells *in vivo* compared to glycolytic cell lines, on mitochondrial biogenesis have not been explored. Furthermore, the effects of this compound in targeted injury models with mitochondrial impairment have also not been characterized.

Mitochondrial dysfunction contributes to oxidant-induced renal cell injury (205), and PGC-1α plays a predominant role in the recovery of mitochondrial function following the initial injury (220). Over-expression of PGC-1α accelerates recovery of mitochondrial and cellular functions after oxidant injury (221), but because of the toxicity limitations in using adenovirus in vivo, there is a need for pharmacological agents that stimulate mitochondrial biogenesis to treat injuries characterized by mitochondrial impairment. In this study, we examined the mechanism of SRT1720 induced mitochondrial biogenesis and function in renal epithelial cells and tested the hypothesis that stimulation of mitochondrial function accelerates recovery from an acute cellular and mitochondrial injury.

EXPERIMENTAL METHODS

Reagents – PGC-1α (H300), NDUFB8, ATP Synthase β, and GAPDH antibodies were obtained from Santa Cruz Biotechnology (Santa Cruz, CA), Invitrogen (Carlsbad, CA), Abcam (Cambridge, MA), and Fitzgerald (Concord, MA), respectively. Acetylated lysine, phosphorylated AMPK (Thr172), and AMPK antibodies were obtained from Cell Signaling Technologies (Danvers, MA). Sirtinol and nicotinamide were purchased from Sigma-Aldrich (St. Louis, MO). All other chemicals were obtained from Sigma-Aldrich.

SRT1720 synthesis and SIRT1 activation – SRT1720 was synthesized according to a procedure previously described (178) and was confirmed by NMR and mass spectrometry and the final product was purified by HPLC. SIRT1 deacetylase activity was measured using a fluorescence-based SIRT1 activity kit (BioMol, Plymouth Meeting, PA) according to manufacturer's protocol as previously described (223).

Isolation and Culture of Renal Proximal Tubules – Female New Zealand White rabbits (~2 kg) were purchased from Myrtle's Rabbitry (Thompson Station, TN). Renal proximal tubules were isolated using an iron oxide uptake method previously described (220). Cells were cultured on 35 mm dishes in a medium consisting of 1:1 DMEM/Ham's F12 (lacking glucose, phenol red, and sodium pyruvate), and supplemented with HEPES (15 mM), glutamine (2.5 mM), pyridoxine HCl (1 uM), sodium bicarbonate (15 mM), and lactate (6 mM). Hydrocortisone (50 nM), selenium (5 ng/ml), human transferrin (5 μg/ml), bovine insulin (10 nM), and L-ascorbic acid-2-phosphate (50 μM) were added daily to fresh culture medium. Experiments with RPTC were conducted on the sixth day after plating when the cells had reached a confluent monolayer. Treatments were

administered for 24 hrs unless otherwise noted. For TBHP injury experiments, cells were

exposed to 400 µM TBHP for 45 min, at which time TBHP media was replaced with

fresh media.

Preparation of cell lysates for immunoblot analysis – Twenty-four hours following

treatment, RPTCs were harvested in RIPA lysis buffer consisting of 25 mM Tris-HCl,

150 mM NaCl, 1% TritonX-100, 1% sodium deoxycholate, and 0.1% SDS. Lysates were

sonicated and total protein was measured by BCA. Immunoblot analysis was performed

as previously described (220).

Immunoprecipitation – Cells were harvested from pooled culture dishes in a

homogenization buffer consisting of 50 mM Tris-HCl, 1 mM β-mercaptoethanol, 1 mM

EDTA, and 0.32 M sucrose. Cells were disrupted by sonication and nuclei were

collected by centrifugation at 900 x g for 10 min. Following centrifugation, the nuclear

pellet was resuspended in a nuclear lysis buffer consisting of 10 mM Tris, 500 mM NaCl,

1% TritonX-100, 10% glycerol, 1 mM sodium pyrophosphate, 1 mM $NaVO_4$, 1 mM NaF,

and protease inhibitors. Immunoprecipitations were carried out according to a protocol

by Roche Diagnostics (Indianapolis, IN). Nuclear protein lysate (500 µg) and 5 µg PGC-

1α antibody were used for experiments. Immunoprecipitates were analyzed by

immunoblotting using antibodies against acetylated lysine residues and PGC-1α.

Supernatants collected from immunoprecipitations were analyzed for Histone H3

expression as a control for initial nuclear protein input.

Quantitative Real-Time PCR – Total RNA was isolated from cells with TRIzol

(Invitrogen, Carlsbad, CA). cDNA was synthesized from 5 µg RNA template using a

SuperScript II Reverse Transcriptase kit (Invitrogen). PCR reactions were carried out using 2.5 μL cDNA template combined with Brilliant II SYBR Green master mix (Stratagene) at a final concentration of 1X and primers (Integrated DNA Technologies) at a concentration of 400 nM. Sequences of primers used for real-time PCR reactions: PGC-1α (FW: 5'-AGG AAA TCC GAG CTG AGC TGA ACA-3', REV: 5'-GCA AGA AGG CGA CAC ATC GAA CAA-3'), and GAPDH (FW: 5'-GAG CTG AAC GGG AAA CTC AC-3', REV: 5'-CAC TGT TGA AGT CGC AGG AG-3').

Mitochondrial DNA content – Real-time PCR was used to determine relative quantities of mitochondrial DNA content in SRT1720-treated cells and control cells. Following a 24 hr treatment, total genomic DNA was extracted using a DNeasy Blood and Tissue Kit (Qiagen). DNA was quantified by measuring A260 values and 50 ng total DNA was used for PCR reactions. Primers specific to the mitochondrial-encoded ND6 gene (FW: ACT GCG ATG GCA ACT GAG GAG TAT, REV: ACC ATA ACT ATA CAA CGC CGC CAC) were used to assess mitochondrial DNA copy numbers. Primers designed against the nuclear-encoded Pou5f1 gene (FW: 5'-GGC CTA TGT CTT TTC CTC TGG-3', REV: 5'-TCC AGG TTC TCT CTC CCT AGC-3') were used for normalization.

Oxygen Consumption (QO₂) and ATP levels – Basal and FCCP-uncoupled oxygen consumption (QO_2) and ATP levels were measured 24 hr following treatment with SRT1720 and/or TBHP. QO_2 was measured using a Clark oxygen electrode as previously described (205). ATP content was measured using an ATP bioluminescent assay kit (BioMol) as previously described and normalized to cellular protein (220).

Statistical Analysis—Data are presented as means +/- SEM and were subjected to one-way ANOVA. Multiple means were compared post-hoc using Student-Newman-Keuls test were considered statistically different when $p<0.05$. RPTC isolated from a single rabbit represented an individual experiment ($n=1$) and were repeated until an n of at least 6 was obtained.

RESULTS

SRT1720 was reported to activate SIRT1 (85, 178), and because SIRT1 activation can increase PGC-1α activity and mitochondrial functioning, we conducted a series of experiments to determine if SRT1720 mediates mitochondrial biogenesis in primary cultures of RPTC, and if so, by what mechanism. To verify SRT1720 potency, a fluorescence-based SIRT1 activity assay kit measuring deacetylation of a peptide target was used to examine SIRT1 deacetylase activity when exposed to SRT1720. SRT1720 increased SIRT1 activity in a concentration-dependent manner with a 3-fold increase in SIRT1 at 1 and 3 μM SRT1720 and a 5-fold increase at 10 μM (Fig. 2-1).
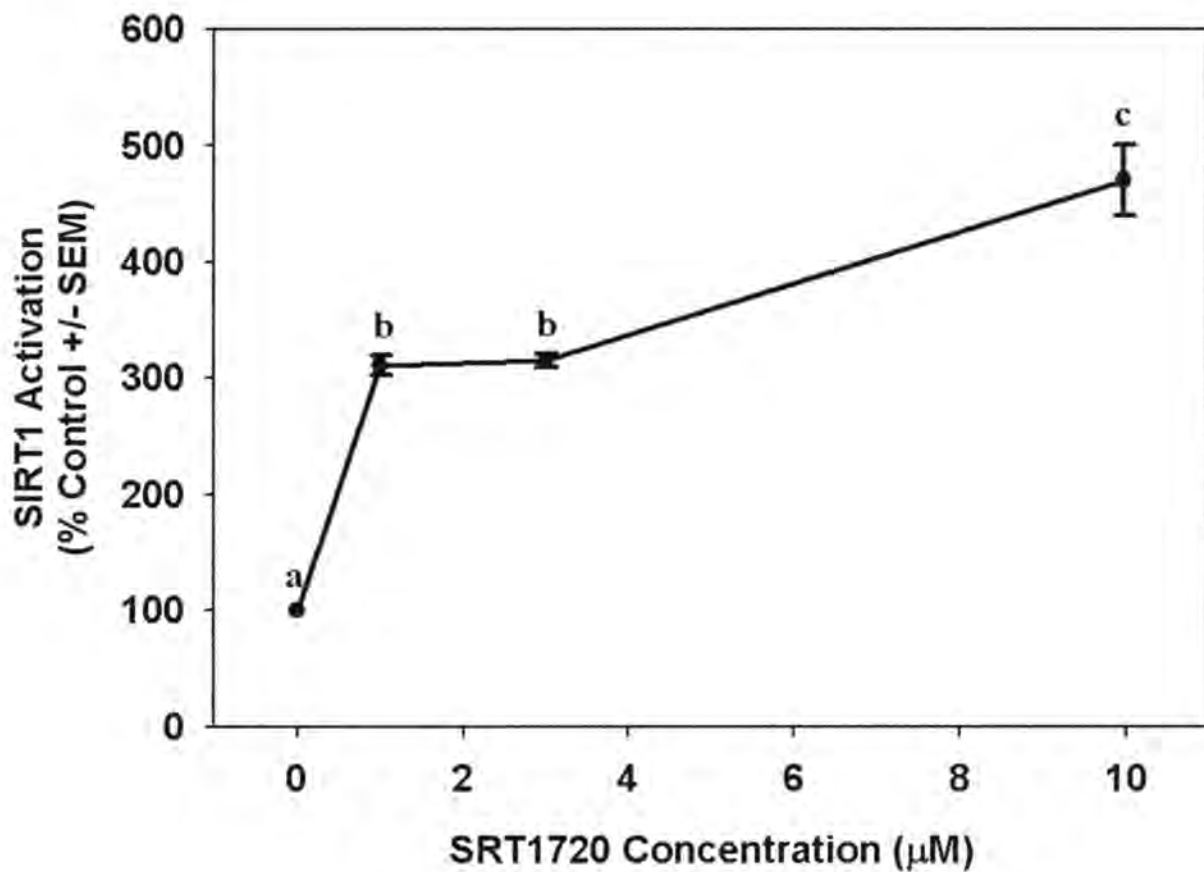
Figure 2-1. SRT1720 enhances SIRT1 deacetylase activity. Recombinant SIRT1 enzyme was incubated with acetylated peptide, NAD^+ and various concentrations of SRT1720. Increasing concentrations of SRT1720 corresponded with increased SIRT1 activity, which was measured indirectly from a fluorescent signal produced that was relative to levels of deacetylated product. Data are presented as mean % control +/- SEM. Different superscripts indicate data are significantly different from each other (p<0.05).

Because SIRT1 can modulate PGC-1α expression and/or activity by deacetylation (196, 229), we assessed the expression and acetylation state of PGC-1α in RPTC exposed to SRT1720 or vehicle for 24 hrs. Immunoblot analysis of nuclear lysates revealed elevated PGC-1α expression (Fig. 2-2a). To further examine nuclear PGC-1α content and acetylation state, PGC-1α protein was immunoprecipitated from nuclear lysates and subjected to immunoblot analysis with antibodies to acetylated lysine residues and PGC-1α (Fig. 2-2b). Time course analysis of acetylated PGC-1α consistently revealed reduced acetylation with 48 hr SRT1720 treatment with no differences at 24 hrs. Total PGC-1α levels in the immunoprecipitate were elevated at 24 and 48 hrs. The ratio of acetylated to total PGC-1α was decreased approximately 50% in SRT1720 cells at 24 hrs, indicating more active PGC-1α in the nucleus with SRT1720 treatment. We confirmed equal loading by measuring histone H3 in the supernatant from the immunoprecipitation experiments by immunoblot analysis (Fig. 2-2b).

Because active PGC-1α promotes transcription of the PGC-1 gene by an autoregulatory feedback loop (68), we examined transcript levels of PGC-1α by real-time PCR, but found no differences between vehicle and SRT1720-treated cells (Fig. 2-2c). Because modifications to PGC-1α may regulate degradation of the protein, we tested whether the increased expression of PGC-1α was due to decreased proteasomal degradation. We have previously characterized the degradation of PGC-1α in RPTC, and showed that it has a short half-life (37 min) (222). RPTC were treated with vehicle or SRT1720 for 24 hrs and then protein translation was inhibited with cycloheximide (100 μM) and samples taken 30 and 60 min later. Nuclear lysates were probed for PGC-1α expression by

immunoblot analysis. No changes in PGC-1α degradation were observed SRT1720 and vehicle treated RPTC (Fig. 2-2d). Taken together, these data provide evidence that SRT1720 treatment induced accumulation of deacetylated nuclear PGC-1α in RPTC that was not the result of either elevated PGC-1αtranscription at 24 hrs treatment or decreased proteasomal degradation.
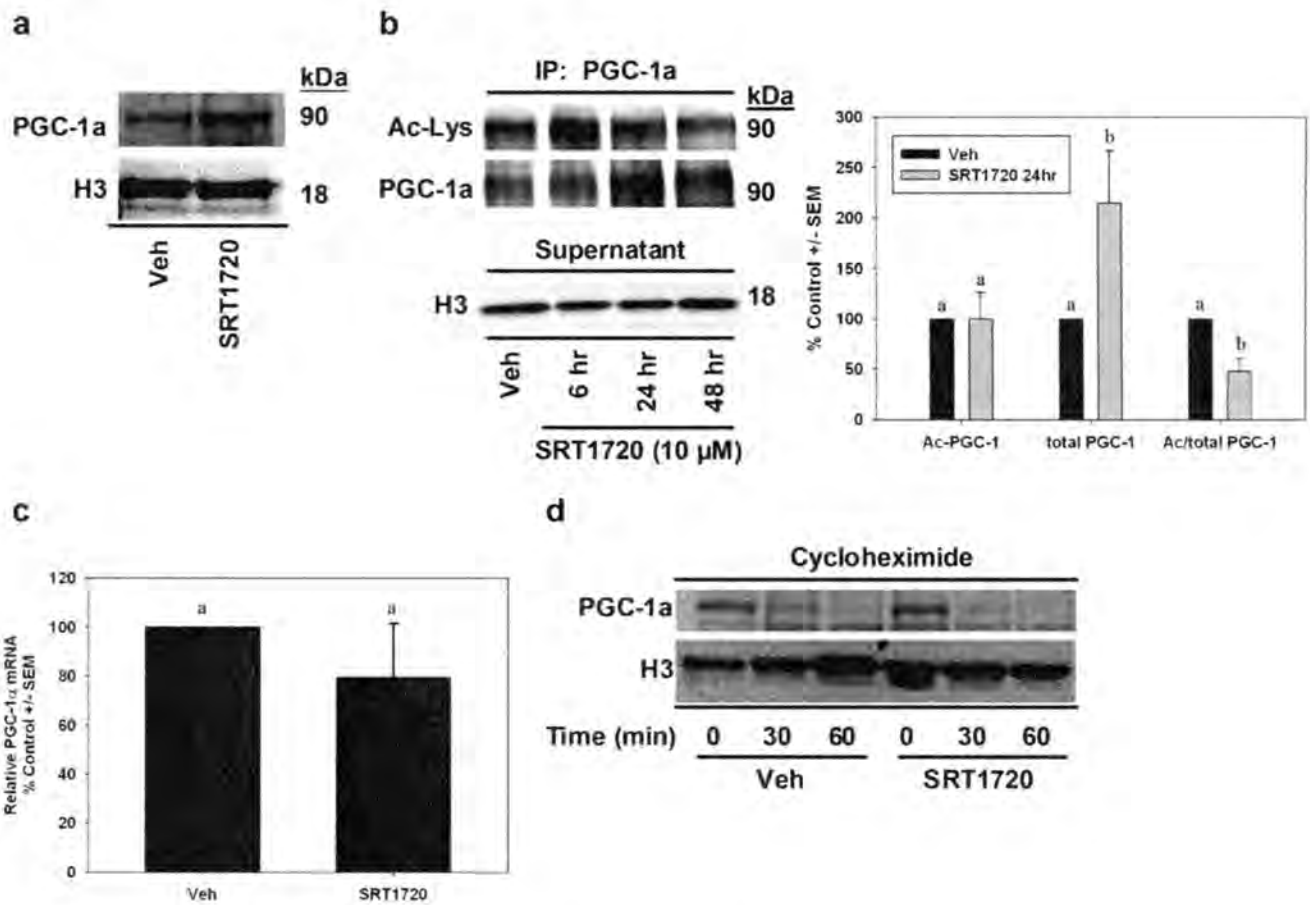
Figure 2-2. Nuclear deacetylated PGC-1α expression is elevated in SRT1720-treated cells. *a*, Nuclear lysates were fractionated from vehicle and SRT1720-treated cells and PGC-1 expression was assessed by immunoblot analysis. Histone H3 expression verified equal protein input within sample groups. *b*, The acetylation state of PGC-1α was examined in nuclear lysates by immunoprecipitating PGC-1α followed by immunoblot analysis of acetylated lysine residues and PGC-1α. Because SRT1720 lysates contained more PGC-1α, supernatants from immunoprecipitations were subjected to Histone H3 immunoblot analysis for input control. *c*, PGC-1α mRNA expression in SRT1720 and vehicle cells was determined by real-time PCR using primers designed to measure PGC-1α transcripts and GAPDH as internal control. *d*, PGC-1α degradation was examined in SRT1720 cells by extracting nuclear protein at 0, 30, and 60 min following cycloheximide exposure and immunoblotting for PGC-1α expression. Histone H3 expression verified protein input. Data are presented as mean % control +/- SEM. Different superscripts indicate data are significantly different from each other (p<0.05).

Mitochondrial biogenesis was determined by assessing mitochondrial DNA copy number, expression of mitochondrial proteins, and mitochondrial function after 24 hrs of SRT1720 treatment. Relative mitochondrial DNA copy number was determined using quantitative real-time PCR to examine the ratio of a select mitochondrial-encoded gene over nuclear DNA in SRT1720 and vehicle-treated cells (Fig. 2-3a). There was a 3.5-fold increase in mitochondrial-encoded NADH dehydrogenase subunit 6 (ND6) DNA in SRT1720 cells compared to controls. Nuclear-encoded Pou5f1 was used for normalization.

Secondly, the effect of SRT1720 treatment on mitochondrial protein levels was explored. SRT1720 (10 μM) elevated ATP Synthase β, a nuclear-encoded protein within the F_1 subunit of the ATP synthase, 1.5-fold over controls (Fig. 2-3b). NDUFB8, a nuclear-encoded complex I subunit, also was elevated approximately 1.5-fold over control by SRT1720.

Mitochondrial function was determined by measuring cellular respiration and ATP levels in RPTC. Compared to controls, basal respiration was elevated approximately 1.5-fold with 3 or 10 μM treatments at 24 hrs (Fig. 2-3c). Uncoupled respiration was elevated approximately 1.5-fold at the same concentrations. Finally, ATP levels were also elevated (1.8-fold) over vehicle controls (Fig. 2-3c). Taken together, the elevations in mitochondrial DNA, proteins, and functional capacity provide strong evidence that mitochondrial biogenesis occurs in RPTC with SRT1720 treatment.
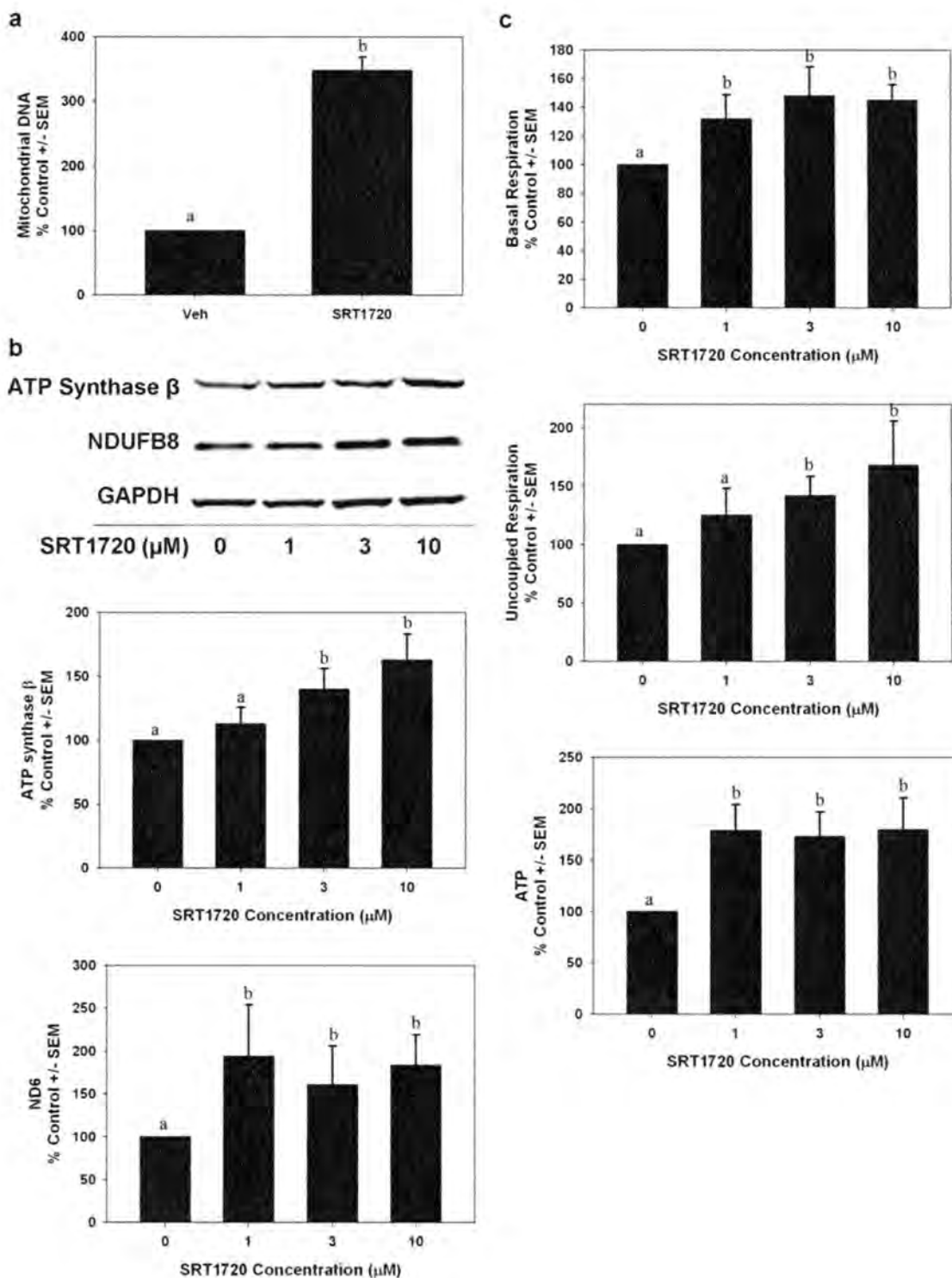
Figure 2-3. SRT1720 induces mitochondrial biogenesis in RPTC within 24 hrs.
a, Mitochondrial DNA copy numbers were assessed by real-time PCR. DNA isolated from RPTC treated with vehicle or 10 µM SRT1720 was analyzed by real-time PCR for relative quantities of the mitochondrial gene ND6 and the nuclear gene Pou5f1. *b*, Mitochondrial proteins ATP Synthase β and NDUFB8 were measured by immunoblot analysis in cells treated with 1, 3, or 10 uM SRT1720. GAPDH immunoblots were performed to verify equal protein input. *c*, Mitochondrial function was assessed in vehicle and SRT1720-treated cells. Basal and FCCP-uncoupled respiration and ATP levels were measured in RPTC treated with 1, 3, or 10 uM SRT1720. Total protein was measured by BCA and used for normalization of data. Data are presented as mean % control +/- SEM. Different superscripts indicate data are significantly different from each other (p<0.05).

71

To verify that the RPTC mitochondrial biogenesis produced by SRT1720 is dependent on SIRT1 activation, pharmacologic inhibitors were used to block SIRT1 activity prior to SRT1720 exposure, and then mitochondrial DNA content and function were analyzed. SRT1720 treatment elevated mitochondrial DNA content compared to vehicle treated cells, whereas cells exposed to SRT1720 in the presence of the SIRT1 inhibitor nicotinamide (NAM, 100 µM) did not show any changes in mitochondrial DNA (Fig. 2-4a). Additionally, RPTC exposed to SRT1720 for 24 hrs demonstrated elevations in ATP levels compared to vehicle cells (Fig. 2-4b). Pretreatment of RPTC with the synthetic SIRT1 inhibitor sirtinol (100 µM) or NAM prevented the SRT1720-mediated increased ATP levels at 24 hrs. The data from these experiments verify that SIRT1 is required for SRT1720-induced mitochondrial biogenesis.
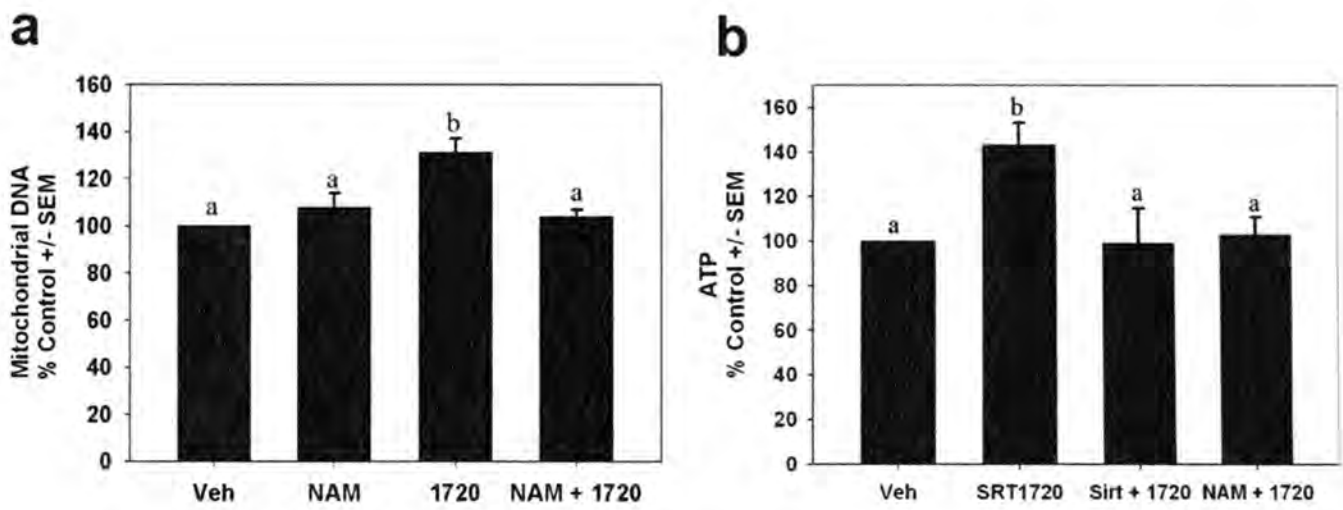
Figure 2-4. SRT1720-induced mitochondrial biogenesis is SIRT1-dependent. *a*, RPTC were treated with 10 μM SRT1720 alone or in the presence of the SIRT1 inhibitor nicotinamide (100 μM NAM) for 1 hr prior to SRT1720 addition. Mitochondrial DNA levels were analyzed by real-time PCR for the mitochondrial gene ND6. The nuclear encoded gene Pou5f1 was used for normalization. *b*, RPTC were treated with SRT1720 alone or in combination with the SIRT1 inhibitors nicotinamide or sirtinol. ATP levels were measured 24 hrs after SRT1720 addition. Total protein was measured by BCA and used for normalization. Data are presented as mean % control +/- SEM. Different superscripts indicate data are significantly different from each other (p<0.05).

AMPK, a primary energy regulator, monitors AMP/ATP levels and activates energy-producing mechanisms when this ratio is elevated (118). AMPK regulates energy supply by directly phosphorylating modulators of metabolic pathways, including PGC-1α (138). Indeed, PGC-1α has at least two sites available for AMPK-mediated phosphorylation, and activators of SIRT1, such as resveratrol, can also induce activation of AMPK (319). To determine if SRT1720 also induces AMPK activation, RPTC were treated for 1 hr and 24 hr with SRT1720 or vehicle and activation of AMPK was detected by immunoblotting for phosphorylated AMPK (Thr172). AICAR and metformin were used concurrently as positive controls for AMPK activation. At both 1 hr and 24 hr, there was no effect on pAMPK levels by SRT1720, whereas a significant induction was observed with metformin treatment at both time points (Fig. 2-5). Contrary to previous reports in other systems (319), we did not observe any changes in pAMPK with AICAR treatment. Total AMPK levels did not change with any treatment. These data provide evidence that SRT1720 acts through SIRT1 activation and not concurrent activation of AMPK.
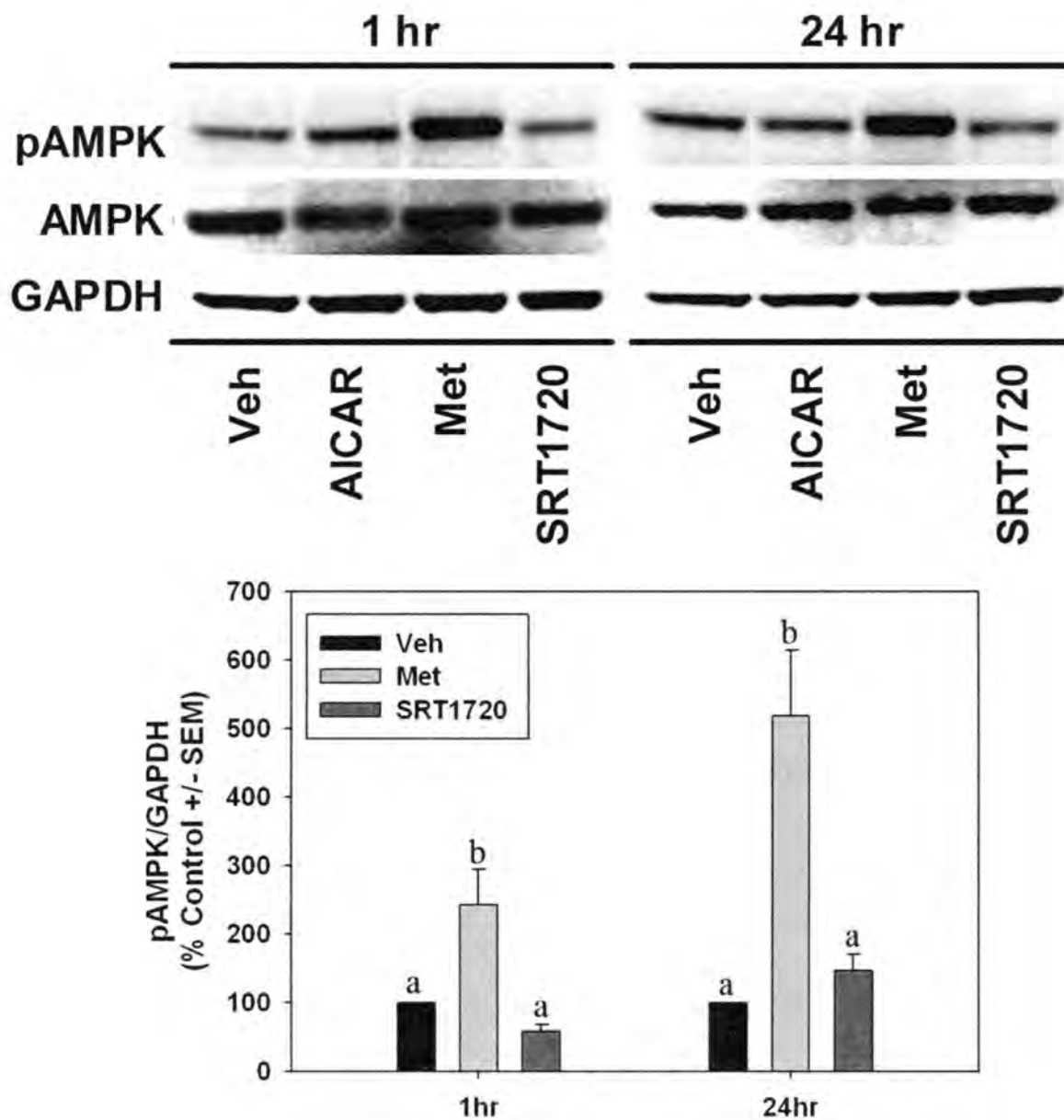
Figure 2-5. SRT1720 does not activate AMP-dependent kinase (AMPK). RPTC treated with 10 µM SRT1720 or vehicle for 1 or 24 hrs were subjected to immunoblot analysis using antibodies to detect phosphorylated AMPK (Thr172), total AMPK, and GAPDH. The known AMPK activators AICAR (500 µM) and metformin (1 mM) were used as positive controls for pAMPK antibody. GAPDH expression was analyzed for load control. Different superscripts indicate data are significantly different from each other ($p<0.05$).

Because PGC-1α and mitochondrial biogenesis have a pivotal role in the recovery of RPTC from oxidant-induced mitochondrial dysfunction (220-221), we tested the hypothesis that pharmacological activation of mitochondrial biogenesis following injury would expedite recovery of mitochondrial functions in RPTC. RPTC were incubated with 400 μM tert-butyl hydroperoxide (TBHP) to induce oxidant injury. At 6 hr post-injury, RPTC were treated with SRT1720 to stimulate mitochondrial biogenesis. At 24 hrs, mitochondrial function and cell morphology of injured RPTC treated with SRT1720 or vehicle were examined. Uncoupled respiration and ATP levels were approximately 60% of control in TBHP-injured RPTC at 24 hr (Fig. 2-6). In contrast, injured cells treated with SRT1720 demonstrated partial recovery of uncoupled respiration and full recovery of ATP levels 24 hrs post-injury (Fig. 2-6).
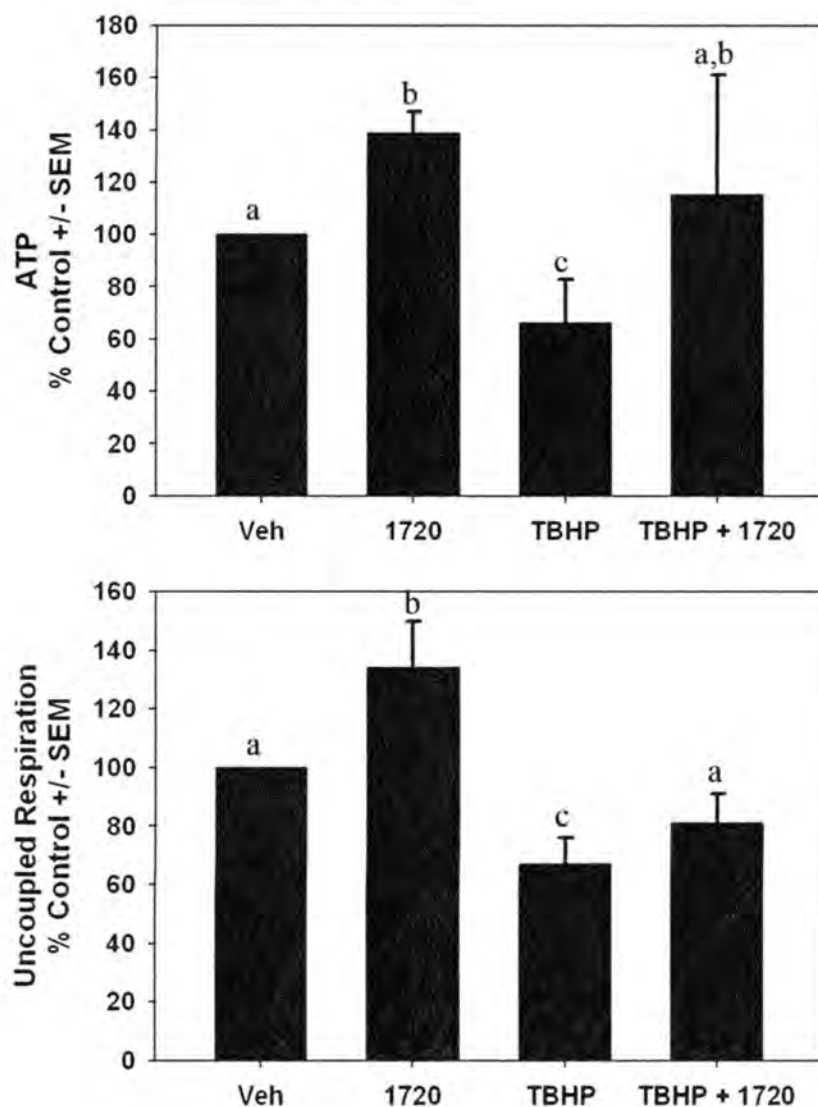
Figure 2-6. Mitochondrial function is rescued in SRT1720-treated cells following oxidant injury. RPTC injured with the oxidant *tert*butyl hydroperoxide (TBHP) were treated with 10 μM SRT1720 or an equal volume of DMSO 6 hrs after injury and ATP levels and FCCP-uncoupled respiration were measured 24 hrs post-injury. Total protein was measured by BCA for data normalization. Data are presented as mean % control +/- SEM. Different superscripts indicate data are significantly different from each other (p<0.05).

Correlating with partial recovery of mitochondrial functions, recovery of RPTC morphology was observed in injured cells treated with SRT1720. Six hours after TBHP exposure, the injury was characterized by a loss of approximately 50% of cells as visualized by denuded areas of the dish as cells had sloughed off the plate surface, as well as a generalized shrinkage and rounding of adherent cells. RPTC treated with SRT1720 for 24 hrs following injury reverted to a pre-injury state characterized by reorganization and migration of surviving cells returning to a confluent monolayer and dome formation indicative of polarized RPTC (Fig. 2-7). This recovery was not as apparent in vehicle-treated injured cells. The data from these experiments indicate that SIRT1 activation can reverse oxidant-induced mitochondrial dysfunction, and recovery of mitochondrial numbers and function may aid in recovery of RPTC morphology following acute injury.

Figure 2-7. RPTC morphology is partially recovered in cells treated with SRT1720 following TBHP toxicity. RPTC exposed to 400 µM TBHP were treated with 10 µM SRT1720 or DMSO 6 hrs after injury and then examined by light microscopy (10 X magnification) for changes in cell morphology at 24 hrs post-injury.
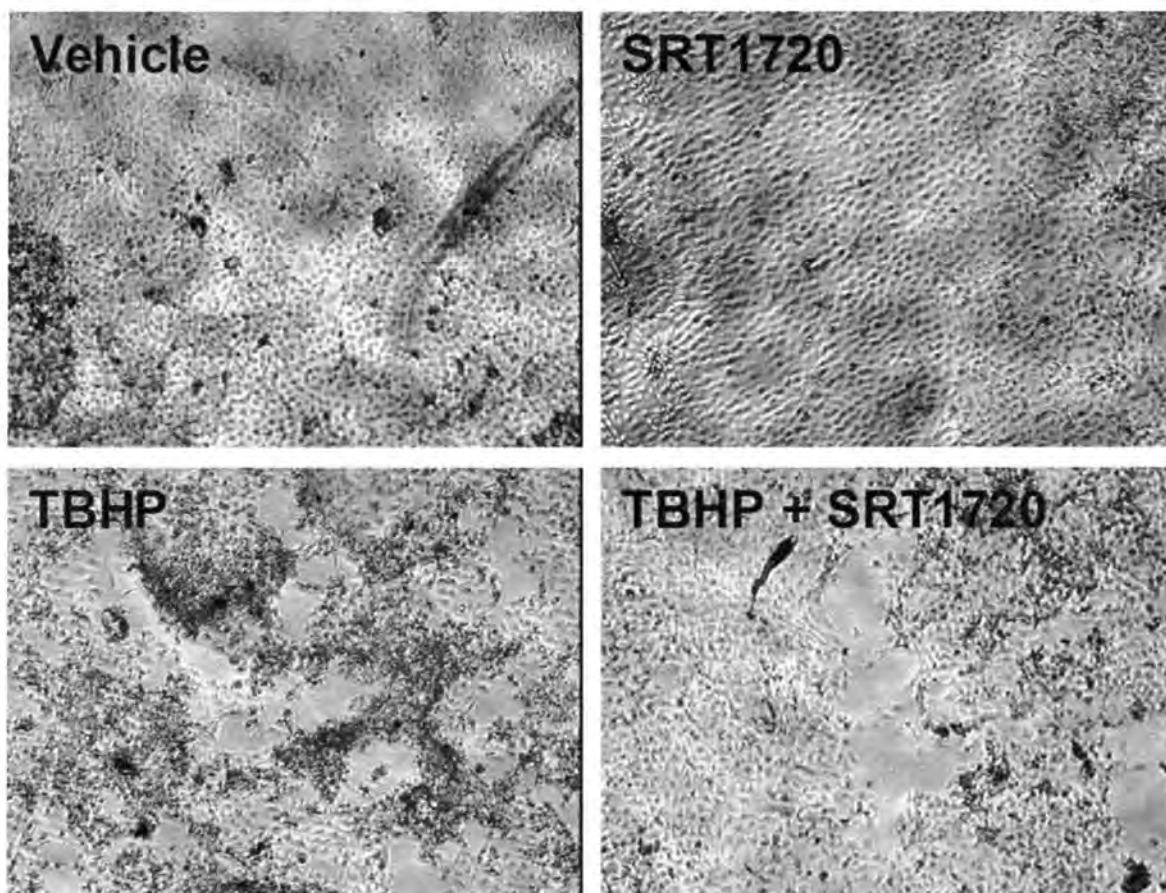
DISCUSSION

Mitochondrial dysfunction is a common mechanism in the etiology of organ injuries and diseases characterized by metabolic insufficiency. Mitochondrial health is essential for cell and organ function due to their role in ATP production, fatty acid and lipid metabolism, signaling pathways, and apoptosis. Despite potential for treating disorders characterized by mitochondrial impairment, very few therapies target the mitochondria to promote its function. In this study we demonstrated that pharmacologically-induced mitochondrial biogenesis enhanced mitochondrial function in RPTC and restored function following an acute injury.

SRT1720 stimulated mitochondrial biogenesis in RPTC within 24 hrs of exposure. Elevated levels of mitochondrial DNA, proteins, and function were observed with 10 μM treatment. The findings agree with results we have previously published linking isoflavone-induced mitochondrial biogenesis with SIRT1 activation (223), as well as others who have demonstrated mitochondrial biogenesis with resveratrol in other cell types (67, 160). The pharmacological advantage of SRT1720 over isoflavones is that SRT1720 produces mitochondrial biogenesis within 24 hrs, a key requirement if targeting acute organ injury.

While SRT1720 was previously reported as a SIRT1 activator, its mechanism of mitochondrial biogenesis in a cellular system is incomplete. Previous studies examining SRT1720-induced mitochondrial biogenesis have based their interpretations primarily on indirect mitochondrial measurements, such as respiration and ATP levels and ETC

activity, predominantly in skeletal muscle cell lines (85, 251). In this study, we sought to explore SRT1720-induced mitochondrial biogenesis in primary kidney cell cultures, which better mimic the metabolic properties of renal cells *in vivo*, not only by examining alterations in functional output, but also by examining direct measurements of mitochondrial protein and DNA expression. When primary RPTC cultures were incubated with SRT1720, mitochondrial proteins NDUFB8 and ATP synthase β, and mitochondrial DNA copy numbers were elevated compared to vehicle-treated cells (Fig. 3), indicating mitochondrial biogenesis occurred within 24 hrs. Furthermore, we confirmed that elevations in mitochondrial components corresponded with increased mitochondrial output by examining cellular respiration and ATP production. Finally, we verified that the observed effects of SRT1720 were dependent on SIRT1 activity by using pharmacologic inhibitors of SIRT1 (Fig. 4), similar to what has been shown previously in other cell types using SIRT1 shRNA (85).

SIRT1 activation results in deacetylation of target proteins, and several substrates have been identified, including PGC-1α. SRT1720 elevated expression of deacetylated nuclear PGC-1α at 24 hrs in RPTC (Fig. 2a and 2b). The elevated expression was neither the result of increased PGC-1 transcription, as we did not observe any changes in PGC-1α mRNA expression (Fig. 2c), nor an increased resistance to proteasomal targeted degradation (Fig 2d). When SRT1720-treated cells were exposed to the inhibitor of protein translation cycloheximide, nuclear PGC-1α degraded at the same rate as vehicle cells, indicating the protein is still susceptible to proteasomal degradation (222, 236). Taken together, these data indicate that SRT1720 did not induce PGC-1α transcription or

increase stability of the protein. However, it is possible that the increased expression of nuclear PGC-1α may have been the result of an earlier transcriptional event that was missed by examining the 24 hr time point or may be the result of increased nuclear sequestration.

We did not observe any activation of AMPK with SRT1720 as examined by immunoblotting for Thr172-phosphorylated AMPK or in total AMPK (Fig. 5), which is consistent with previous reports that this compound exerts its effects in an AMPK-independent mechanism (85). Interestingly, metformin induced a robust phosphorylation of AMPK within 1 hr of treatment which was maintained for at least 24 hrs. In contrast AICAR, which has previously been shown to induce phosphorylation of AMPK in other cell types (319), did not have any effect on pAMPK expression after 1 or 24 hr treatment in RPTC. We have not explored the reason for the differential effects of AICAR in RPTC and other cell types

PGC-1α is an emerging therapeutic target for mitochondrial abnormalities due to its regulatory role in controlling metabolic processes and mitochondrial activities and biogenesis within the cell. Enhancing PGC-1α expression or activity has proven effective in reversing the phenotypic consequences of mitochondrial impairment. Mitochondrial myopathies can be rescued through transgenic expression of PGC-1α or the pharmacologic PPAR pan-agonist bezafibrate, both of which induce mitochondrial biogenesis, enhance respiratory capacity, conserve ATP levels, and prolong lifespan (299). Pharmacological stimulation or adenoviral upregulation of PGC-1α rescued

mitochondrial function and bioenergetics and restored insulin signaling in insulin-resistant skeletal muscle cells (209). Finally, the benefits of exercise and caloric restriction to rescue or protect against metabolic deficiencies has been linked to enhanced PGC-1α activity (27, 155).

Recent evidence indicates that induction of PGC-1α and mitochondrial biogenesis is a critical adaptive response to maintain energy levels and metabolic demands required during recovery from certain acute injuries to cells and organs (220, 294, 310). In response to partial hepactectomy, C/EBPβ transcriptionally induces PGC-1α in order to maintain metabolic homeostasis and energy demands of the regenerating liver (294). In response to oxidant-induced mitochondrial dysfunction in RPTC, induction of PGC-1α and mitochondrial biogenesis is an adaptive repair mechanism initiated by the cell, which can be stimulated by PGC-1α over-expression (220-221). Here, we show that pharmacologically-induced mitochondrial biogenesis also rescues mitochondrial functions following oxidant-induced injury. Within 24 hrs SRT1720 reversed mitochondrial dysfunction and ATP depletion resulting from TBHP toxicity (Fig. 6).

Although the majority of studies investigating PGC-1α-mediated mitochondrial regulation through AMPK or SIRT1 are focusing on its role in chronic or age-related metabolic deficiencies (106, 179), this pathway offers a unique target for the treatment of acute organ injuries that are also plagued by mitochondrial impairment. As observed in this study as well as previous reports (220-221), mitochondrial biogenesis has a pivotal role in recovery of critical mitochondrial functions in oxidant-injured renal cells. Acute

organ injuries, such as ischemic acute kidney injury (AKI), are characterized by de-energization of the mitochondria as well as loss of mitochondrial proteins and depletion of cellular energy stores (29, 86, 297), which could exacerbate cell death and organ failure or limit energy-dependent repair processes if mitochondrial function is not restored. These studies provide evidentiary basis to study the involvement of mitochondrial repair processes in the recovery from organ injuries such as AKI, and highlights the therapeutic potential of pharmacological inducers of mitochondrial biogenesis to rescue mitochondrial function in injuries and disorders plagued by mitochondrial impairment.

CHAPTER 3:

Persistent Disruption of Mitochondrial Homeostasis after Acute Kidney Injury

ABSTRACT

While mitochondrial dysfunction is a pathological process that occurs after acute kidney injury (AKI), the state of mitochondrial homeostasis during the injury and recovery phases of AKI remains unclear. We examined markers of mitochondrial homeostasis in two non-lethal rodent AKI models. Myoglobinuric AKI was induced by glycerol injection into rats, and mice were subjected to ischemic AKI. Animals in both models had elevated serum creatinine 24 h after injury which recovered between 24 h and 144 h. Markers of proximal tubule function/injury, including NGAL and urine glucose, did not recover during this same period. The persistent pathological state was confirmed by sustained caspase 3 cleavage and evidence of tubule dilation and brush border damage. Respiratory proteins NDUFB8, ATP synthase β (ATPβ), cytochrome c oxidase subunit I (COX I), and COX IV were decreased in both injury models and did not recover by 144 h. Immunohistochemical analysis confirmed that COX IV protein was progressively lost in proximal tubules of the kidney cortex after I/R. Expression of mitochondrial fission protein Drp1 was elevated after injury in both models, whereas the fusion protein Mfn2 was elevated after glycerol injury but decreased after I/R AKI. LC3-I/II expression revealed that autophagy increased in both injury models at the later time points. Markers of mitochondrial biogenesis, such as PGC-1α and PRC, were elevated in both models.

These findings reveal that there is persistent disruption of mitochondrial homeostasis and sustained tubular damage after AKI, even in the presence of mitochondrial recovery signals and improved glomerular filtration.

INTRODUCTION

Acute kidney injury (AKI) is an increasingly prevalent, complex clinical disorder. Intrinsic AKI, produced from direct damage to the kidney, may arise in a number of ways, including drug/toxicant exposure or ischemia (46, 60, 273). Although numerous mechanisms of AKI are observed clinically and in experimental models, it is generally recognized as a multi-factorial injury with overlapping elements as opposed to a single-component injury.

Renal ischemia/reperfusion (I/R) is a common cause of AKI. An ischemic insult occurs when there is reduced blood flow to the kidney and may occur after drug or toxicant exposure, vascular diseases, sepsis, or blood volume depletion and hypotension (29, 273). The pathophysiology of ischemic AKI is comprised of both microvascular and tubular components. The microvascular injury is characterized by increased vasoconstriction and decreased vasodilation, endothelial and smooth muscle cell damage, and leukocyte infiltration (29, 59, 252).

Rhabdomyolysis is a condition in which heme proteins, released in the form of myoglobin from muscle cells or hemoglobin from erythrocytes, produce secondary organ toxicity, predominantly AKI (36, 195). Although the mechanism of myoglobinuric-induced AKI is not entirely known, a number of factors including ischemic injury resulting from vasoconstriction and blood volume depletion as blood pools at the site of muscle injury, direct tubule toxicity from iron influx and hydroxyl radical formation, and tubular obstruction contribute to the disease process (36, 215-216).

Subcellular injury to the tubular epithelium is a primary component of AKI, and although

different injuries may manifest by particular mechanisms, common pathogenic elements

are observed in multiple injury models. Mitochondrial damage is a major contributor to

the lethal and sublethal tubular cell injury observed in the disease progression of AKI

(86, 112, 139-140, 297). Increased production of ROS and NO, formed prominently

within the mitochondria, as well as compromised antioxidant mechanisms following

ischemic periods make the mitochondria particularly susceptible (215-216, 249, 317).

Additionally, elevations in intracellular and mitochondrial Ca^{2+} and Fe^{3+} may contribute

to the central role of the mitochondria in the disease process (65, 140). Subsequent

disruption of mitochondrial respiratory complexes, membrane depolarization, ATP

depletion, lipid peroxidation, membrane permeabilization and release of apoptotic

proteins contribute to mitochondrial and cellular injury (28-29, 36, 112).

The dynamic nature of mitochondria lends to dramatic alterations in structural integrity

and population following acute toxic challenge. Mitochondrial fragmentation has been

observed in models of AKI, and this process contributes to the resulting injury (39).

However, the role of mitochondrial fission and fusion following initial injury and during

the recovery and maintenance phase is still not completely understood. Mitochondrial

biogenesis is initiated after acute organ injuries (227, 310), including cellular models of

AKI (220). There is an immediate induction of the transcriptional co-activator

peroxisome proliferator-activated receptor gamma co-activator 1-alpha (PGC-1α) in

experimental models of stroke, liver damage, heart failure, and neuromuscular disorders

in response to the increased energy demand in such tissues (227, 294, 299, 310). PGC-1α is a primary regulator of mitochondrial biogenesis and is known to associate with transcription factors responsible for mitochondrial gene expression, including the nuclear respiratory factors (NRFs) and mitochondrial transcription factor A (Tfam) (308). There is significantly less known about other members of the PGC-1 family, PGC-1β and PGC-1 related co-activator (PRC), in acute injury models or in mitochondrial biogenesis, and the role of mitochondrial biogenesis during the acute injury phase and throughout sustained injury and recovery has not been fully established.

In this study we asked how mitochondria would initially respond to an acute injury to the kidney and during recovery of function. There is evidence that the health of this organelle is a critical determinant in both injury progression and recovery in AKI, and there is a need to obtain a more complete understanding of mitochondria in this type of injury. We assessed several mitochondrial parameters in two rodent AKI models, examined expression of respiratory proteins, fission and fusion processes, autophagy, and determined mitochondrial biogenesis at initiation of injury and throughout recovery of renal function.

EXPERIMENTAL PROCEDURES

Glycerol model of myoglobinuric AKI

Male Sprague-Dawley rats, 180-200g, were injected with an equally divided hypertonic glycerol solution (50% glycerol/H_2O, 10mL/kg, i.m.) into the muscle of each hind limb as previously described (313). Renal function was monitored as described below starting at 24 h post-injection until rats were euthanized at 24, 72, or 144 h after injections, at which time kidneys were harvested and snap-frozen for molecular analysis. All procedures involving animals were performed with approval from the Institutional Animal Care and Use Committee (IACUC) in accordance with the NIH Guide for the Care and Use of Laboratory Animals.

Ischemia/reperfusion model of AKI

8-week old male C57BL6 mice weighing 25-30g were subjected to bilateral renal pedicle ligation as described previously (323). Briefly, renal artery and vein were isolated and blood flow was occluded with a vascular clamp for 20m, and mice were euthanized at 24, 72, or 144hr after procedure, at which time kidneys were harvested for molecular analysis. All procedures involving animals were performed with approval from the Institutional Animal Care and Use Committee (IACUC) in accordance with the NIH Guide for the Care and Use of Laboratory Animals.

Assessing renal function

Tail vein blood was collected from rats at various time points after glycerol injection, and serum was used to measure serum creatinine levels. For mice, blood was collected by

retro-orbital eye bleed. Creatinine levels were measured using a Quantichrom™ Creatinine Assay Kit (BioAssay Systems, Hayward, CA) according to manufacturer's protocol. Urine was collected from rats housed in metabolic cages overnight (16 hrs) at various time points throughout the study. Urine samples were used to determine creatinine levels (Quantichrom Creatinine Assay Kit, BioAssay Sytems), glucose (Quantichrom Glucose Assay Kit, BioAssay Systems), and neutrophil gelatinase-associated lipocalin (NGAL) levels (NGAL ELISA Kit, BioPorto) according to manufacturers' instructions.

Immunoblot analysis

Renal cortical tissue was lysed in RIPA buffer containing cocktail protease and phosphatase inhibitors. Total protein content was measured by the BCA assay. Fifty µg total protein was loaded into SDS-PAGE gels and immunoblots were performed as previously described (220).

mRNA analysis

Total RNA was isolated renal cortical tissue with TRIzol (Invitrogen) according to manufacturer's protocol and cDNA synthesized using RevertAid First Strand cDNA Synthesis Kit (Fermentas). PCR reactions were performed using 3uL diluted cDNA product as described previously (90). Primer sets used for PCR are listed in Table 1.

Immunohistochemistry

Paraffin-embedded sections were cleared in xylenes, and then rehydrated in a graded ethanol wash. Antigen unmasking was performed by boiling sections in citrate buffer for 10 min followed by cooling at room temperature for 30 min. Endogenous peroxidase activity was quenched by incubating sections in 3% H_2O_2 for 10 min. Sections were then blocked in 10% normal goat serum for 1 hr, followed by COX IV (Abcam, 1:700 dilution) antibody incubation for 1 hr. Sections were then incubated in biotinylated anti-rabbit secondary antibody for 30 min followed by HRP-linked avidin-biotin complex reagent (Vectastain) for 30 min. Finally, antibody detection was visualized by DAB peroxidase substrate developer (Vectastain), counterstained with hematoxylin, mounted and coverslipped. Images were acquired with a Nikon microscope under control of QCapture imaging software. Low magnification images are at 10X and high magnification images were captured at 40X.

ATP measurement

Renal cortical tissue ATP was measured as previously described (290, 299). ATP was extracted from flash frozen kidney cortex with 0.4 M $HClO_4$, and ATP levels were determined using an ATP bioluminescence assay kit (Roche) and normalized to protein concentration.

Statistical analysis

Graphs represent a sample size of 3 to 6 for each group. Data were analyzed by ANOVA based on ranks followed by the Mann-Whitney rank-sum test for individual group comparisons of non-parametric data.

RESULTS

Rats exposed to intramuscular injection of glycerol exhibited kidney injury within 24 h as determined by an increase in serum creatinine (SCr) levels (Fig 3-1A). At time of injection (t=0 h), control and glycerol rats had similar SCr levels. SCr in glycerol-treated rats increased ~4-fold at 24 h, and then gradually decreased at 72 and 144 h without reaching control levels.

Although SCr measurements demonstrated functional recovery between 24 and 144 h after glycerol treatment, urinary measurements reveal sustained renal injury. Urinary creatinine (UCr) concentrations were reduced 85% at 48 h after glycerol injection, and remained decreased at 144 h after injury (Fig 3-1B). Because glucose is freely filtered by the glomerulus and nearly 100% reabsorbed in the proximal tubule (305), urinary glucose is a marker of proximal tubular function. Urine glucose levels increased ~6-fold at 48 h and remained at this level at 144 h after glycerol injection (Fig 3-1C). Neutrophil gelatinase-associated lipocalin (NGAL) is expressed in low abundance in proximal tubular cells, and is upregulated and excreted into the urine after injury, and is now used as a biomarker of AKI (182). NGAL increased 40-fold at 48 h and remained elevated at 144 hr following glycerol injection (Fig 3-1D). Overall, these results reveal partial recovery of glomerular function (e.g. glomerular filtration) following AKI, but persistent proximal tubular dysfunction.
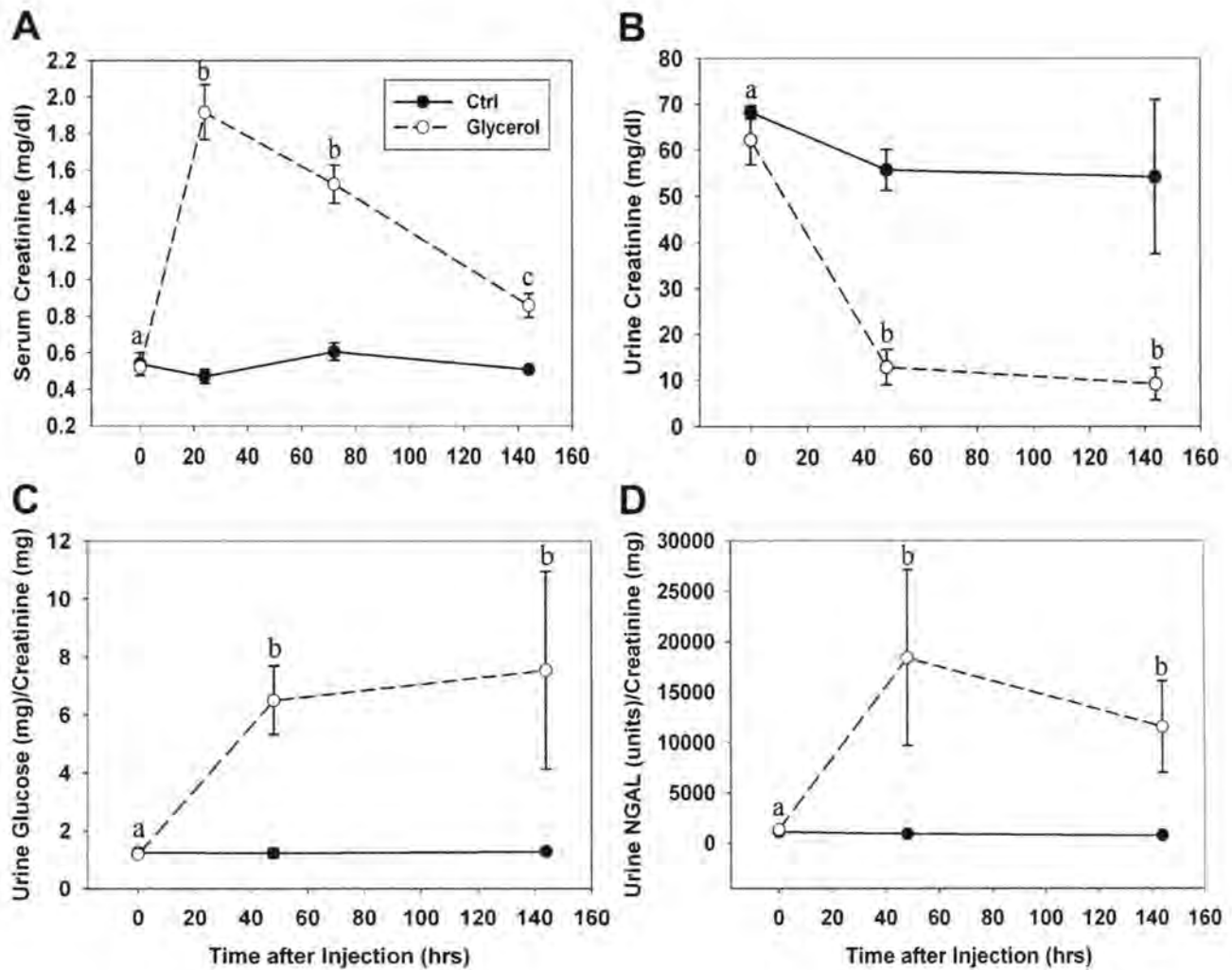
Figure 3-1. Renal dysfunction after glycerol-induced myoglobinuria. *A*: serum creatinine was maximal 24 h after injection and partially recovered between 24 and 144 h after injury without returning to normal levels. *B*: urine creatinine was reduced 48 h after injury and remained decreased at 144 h. Urine glucose (*C*) and neutrophil gelatinase-associated lipocalin (NGAL; *D*) were elevated 48 h after glycerol injection and remained elevated at 144 h. Different superscripts above data points are significantly different from one another ($P < 0.05$).

Apoptosis is known to be a primary mechanism of cell death in models of AKI. To evaluate apoptosis in our AKI models, we performed caspase-3 immunoblot analysis on renal cortical tissue collected at 24 h, 72 h, and 144 h after glycerol-induced AKI (Fig 3-2A). Cleaved-caspase 3 expression increased and remained elevated throughout the experimental period following glycerol injection, suggesting continued activation of apoptotic signaling. Additionally, histological evidence revealed persistent tubule dysfunction. Tissue structure was examined following Periodic acid-Schiff (PAS) staining, and revealed proximal tubule dilation and brush border damage at 24 h after glycerol that was sustained throughout the study (Fig 3-2B).
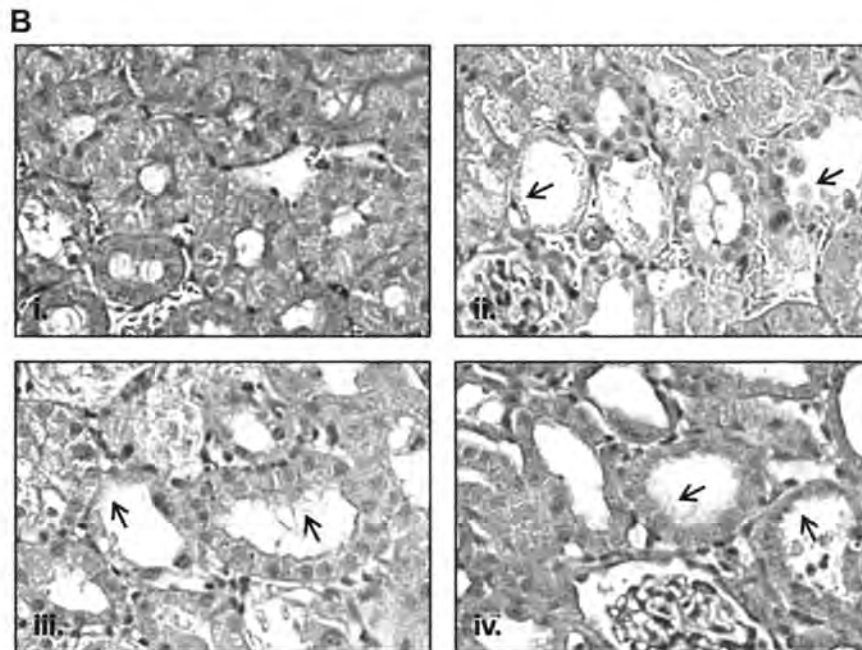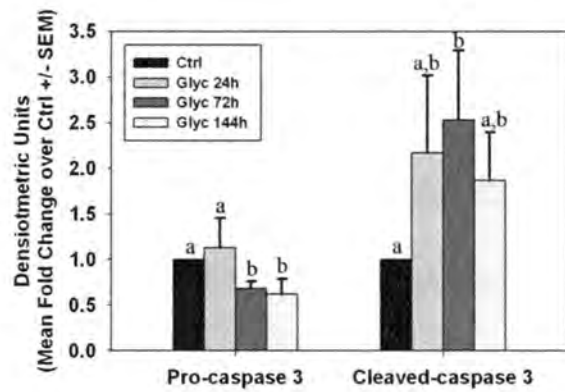
Figure 3-2. Persistent tubule pathology after glycerol-induced acute kidney injury (AKI). *A*: activation of caspase 3 was observed by the presence of a caspase 3 cleavage fragment at 24, 72, and 144 h after glycerol injection. Bars with different superscripts are significantly different from one another ($P < 0.05$). *B*: periodic acid-Schiff (PAS) staining in control rats (*i*) and 24 h (*ii*), 72 h (*iii*), or 144 h (*iv*) after glycerol injection at ×40 magnification. Arrowheads indicate dilated tubules and brush-border damage after injury.

Transcript and protein levels of several mitochondrial respiratory genes were examined over time after AKI in renal cortical lysates. After glycerol-induced AKI, mRNA for the mitochondrial-encoded genes NADH-ubiquinone oxidoreductase chain 6 (ND6) and cytochrome c oxidase subunit I (COX I) were decreased between 72-144 h after injection (Fig 3-3A). In contrast, mRNA expression for the nuclear-encoded mitochondrial protein NDUFB8 did not change at any time after injury, and expression of ATP synthase β increased 144 h after glycerol injection. Similar to mRNA levels, COX I protein decreased after injury, although this was seen much earlier than mRNA, and the decrease was maintained until 144 h post-injection (Fig 3-3B). In contrast to the results observed for NDUFB8 and ATP synthase β mRNA, protein levels for these were reduced early after injury and remained decreased throughout the study period.
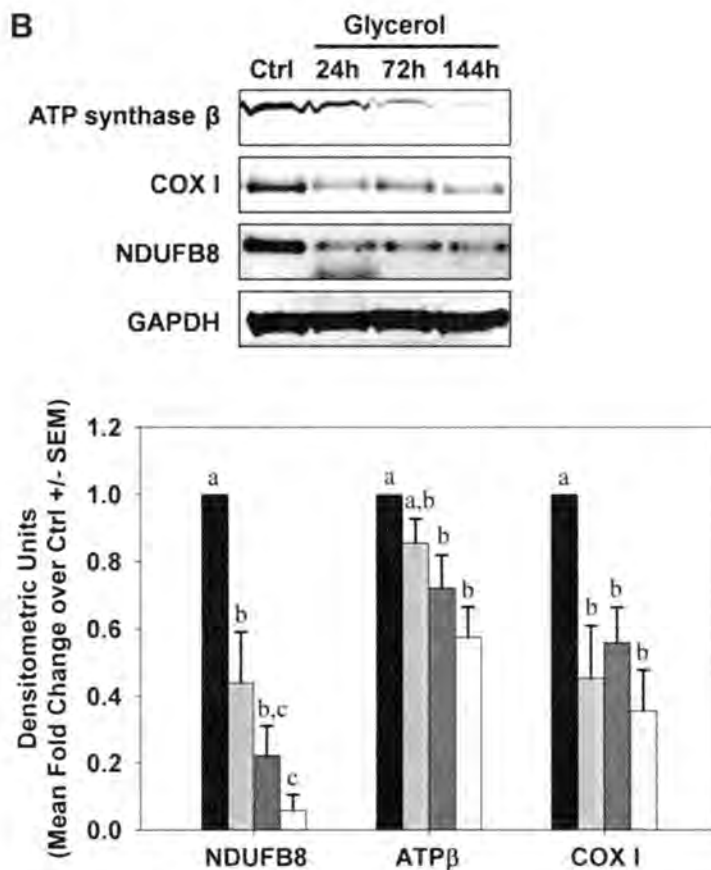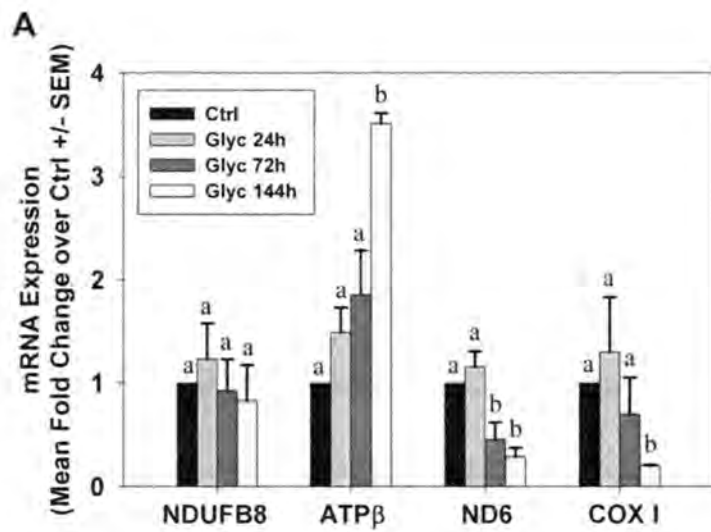
Figure 3-3. Sustained depletion of mitochondrial proteins after glycerol-mediated AKI. *A*: mRNA from control and glycerol rats was analyzed by qRT-PCR for expression of nuclear-encoded respiratory genes NDUFB8 and ATP synthase β and the mitochondrial-encoded genes ND6 and COX I at 24, 72, and 144 h after injury. *B*: expression of mitochondrial respiratory proteins from kidneys of control and glycerol rats was examined by immunoblot analysis. Bars with different superscripts are significantly different from one another ($P < 0.05$).

Because alterations in mitochondrial fission/fusion proteins can change in AKI models (39), we examined markers of fission/fusion over time in the glycerol model. Twenty-four hours after glycerol injection renal dynamin-related protein (Drp1) mRNA was elevated approximately 4-fold over control rats and remained at this level through 144 h (Fig 3-4A). Correspondingly, Drp1 protein levels were also elevated early and remained elevated through 144 h (Fig 3-4B). No changes were observed in mitofusin 2 (Mfn2) mRNA levels (Fig 3-4A); however, Mfn2 protein increased 24 h after injection and remained elevated until 144 h (Fig 3-4B).
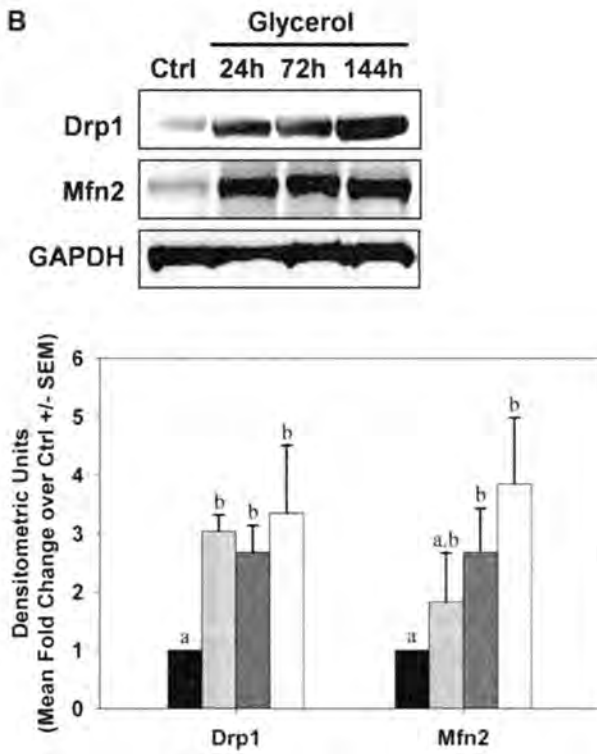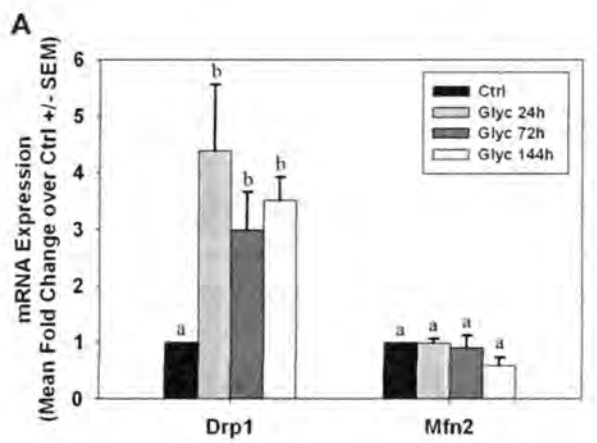
Figure 3-4. Alterations in mitochondrial fission and fusion proteins after glycerol-mediated AKI. mRNA (*A*) and protein (*B*) expressions from kidneys of control (Ctrl) and glycerol (Glyc) rats were analyzed by qRT-PCR and immunoblot analysis for expression of Drp1 and Mfn2 at 24, 72, and 144 h after injury. Bars with different superscripts are significantly different from one another ($P < 0.05$).

Autophagy has been observed in multiple acute injury models, including AKI (152), and has been intimately linked with induction of Drp1 expression and mitochondrial fission (279). Thus, we examined microtubule-associated protein light chain 3 (LC3)-I/II expression over time following glycerol. An increase in the autophagic marker LC3-II was not observed until 144 h (Fig 3-5A). These results provide evidence that autophagy occurs late in the course of AKI.
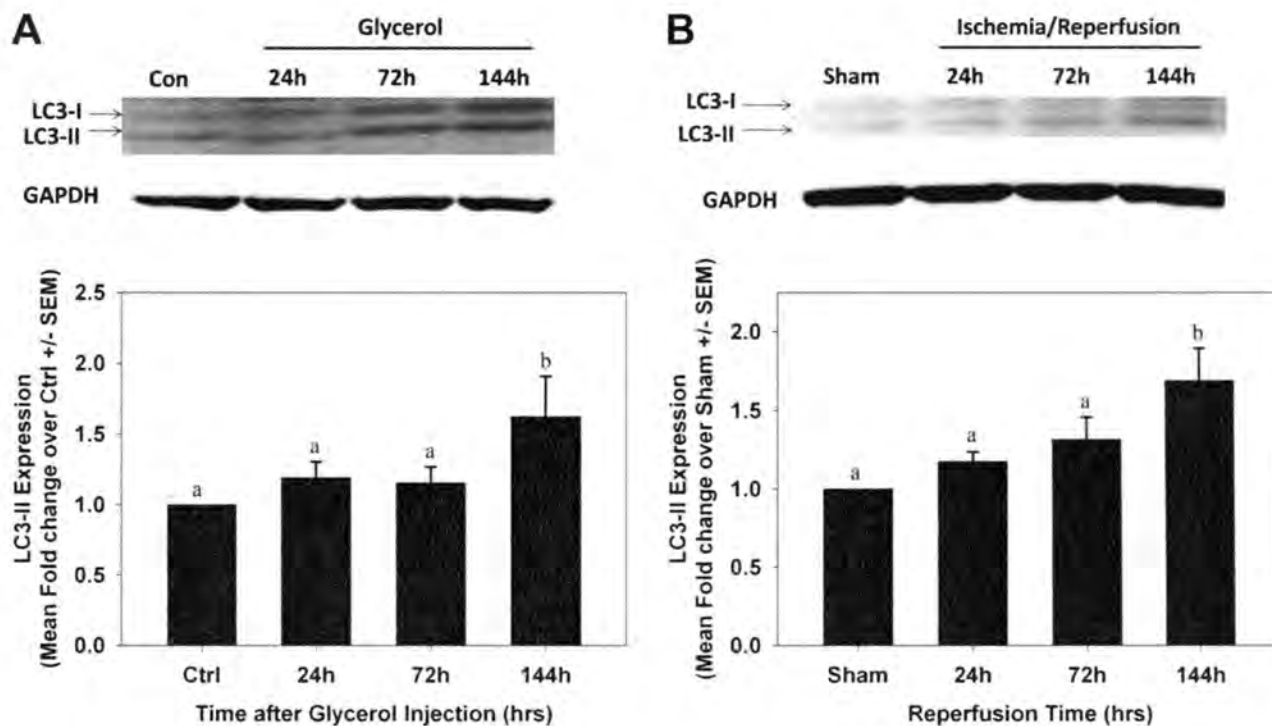
Figure 3-5. Induction of autophagy after AKI. LC3-I/II protein expression was measured by immunoblot analysis in control and glycerol-treated rats (*A*) and sham and ischemia-reperfusion (I/R) mice (*B*). Bars with different superscripts are significantly different from one another (*P* < 0.05).

Initiation of mitochondrial biogenesis occurs in acute injury models (220, 227, 294, 310).

We assessed expression of several known mediators of mitochondrial biogenesis by PCR

and immunoblot analysis. Peroxisome proliferator activated receptor gamma co-

activator-1α (PGC-1α), PGC-1 related co-activator (PRC), and nuclear respiratory factor

(NRF)-1 mRNA levels were elevated within 24 h after glycerol injection, and remained

elevated throughout 144 h (Fig 3-6A). PGC-1β decreased at 144 hr and no changes were

observed in NRF-2α or mitochondrial transcription factor A (Tfam) mRNA.

Correspondingly, there was an elevation in the biogenic proteins PGC-1α, NRF-1, and

Tfam after injury (Fig 3-6B), and the elevation was sustained throughout the study

period.
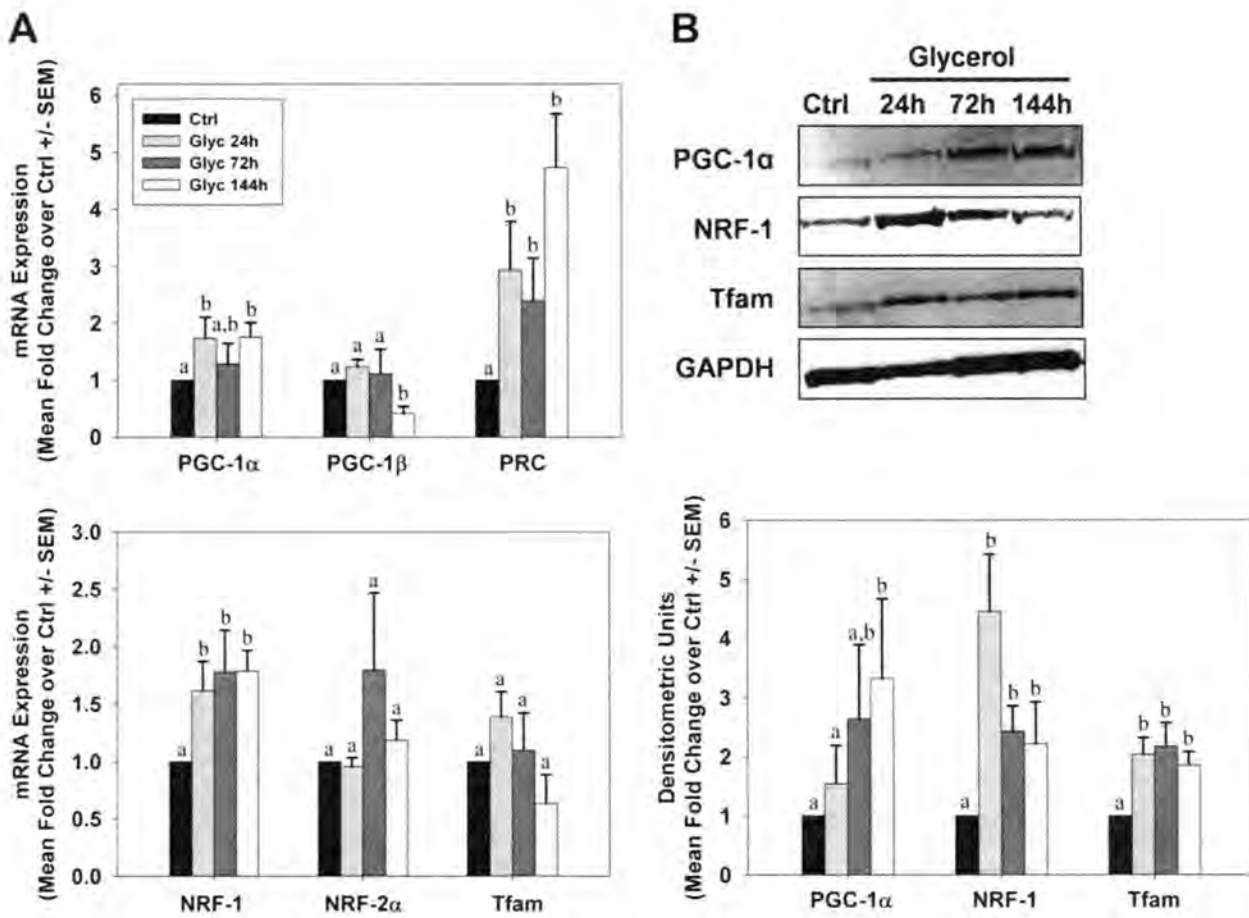
Figure 3-6. Mitochondrial biogenesis after glycerol-mediated AKI. *A*: kidneys from control and glycerol-treated rats were analyzed for expression of genes associated with mitochondrial biogenesis by qRT-PCR. *B*: peroxisome proliferator-activated receptor γ co-activator 1-α (PGC-1α), nuclear respiratory factors (NRF-1), and mitochondrial transcription factor A (Tfam) protein expressions were examined in kidneys of control and glycerol-treated rats by immunoblot analysis. Bars with different superscripts are significantly different from one another (*P* < 0.05).

Consistent with expression of biogenic proteins, but in contrast to reduced respiratory proteins, tissue ATP levels did not change at 24 h, increased at 72 hr, and was not different from controls at 144 h (Fig 3-7A).
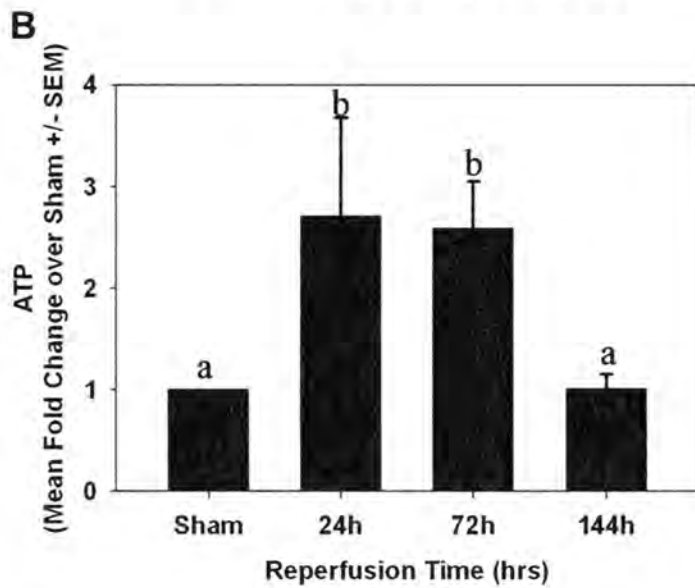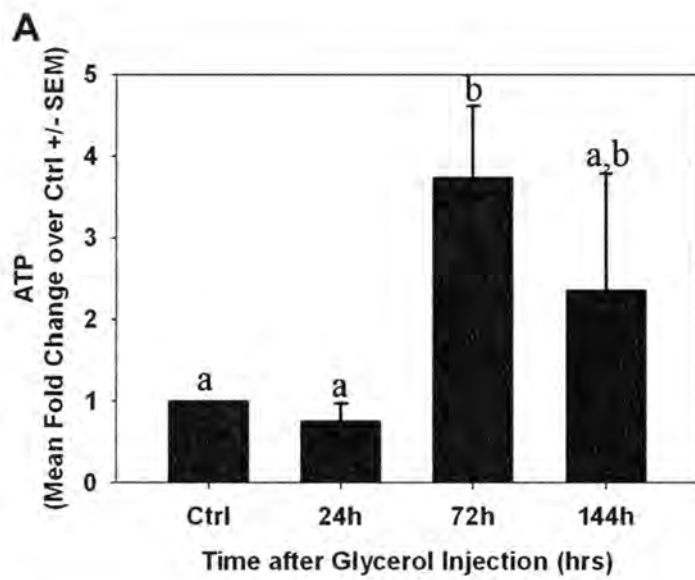
Figure 3-7. ATP levels after AKI. ATP was measured in flash-frozen kidney cortex from control/sham animals and at 24, 72, and 144 h after glycerol (*A*)- or I/R (*B*)-induced AKI. Bars with different superscripts are significantly different from one another ($P < 0.05$).

To determine whether the observed changes following myoglobinuric AKI were specific to the species and/or injury model used, we examined mitochondrial homeostasis markers in a mouse ischemia-reperfusion (I/R) injury model. Following a similar pattern to the rat myoglobinuria model, mice subjected to renal ischemia-reperfusion injury (I/R) exhibited kidney injury within 24 h after reperfusion, with a 7-fold rise in SCr levels at 24 h (Fig 3-8). Recovery of SCr levels occurred over time but did not reach control levels at 144 h.
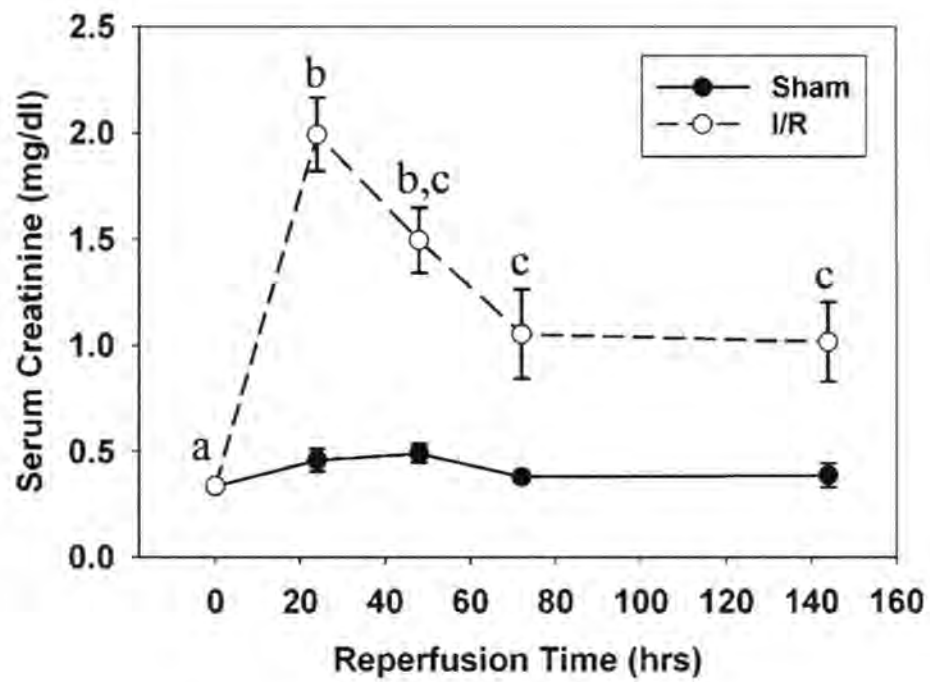
Figure 3-8. Kidney dysfunction after I/R injury. Serum creatinine levels were significantly elevated 24 h after reperfusion, and then slowly decreased between 24 and 144 h without returning to normal levels. Different superscripts above data points are significantly different from one another ($P < 0.05$).

Persistent apoptosis was also observed following I/R injury, where accumulation of cleaved-caspase 3 was noted at 72 and 144 h (Fig 3-9A). Histological evidence also revealed persistent tubule damage with proximal tubule dilation and brush border damage at 24 h after I/R and that was sustained throughout the study (Fig 3-9B).
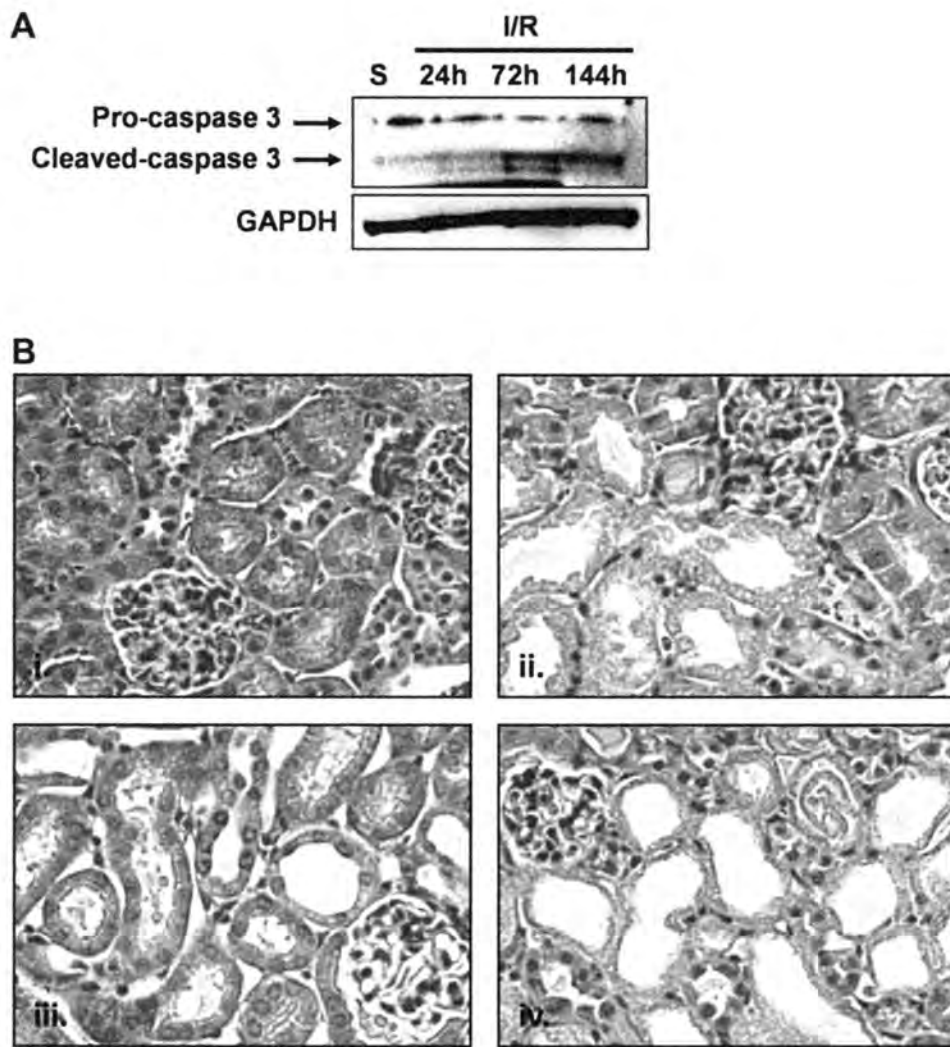
Figure 3-9. Persistent tubule pathology after I/R AKI. *A*: activation of caspase 3 was observed by the presence of a caspase 3 cleavage fragment at 72 and 144 h after reperfusion. *B*: hematoxylin and eosin (H&E) staining in sham mice (*i*) and 24 h (*ii*), 72 h (*iii*), or 144 h (*iv*) after I/R at ×40 magnification.

Loss of proximal tubule basolateral-apical polarity occurs after ischemic injury as a result of changes in cytoskeletal components. Depolarized and dedifferentiated proximal tubule cells undergo numerous morphological and biochemical changes, which can be evident by alterations in the expression of various epithelial and mesenchymal markers. One such alteration is the redistribution and loss of Na^+,K^+-ATPase expression early after injury in conjunction with loss of polarity. Normally expressed on the basolateral membrane, Na^+,K^+-ATPase (along with other membrane components such as integrins) relocates to the apical membrane or cytosol where it is subject to degradation. Examining expression in our model by IHC revealed that Na^+,K^+-ATPase was ubiquitously expressed specifically on the basolateral membrane of every proximal tubule in sham animals (Fig 3-10i). Twenty-four hours after ischemic injury, Na^+,K^+-ATPase redistributed from the basolateral membrane into the cytosol, and there was a generalized loss of expression throughout the cortex (Fig 3-10ii). At 72h and 144h after I/R, Na^+,K^+-ATPase expression was not restored (Fig 3-10iii, Fig 3-10iv), suggesting that the persistent tubule pathology is associated with a lack of repolarization and redifferentiation of the proximal tubule epithelium within the 144h study period.
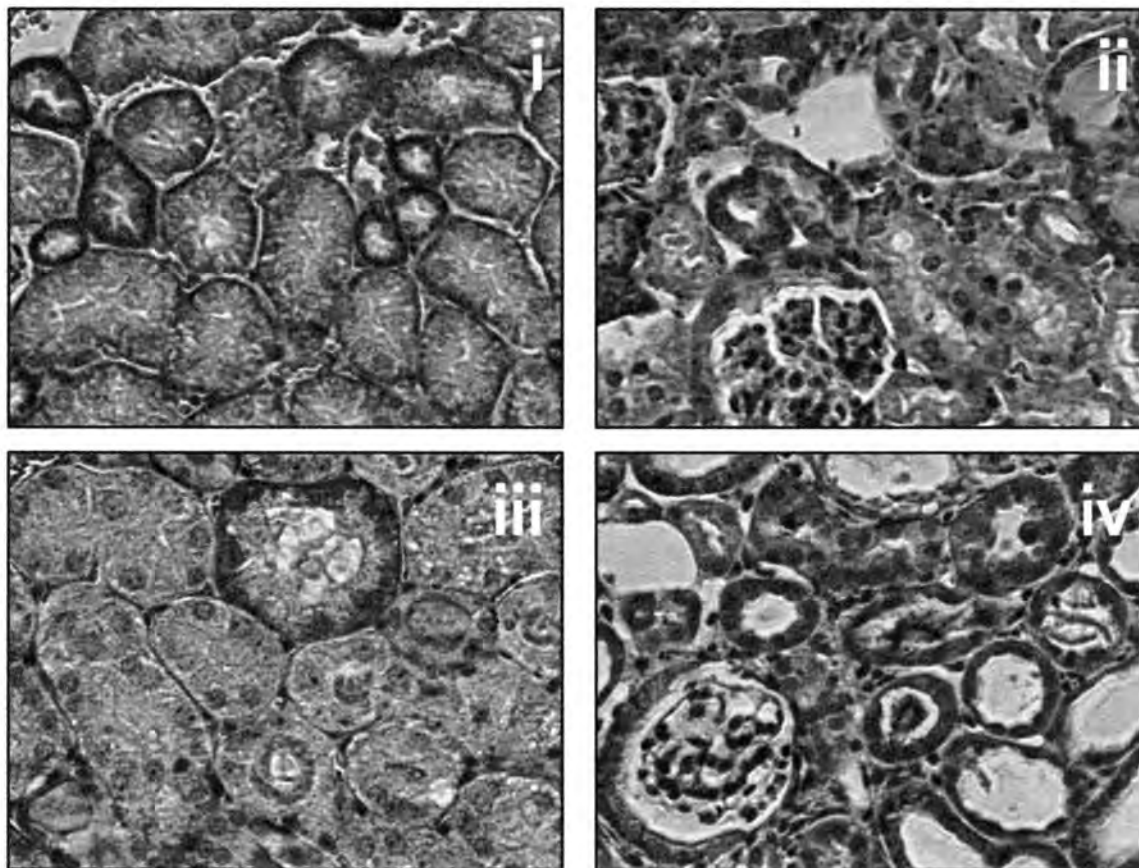
Figure 3-10. Sustained loss of Na$^+$,K$^+$-ATPase expression and localization in renal cortex proximal tubules after I/R. Expression of Na$^+$,K$^+$-ATPase was examined after I/R by immunohistochemistry in sham (i), and 24h (ii), 72h (iii), and 144h (iv) after I/R. Brown stain on basolateral membrane in (i) indicates Na$^+$,K$^+$-ATPase immunoreactivity visualized by DAB development and hematoxylin counterstain.

Twenty-four hours after I/R injury renal ND6, COX I, and ATP synthase β mRNA levels decreased and remained decreased at 72 h and 144 h after injury (Fig 3-11A). Immunoblot analysis on renal cortical lysates revealed that NDUFB8, ATP synthase β, and COX I protein levels decreased after I/R injury and did not recover over 144 h, similar to what was observed in the myoglobinuria model (Fig 3-11B).

Immunohistochemical analysis confirmed decreases in mitochondrial protein expression in proximal tubules of the kidney cortex. COX IV, which followed the same expression pattern as other respiratory proteins (Fig 3-11B, 3-11C), was localized throughout the kidney cortex, particularly the proximal tubule in sham animals (Fig 3-11Di). Twenty-four hours after I/R, COX IV immunoreactivity was less intense and more diffuse, although most proximal tubules were still positive for COX IV protein expression (Fig 3-11Dii). Immunoreactivity of COX IV within the kidney cortex, particularly with proximal tubules, became progressively less intense 72 h and 144 h after injury (Fig 3-11Diii, iv, inset).
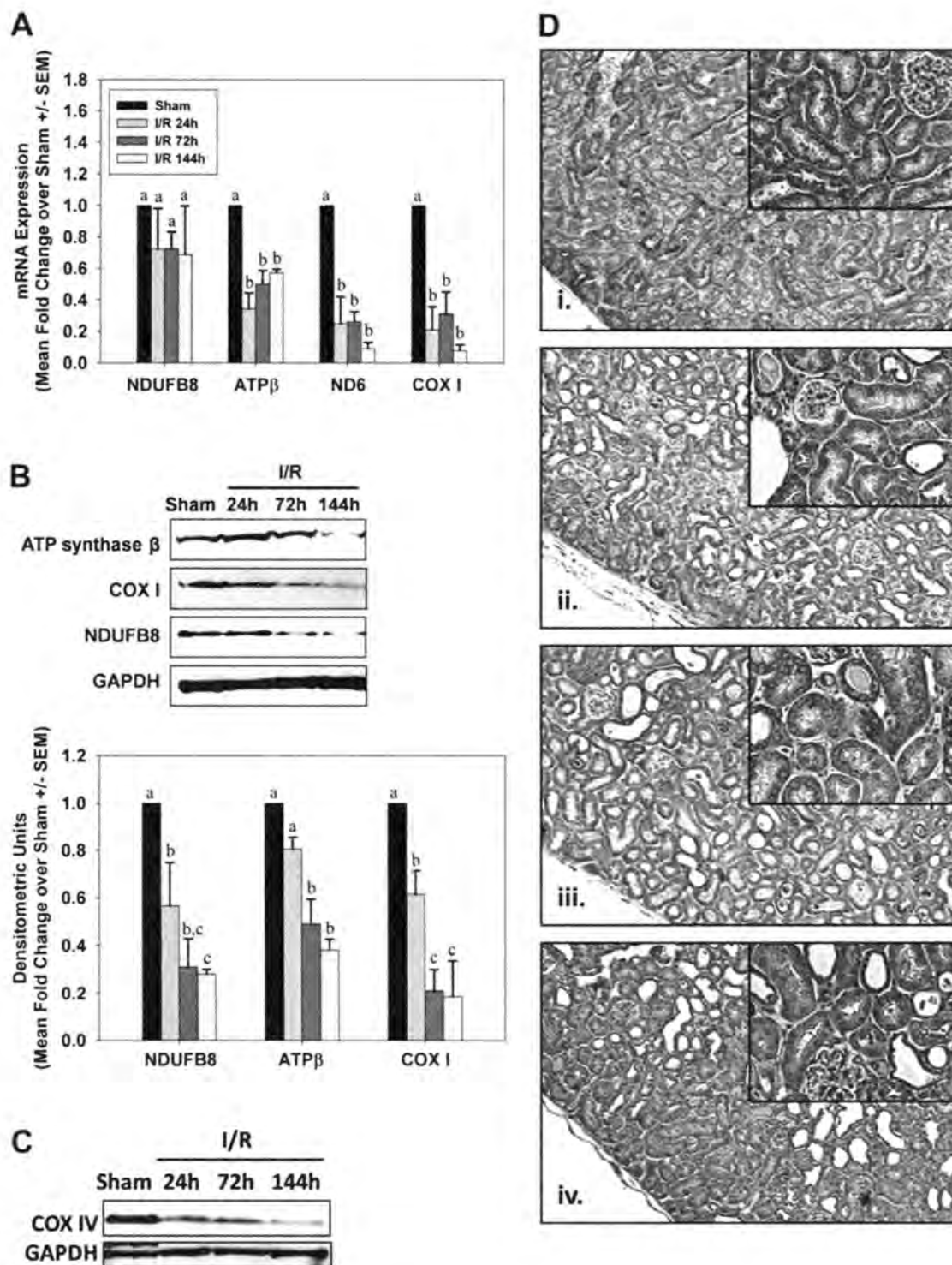
Figure 3-11. Sustained depletion of mitochondrial proteins after I/R AKI. *A*: mRNA from sham and I/R mice was analyzed by qRT-PCR for expression of nuclear-encoded respiratory genes NDUFB8 and ATP synthase β and the mitochondrial-encoded genes ND6 and COX I at 24, 72, and 144 h after injury. *B*: expression of mitochondrial respiratory proteins from kidneys of sham and I/R mice was examined by immunoblot analysis. Bars with different superscripts are significantly different from one another ($P < 0.05$). *C*: immunoblot analysis confirmed reduced COX IV protein expression in kidney cortex from mice 24, 72, and 144 h after I/R. *D*: COX IV immunohistochemistry (brown stain) in sham mice (*i*) or 24 h (*ii*), 72 h (*iii*), or 144 h (*iv*) after reperfusion in I/R mice, with hematoxylin counterstain. Low-magnification images were captured at ×10 and higher-magnification *insets* were captured at ×40.

115

No changes in Drp1 or Mfn2 mRNA were detected in kidneys of mice subjected to I/R injury (Fig 3-12A). However, immunoblot analysis revealed an increase in Drp1 protein at 72 and 144 h post-reperfusion (Fig 3-12B). Mfn2 protein decreased within 24 h and remained decreased at 72 h after I/R injury.
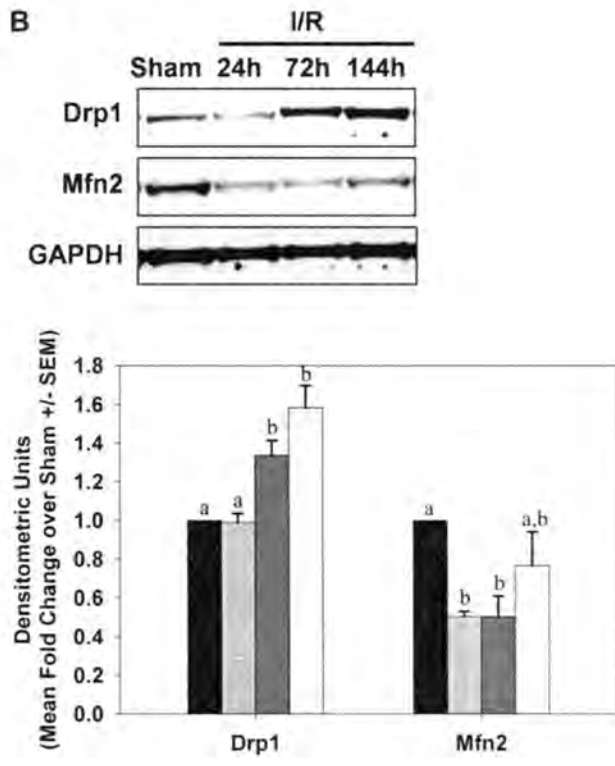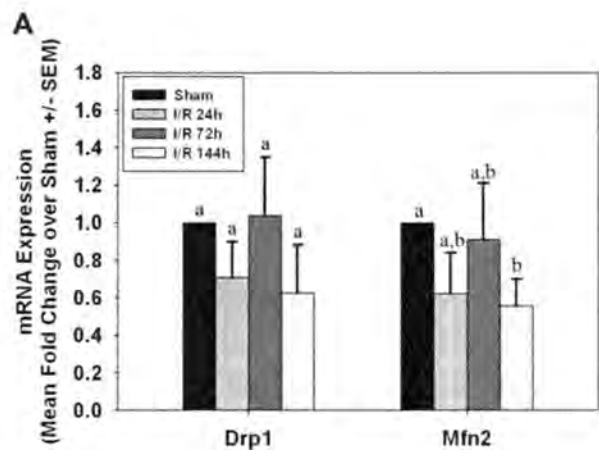
Figure 3-12. Alterations in mitochondrial fission and fusion proteins after I/R AKI. mRNA (*A*) and protein (*B*) expressions from kidneys of sham and I/R mice were analyzed by qRT-PCR and immunoblot analysis of Drp1 and Mfn2 at 24, 72, and 144 h after injury. Bars with different superscripts are significantly different from one another ($P < 0.05$).

Autophagy, was measured by LC3-I/II expression over time after I/R (Fig 3-5B). Similar to the findings observed in the myoglobinuric model, LC3-II expression increased at 144 h after reperfusion, again suggesting autophagy was active late in the injury/recovery process (Fig 3-5B).

Following I/R injury, only PRC mRNA was elevated and sustained throughout the study period (Fig 3-13A). PGC-1α, PGC-1β, Tfam, and NRF-1 mRNA tended to decrease slightly immediately after injury. In contrast to mRNA expression, protein levels of PGC-1α and Tfam increased after injury, but NRF-1 protein levels did not change (Fig 3-13B). Similar to what was observed in the myoglobinuria model, tissue ATP levels were elevated 24 and 72 h after I/R injury and returned to control levels at 144 h (Fig 3-7B). ATP was increased 24 h and 72 h after reperfusion, but back to pre-injury level at 144 h.
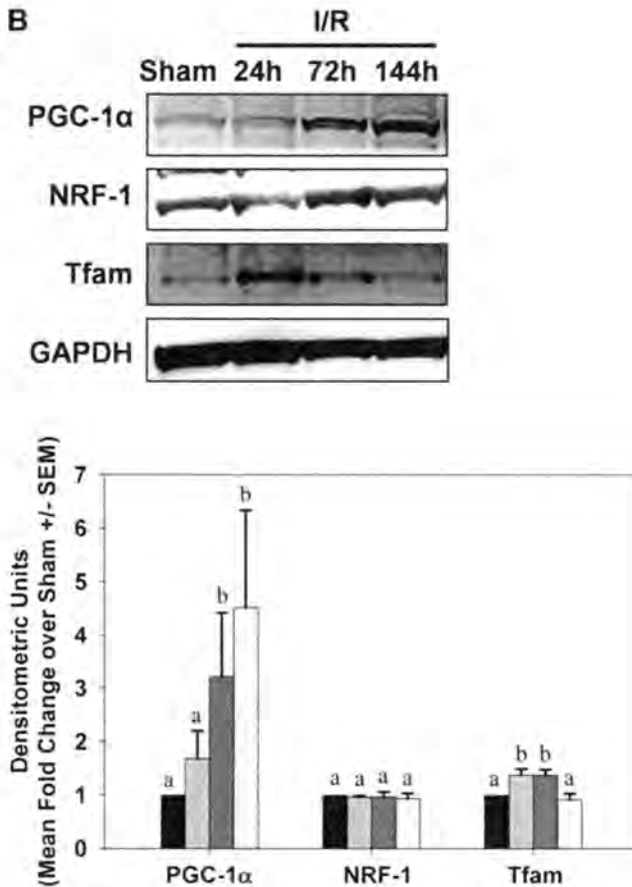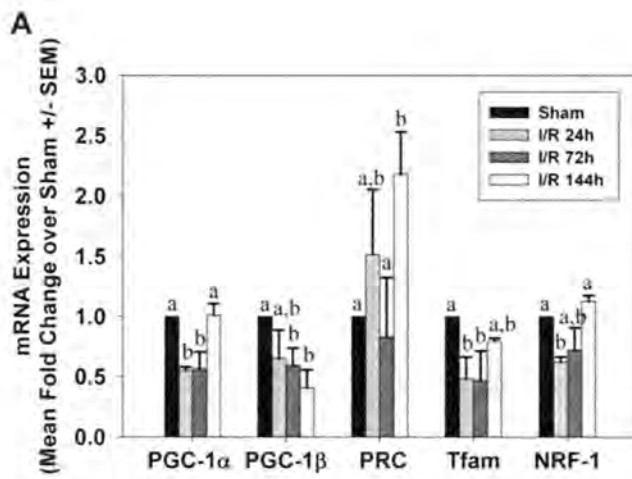
Figure 3-13. Mitochondrial biogenesis after I/R AKI. *A*: kidneys from sham and I/R mice were analyzed for mRNA expression of genes associated with mitochondrial biogenesis by qRT-PCR. *B*: PGC-1α, NRF-1, and Tfam protein expressions were examined by immunoblot analysis in kidneys from sham and I/R mice. Bars with different superscripts are significantly different from one another ($P < 0.05$).

Because we did not see restoration of normal protein expression within the 6 day time frame of the current study, we decided to extend the recovery time twice as long to 12 days after ischemic injury. Extending the recovery time to 12 days allowed for SCr levels to return all the way back to normal (Fig 3-14A). Of the mitochondrial proteins examined, only COX I was slightly reduced still, whereas both ATP synthase β, and NDUFB8 were back to normal levels (Fig 3-14B). Drp1 and PGC-1α were both still slightly elevated compared to sham animals, and Na^+,K^+-ATPase expression was still slightly reduced (Fig 3-14B). Taken together, the results from these studies reveal that although expression of proteins altered after ischemic injury are not completely back to normal levels, they are mostly restored at 12 days after injury.
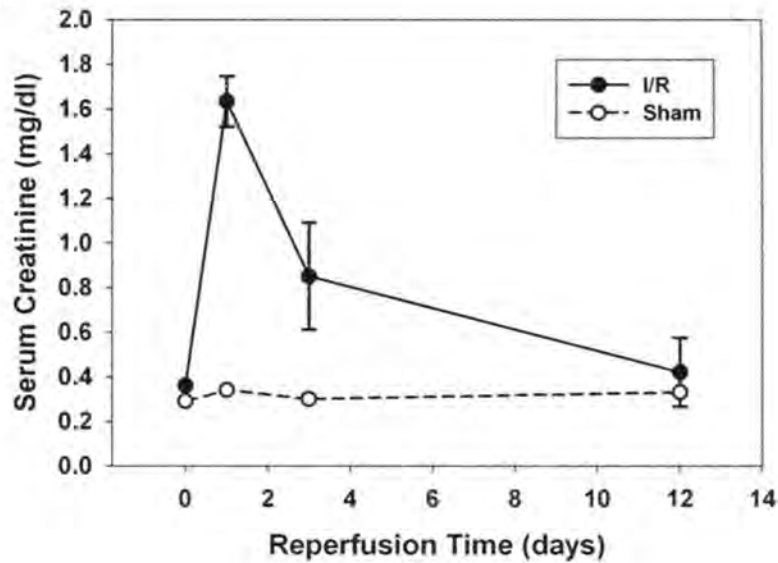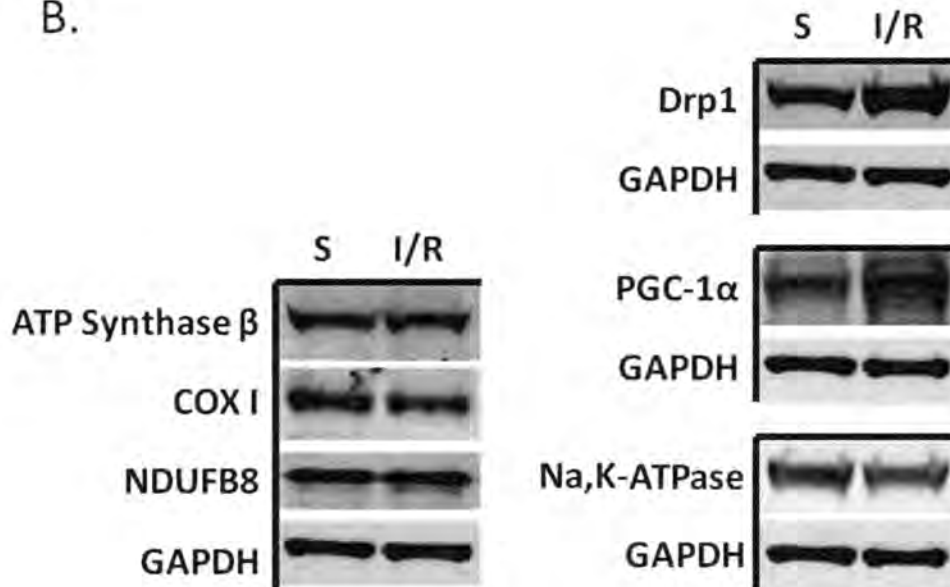
Figure 3-14. Protein expression mostly restored by 12 days after I/R. (A) SCr measurements were taken to monitor kidney function after I/R. (B) Expression of proteins altered after ischemic injury were examined at 12 days after injury by immunoblot analysis. Representative blots are shown for mitochondrial proteins ATP synthase β, COX I, and NDUFB8, as well as fission protein Drp1, biogenesis protein PGC-1α, and ion transporter protein Na^{+},K^{+}-ATPase.

DISCUSSION

In this study, we examined mitochondrial homeostasis in two different rodent AKI models. Previous studies have illustrated a central role of the mitochondria in acute injuries and provide evidence that the health of this organelle is a primary determinant in both the pathogenesis and recovery of organ function. However, many questions need to be answered in regards to duration of mitochondrial dysfunction, mechanisms of mitochondrial recovery, and influence of mitochondrial biogenesis on restoration of renal function. In the current study, we begin to address these questions by evaluating mitochondrial respiratory gene and protein expression, fusion and fission processes, autophagy, and biogenesis immediately after injury and during a 1 week recovery period.

In the glycerol model, the levels of mitochondrial proteins (e.g. NDUFB8, ATP synthase β, COXI) decreased and remained decreased throughout the partial recovery of glomerular function. While mRNA for the mitochondrial-encoded genes ND6 and COXI were decreased after injury, transcript levels for the nuclear-encoded mitochondrial proteins NDUFB8 and ATP synthase β either did not change (NDUFB8) or were elevated after injury (ATP synthase β). This finding would suggest differential regulation of transcription occurring in the nucleus versus the mitochondria following injury-induced mitochondrial protein degradation. The up-regulation of the mitochondrial biogenesis signaling molecules PGC-1α, PRC, and NRF-1 provides evidence of active transcription of nuclear-encoded mitochondrial proteins, whereas persistent pathological signals or damage may prevent active transcription of the mitochondrial genome. Similar to the glycerol model, mitochondrial proteins were decreased and remained decreased

throughout the partial recovery of glomerular function after I/R. IHC analysis following I/R confirmed the loss of COX IV in cortical proximal tubules after injury. However, following I/R-induced AKI, transcript levels of both nuclear- and mitochondrial-encoded proteins were depressed early after injury and throughout the recovery phase. These findings reveal differences in mitochondrial recovery signals in response to different inducers of AKI and that active transcription of mitochondrial encoded genes is inhibited even in the presence of elevated PGC-1α and other biogenic factors.

In cellular AKI models we have observed mitochondrial protein loss immediately after injury, and recovery of protein expression that was dependent on PGC-1α and mitochondrial biogenesis (221). As expected, mitochondrial biogenesis signaling was prominent following AKI, as reflected by early and continued elevations in PGC-1α, PRC and NRF-1 transcript and protein levels after injury. These findings are consistent with previous reports of induction of PGC-1α and mitochondrial biogenesis in acute organ injuries (220, 294, 299, 310). Significantly less has been reported about the roles of other PGC-1 family members, PGC-1β and PRC, in mitochondrial biogenesis and following acute injury. PGC-1β mRNA expression did not change after glycerol injury; however, PRC mRNA was robustly elevated immediately after injury and remained elevated throughout the 1-week recovery period. There were also elevations in NRF-1 and Tfam mRNA and/or protein, which are critical regulators of biogenesis (308).

Following I/R injury, PRC mRNA was elevated early after injury and remained elevated throughout the study period; however, no increase in transcript levels for any other gene

was observed. There were, however, alterations in protein expression of PGC-1α and Tfam. PGC-1α was elevated 72 h after injury and Tfam was transiently elevated between 24 h and 72 h reperfusion. These findings suggest that mitochondrial biogenesis is a component of the recovery phase after AKI, and that PGC-1α actively participates in response to mitochondrial injury. These studies also reveal a prominent response from PRC, which may be a critical regulator of mitochondrial biogenesis and maintenance following AKI and the role of each of the PGC-1 family members may depend on injury- or tissue-specific responses. Future studies are needed to distinguish the contribution of each family member following AKI.

Initially, the observation that electron transport chain proteins were severely depleted early after injury and did not recover while SCr levels returned to normal was inconsistent with our expectations that mitochondrial proteins would be restored as glomerular function recovered. In part, this was the result of the inherent limitations of using only one marker of renal function. However, upon further inspection the loss of COX IV in the proximal tubules and the loss of other mitochondrial proteins in the renal cortex were consistent with the sustained decrease in proximal tubular function, as determined histologically and from urinary glucose and NGAL measurements.. A direct causal relationship between loss of mitochondrial proteins and proximal tubular dysfunction cannot be established in the current study. It is possible that the correlation is merely a secondary effect from numerous pathological signals contributing to the injury. Future studies will directly address these questions to elucidate the role of mitochondrial biogenesis and function in recovery from AKI.

Although mitochondrial electron transport chain proteins remained decreased throughout the study period, ATP levels paralleled PGC-1α, and did not decrease but increased above control levels. Previous studies have demonstrated that ATP is reduced dramatically during ischemia, but is mostly recovered 24 h after reperfusion (135, 259, 278). Similarly, ATP is decreased within 1 h following glycerol-induced AKI (313). In both models, ATP was elevated at 72 h after injury and trended back to control levels at 144 h. The mechanism or source of higher than normal ATP after injury is still unclear, particularly under conditions of extended mitochondrial disruption and reduced oxidative phosphorylation proteins. Elevated nucleotide pools have been reported in plasma and red blood cells in human and rodent renal failure studies (75, 192) and it has been suggested that this may be the result of under excretion in the urine or from salvage pathways due excessive accumulation of inorganic phosphate (Pi). Additionally, increased gluconeogenesis has been reported in proximal tubules isolated from rat kidneys 1-3 days after I/R that may compensate for an increased energy demand (154). It is not known if any of these mechanisms contribute to the elevated renal ATP levels observed in the current study. The observation warrants additional exploration, though, and illustrates the complex nature of the organelle and the limitations of using only one parameter to gauge mitochondrial function.

Following AKI there were marked changes in mitochondrial fission and fusion protein expression. In the myoglobinuria model, both Drp1 and Mfn2 protein expression were

elevated after injury and remained elevated throughout the recovery period. However, increased Drp1 protein levels was correlated with increased Drp1 mRNA while Mfn2 protein levels were not associated with increased Mfn2 mRNA, suggesting an altered post-transcriptional regulation. In contrast, in the I/R model elevated Drp1 protein expression was delayed until the recovery phase without any change in Drp1 mRNA expression throughout the study, suggesting there may be changes in protein degradation after I/R. Mfn2 protein levels decreased after injury and during recovery without a change in Mfn2 mRNA levels. These results reveal differences between the two AKI models with respect to mitochondrial fusion protein expression; however, fission protein Drp1 was elevated after injury in both models, suggesting that mitochondrial fission may be a more general process in AKI whereas fusion protein expression may be more specifically-regulated.

Induction of Drp1 protein and mitochondrial fragmentation has been reported previously in I/R AKI models and this process is a major contributor to injury progression (39). Brooks, et al., demonstrated that by inhibiting Drp1 either pharmacologically or by molecular techniques, attenuated mitochondrial fragmentation, cytochrome *c* release, apoptosis, and kidney injury in both cellular and animal models of AKI. Both of the AKI models used in the current study are consistent with the results obtained by Brooks, et al., and others, which have demonstrated induction of Drp1 is correlated with caspase 3 cleavage and apoptosis (89, 164, 275). However, the current study also demonstrates alterations in the mitochondrial fusion protein Mfn2 following AKI, and the contribution

of this protein to mitochondrial fragmentation and injury progression has not been fully evaluated and warrants additional attention in future studies.

Autophagy has been reported in a number of acute injury models, including AKI (152). Induction of autophagy is thought to be crucial in the removal of damaged proteins and organelles (i.e. mitochondria) after injury, and blocking this response may prevent efficient cellular and organ recovery (152). Additionally, autophagy has been linked with changes in mitochondrial dynamics, which includes selective mitochondrial fission, fusion, and sequestration in the course of removal of damaged mitochondria (279). It is interesting that this response was not upregulated until the recovery phase in both models, somewhat paralleling the results observed for mitochondrial biogenesis.

There is an overwhelming need to develop new treatment strategies for AKI as there are currently no methods to improve renal function, but rather only procedures to prevent further damage and to maintain functional output, such as dialysis. Mitochondria undergo significant alterations following AKI and influence the pathophysiology as well as recovery of organ function during and after injury. We demonstrated that persistent mitochondrial dysfunction occurs within damaged proximal tubules after AKI and may contribute to the sustained injury observed within these structures. This phenomenon occurs even in the process of active repair signals and during improved glomerular function. Additionally, persistent mitochondrial dysfunction may also lead to chronic deficiencies in cell and organ function similar to disorders of the heart, brain, and kidney which are known to be associated with mitochondrial disease. As such, strategic

development of methods to improve mitochondrial functions, i.e. mitochondrial

biogenesis, following injury may offer unique therapeutic targets for the treatment of

AKI.

Chapter 4:

SRT1720 improves renal cortical mitochondrial and tubular function following ischemia-reperfusion injury.

ABSTRACT

Ischemia-reperfusion (I/R) injury in the kidney primarily targets lethal and sub-lethal injury in the proximal tubule, most notably observed in the necrotic region in the outer stripe of the outer medulla. Sub-lethal injury consists of numerous injury and repair mechanisms that occur in response to oxygen deprivation during the ischemic period and robust oxidant damage and inflammation as a component of the reperfusion injury. Mitochondrial dysfunction is a primary pathological consequence of I/R injury, and promoting mitochondrial biogenesis as a repair mechanism after injury may offer unique benefits to restore mitochondrial and organ function. Rats subjected to bilateral renal pedicle ligation for 22m were treated once daily with the SIRT1 activator SRT1720 (5 mg/kg, i.p.) or vehicle starting at 24h after reperfusion until 72h or 144h. Mitochondrial proteins ATP synthase β, cytochrome c oxidase subunit I (COX I), and NDUFB8 were diminished at 24h, 72h and 144h in rats subjected to I/R plus vehicle treatment. Rats treated with SRT1720 after I/R (IR+SRT1720) had improved mitochondrial protein expression by 144h, which was associated with restored state 2 and uncoupled mitochondrial respiration. PGC-1α was elevated at 72h and 144h in both IR and IR+SRT1720 rats; however, SRT1720 treatment was associated with reduced acetylated

PGC-1α, the more active form. Kidney injury molecule-1 (Kim-1), a sensitive and specific marker of tubular injury, was persistently elevated in the urine of both IR and IR+SRT1720 rats. Tissue analysis revealed that Kim-1 was also persistently expressed in the renal cortex of IR rats but was attenuated in IR+SRT1720 rats. Additionally, sustained loss of Na,K-ATPase expression and elevated vimentin in IR rats was normalized in IR+SRT1720 rats, suggesting treatment was associated with restoration of a differentiated, polarized proximal tubule epithelium. Taken together, these results suggest that treatment with SRT1720 expedited recovery of mitochondrial proteins expression and function by enhancing mitochondrial biogenesis. Rescue of mitochondrial function was associated with a faster recovery of proximal tubule integrity. Targeting mitochondrial biogenesis may offer unique therapeutic benefits as a strategy to improve tubule repair following ischemic injury.

INTRODUCTION

Ischemia-reperfusion (I/R) is a primary cause of acute kidney injury (AKI), and the proximal tubule epithelium is particularly sensitive to the damage associated with ischemic injury. In addition to lethal injury to proximal tubule cells, sub-lethal injury account for much of the functional impairment observed in the post-ischemic kidney. For example alterations in cytoskeletal components and loss of polarity, characterized by the redistribution of membrane-specific lipids and proteins, such as the basolaterally-expressed Na^+,K^+-ATPase, contribute to defective ion and water reabsoption after injury (184-185). Loss of both viable and non-viable cells into the tubular lumen also account for the reduced functional capacity of the proximal tubule after injury, and surviving cells must replace the denuded basement membrane by dedifferentiating, migrating, and proliferating to reform an intact redifferentiated tubular epithelium (76). During the transformation to an undifferentiated phenotype, the cells lose epithelial-like markers, such as the intermediate filament cytokeratin, and express mesenchymal and developmental markers such as vimentin and PCNA (302). AKI is generally considered a reversible injury; however, the extent of recovery may not always be complete, as a number of factors can influence the regenerative process, such as persistent inflammation and fibrosis (30, 76).

Mitochondria are a primary subcellular target of I/R injury. Weinberg, et al., demonstrated that 60m hypoxia followed by 60m reperfusion resulted in high amplitude swelling of mitochondria, indicative of depolarization and initiation of mitochondrial permeability transition (297). We have recently shown that I/R in mice results in early

and persistent loss of mitochondrial electron transport chain proteins in the outer cortex of the kidney, a zone not generally susceptible to the overt necrotic cell death usually seen in the outer medulla (91). ATP synthase β, NDUFB8, and mitochondrial-encoded cytochrome c oxidase subunit I (COX I) were depleted within 24h after I/R and did not recover by 144h after reperfusion. In fact, our unpublished observations have revealed that it took approximately two weeks for mitochondrial protein expression to be restored. Additionally, we showed that other markers of mitochondrial homeostasis were persistently disrupted, including increased expression of the mitochondrial fission protein Drp1, reduced expression of the fusion protein Mfn2, and up-regulation of proteins associated with mitochondrial biogenesis (91). These results were consistent with the findings of Brooks, et al., when they demonstrated that induction of Drp1 and mitochondrial fragmentation was a contributor of kidney injury, and inhibiting mitochondrial fragmentation preserved mitochondrial integrity, inhibited release of cytochrome c and apoptosis, and protected against renal dysfunction in a mouse I/R model (39).

Previous work from our laboratory demonstrated that signaling of mitochondrial biogenesis through PGC-1α was essential for recovery of mitochondrial function in renal cells following oxidant-induced injury (220-221). Expression of PGC-1α was induced after oxidant exposure in renal proximal tubule cells (RPTC), and it corresponded with recovery of mitochondrial oxygen consumption and cellular ATP levels, which took approximately 5-6 days to restore to pre-injury levels (220). Additionally, over-

expression of PGC-1 after oxidant injury expedited recovery of mitochondrial and cellular function to approximately 2 days (221).

We have previously characterized several pharmacological activators of mitochondrial biogenesis in RPTC (90, 223-224). SRT1720 was initially reported as a potent SIRT1 activator, and treatment for 8 weeks in either a diet-induce obesity model or a genetic diabetic mouse model improved glucose tolerance and insulin sensitivity compared to vehicle-treated mice (178). In our hands, SRT1720 stimulated mitochondrial biogenesis in RPTC within 24h of exposure, with elevated mitochondrial protein expression, basal and uncoupled oxygen consumption, and total cellular ATP in SRT1720-treated cells (90). The effects of SRT1720 were dependent on SIRT1 activity, and occurred in the absence of AMPK activation. Finally, SRT1720 restored mitochondrial and cellular function in an acute oxidant injury model which is known to initiate mitochondrial toxicity. Feige, et al., demonstrated that 15 weeks of SRT1720 treatment mimicked energy deprivation pathways typically stimulated during exercise, preventing diet-induced obesity, improving glucose and cholesterol homeostasis, and stimulating energy expenditure in fat tissue (85). SRT1720 treatment activated genes associated with mitochondrial metabolism and function, and fatty acid oxidation in a number of tissues. Additionally, SRT1720 was recently studied in a high fat diet model in which mice given SRT1720 in combination with a high fat diet showed prolonged mean lifespan and improved health (180). SRT1720-treated mice had reduced liver steatosis and pancreatic toxicity, improved blood glucose levels and insulin sensitivity, and improved locomoter

function. Improved metabolic health was associated with reduced PGC-1α acetylation, and restored mitochondrial respiratory capacity.

The purpose of the current study was to test the hypothesis that mitochondrial biogenesis is an essential component of the repair process following AKI, and to examine whether SRT1720 treatment could rescue mitochondrial function in an acute injury model. To do so, we examined recovery of mitochondrial and renal function in rats treated with SRT1720 24h after I/R-induced AKI. Our results demonstrate that SRT1720 treatment expedited recovery of mitochondrial proteins and function after I/R. Markers of tubular injury/function were also restored in treated animals, including reduction in Kim-1 expression, and restoration of a polarized, differentiated proximal tubule.

EXPERIMENTAL PROCEDURES

Ischemia/reperfusion model of AKI

Eight-week old male Sprague-Dawley rats weighing 180-200g were subjected to bilateral renal pedicle ligation as previously described (323). Briefly, renal artery and vein were isolated and blood flow was occluded with a microvascular clamp for 22m. After reperfusion, the abdominal opening was sutured and rats were allowed to recover from anesthesia. Dosing was initiated at 24h after reperfusion, and rats were given either a daily injection of SRT1720 (5 mg/kg, i.p.) or vehicle, which was continued until rats were euthanized at 72h or 144h. All procedures involving animals were performed with approval from the Institutional Animal Care and Use Committee (IACUC) in accordance with the NIH Guide for the Care and Use of Laboratory Animals.

Assessing renal function

Tail vein blood was collected and serum was used to measure creatinine levels using a Quantichrom™ Creatinine Assay Kit (BioAssay Systems, Hayward, CA) according to manufacturer's protocol. Urine was collected from rats housed in metabolic cages overnight (16h) at various time points throughout the study. Urine samples were used to determine kidney injury molecule-1 (Kim-1, Argutus Medical Rat Kim-1 ELISA, Dublin, Ireland).

Immunoblot analysis

Surface regions of renal cortex, which are not generally within the zone of extensive necrosis, was dissected from flash frozen kidneys, and tissue was lysed in RIPA buffer containing cocktail protease and phosphatase inhibitors. Total protein content was measured by the BCA assay. Fifty µg total protein was loaded into SDS-PAGE gels and immunoblots were performed as previously described (220).

Immunohistochemistry

Paraffin-embedded sections were cleared in xylenes, and rehydrated in a graded ethanol wash. Antigen unmasking was performed by boiling sections in citrate buffer for 10 min followed by cooling at room temperature for 30m. Endogenous peroxidase activity was quenched by incubating sections in 3% H_2O_2 for 10 min. Sections were then blocked in 10% normal goat serum for 1h, followed by primary antibody (Kim-1, R&D Systems; Na^+,K^+-ATPase, Upstate Antibodies) overnight at 4°C. Sections were then incubated in

biotinylated anti-rabbit secondary antibody for 30 min followed by HRP-linked avidin-biotin complex reagent (Vectastain) for 30 min. Finally, antibody detection was visualized by DAB peroxidase substrate developer (Vectastain), counterstained with hematoxylin, mounted and cover slips applied. Images were acquired with a Nikon microscope under control of QCapture imaging software. Low magnification images are at 10X and high magnification images were captured at 40X.

Mitochondrial isolation and oxygen consumption

At the time of euthanasia, kidneys were excised from rats and submerged in an ice-cold mitochondrial isolation buffer on ice. Mitochondria were isolated by differential centrifugation as previously described (64). The mitochondrial pellet was resuspended in an incubation buffer and oxygen consumption (QO_2) was measured using a Clark oxygen electrode. Briefly, 1.5 ml of mitochondrial suspension was added to the chamber and state 2 respiration was measured. Uncoupled oxygen consumption was determined by injecting FCCP for a final concentration of 1 μM. An aliquot of the mitochondrial suspension was saved for protein measurement, and rates were calculated as nmol O_2 consumed per minute, and were normalized to the amount of total protein in each sample.

Statistical Analysis

Graphs represent a sample size of 3 to 6 for each group. Data were analyzed by ANOVA based on ranks followed by the Mann-Whitney rank-sum test for individual group comparisons of non-parametric data.

RESULTS

Approximately 8-week old Sprague-Dawley rats were divided into four groups that would undergo either a sham or renal ischemia-reperfusion (I/R) procedure, followed by treatment with either SRT1720 (5 mg/kg, i.p.) or vehicle starting at 24h after the procedure. The four groups were designated as: sham + vehicle (V), sham + SRT1720 (S), I/R + vehicle (IRV), and I/R + SRT1720 (IRS), and the rats were euthanized at 72h or 144h after the sham or I/R procedure. Mitochondrial DNA (mtDNA) copy number is an indirect measure of the number of mitochondria in a certain tissue. Renal cortical mtDNA increased approximately 60% in S rats compared to the V group at 144 h (Fig 4-1A). mtDNA were not different in either of the I/R groups compared to V at this time point. PGC-1α is increased and mitochondrial biogenesis is induced during recovery from AKI (91). PGC-1α protein was up-regulated after injury at both 72h and 144h in both SRT1720- and vehicle-treated rats (Fig 4-1B). Because SIRT1 is a protein deacetylase and PGC-1α is a SIRT1 target, and because we have previously shown that SRT1720 treatment results in deacetylated PGC-1 in primary RPTC (90), we examined PGC-1α acetylation in our model. Renal cortical lysates were subjected to immunoprecipitation with an acetylated-lysine antibody, and then subjected to immunoblot analysis with an antibody to PGC-1α. There was increased acetylated PGC-1α in IRV rats at both 72h and 144h after injury that was reduced to control levels in IRS rats, suggesting that the majority of PGC-1 which is up-regulated in IRS rats after injury is in the deacetylated form (Fig 4-1C). Because differences in nuclear localization of PGC-1α can affects its activity and because we have previously shown increased nuclear PGC-1α with SRT1720 treatment (90), we examined whether there were any differences

137

in nuclear localization of PGC-1 with treatment or after injury. Similar to the cortical tissue lysates, PGC-1α expression was increased in nuclear lysates after I/R, but there were no differences between the IRV and IRS groups (Fig 4-1D). During the course of activation of the mitochondrial biogenesis program, mitochondrial transcription factors are up-regulated and translocated to the mitochondria to transcribe and replicate the mitochondrial genome. Protein expression of mitochondrial transcription factor A (Tfam) was not changed after injury or treatment in whole cortex tissue lysates (data not shown); however, in isolated mitochondria, Tfam expression was increased in both groups that received SRT1720, suggesting that there is increased mitochondrial Tfam localization with SRT1720 treatment (Fig 4-1E). Some evidence suggests that SIRT1 activators may act on AMPK either instead of or in conjunction with SIRT1 (15, 73). In our model, we observed increased pAMPK (Thr172) in both IRV and IRS rats; however, we did not see any effect of SRT1720 treatment on pAMPK expression (Fig 4-1F). Overall, we suggest that SRT1720 is inducing a mitochondrial biogenic response to increase mtDNA, and after injury is activating PGC-1α through deacetylation and increasing the mitochondrial levels of Tfam, a target of PGC-1α.
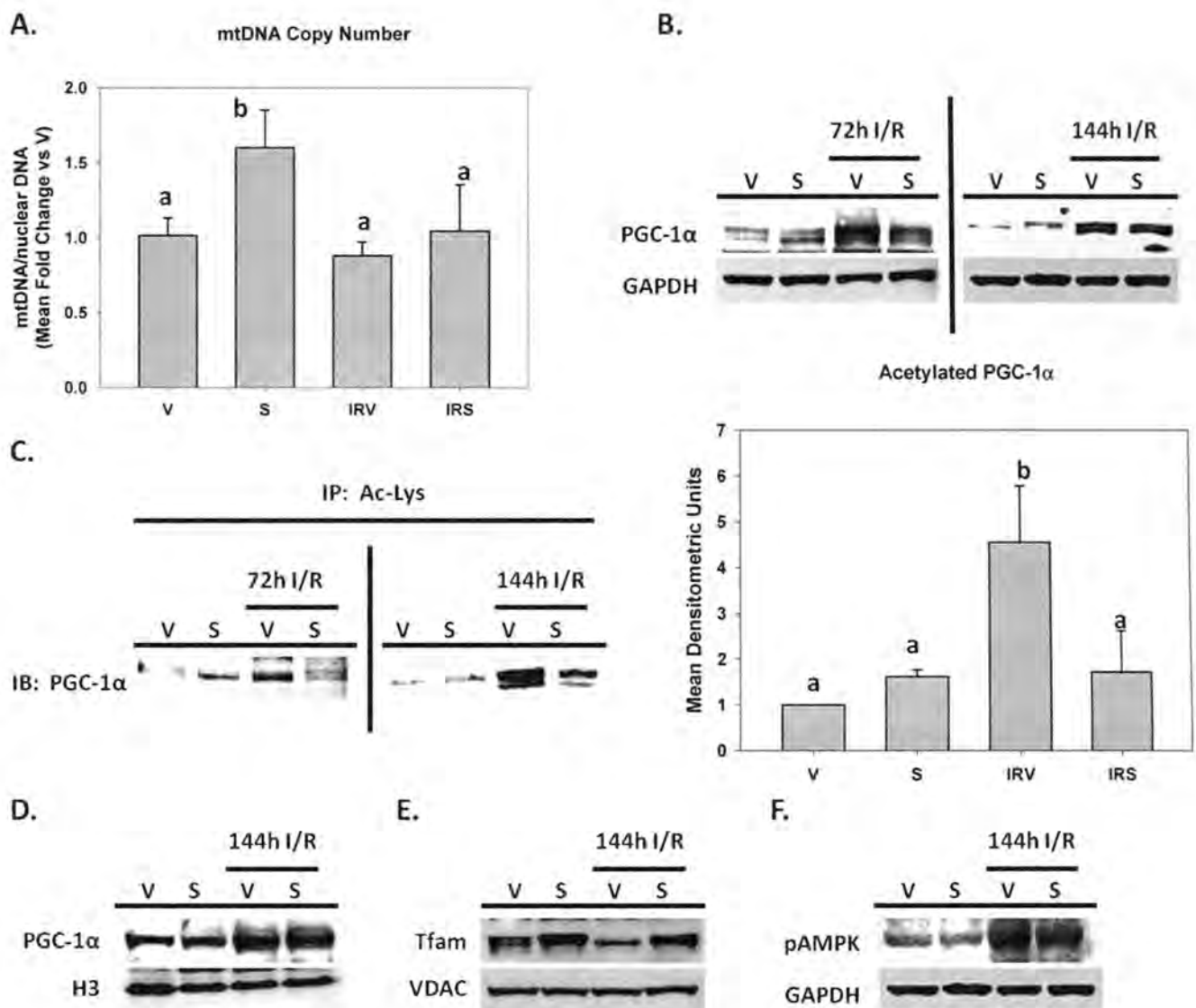
Figure 4-1. SRT1720 induces renal mitochondrial biogenesis and increases deacetylated PGC-1α after I/R. (A) Mitochondrial DNA (mtDNA) copy number was quantified in total genomic DNA isolated from the renal cortex at 144h. (B) PGC-1α expression was determined by immunoblot analysis in protein isolated from the renal cortex at 72h and 144h. (C) Acetylated PGC-1α was examined in tissue lysates from the renal cortex by immunoprecipitating with an acetylated-lysine antibody, followed by immunoblot analysis with an antibody against PGC-1α. Densitometric quantification of the 144h bands are shown in the graph to the right of the representative blots. (D) Nuclear PGC-1α expression was examined by immunoblot analysis in lysates of isolated nuclei from the renal cortex at 144h. (E) Mitochondrial transcription factor A (Tfam) expression was analyzed in lysates generated from isolated mitochondria from the renal cortex at 144h. (F) pAMPK expression was examined by immunoblot analysis in renal cortical tissue lysates at 144h.

From mouse renal I/R studies, we have shown that mitochondrial proteins are depleted early after injury and are persistently down-regulated until at least 144h after injury (91). In fact, in our unpublished observations, it took approximately two weeks for mitochondrial protein expression to recover after I/R. Because we were able to stimulate a mitochondrial biogenic response with SRT1720 treatment, we next examined recovery of mitochondrial protein expression the rats after injury (Fig 4-2). Twenty-four hours after ischemia, prior to initial dosing, the nuclear-encoded proteins ATP synthase β and NDUFB8, and the mitochondrial-encoded protein COX I were all decreased (Fig 4-2A). As expected, mitochondrial proteins were still diminished at 72h and 144h in IRV rats (Fig 4-2A). Rats in the IRS group had higher levels of mitochondrial protein expression by the 144h time point, but not at 72h (Fig 4-2A). We next examined mitochondrial proteins in mitochondria isolated from the renal cortex to determine whether the reduction in mitochondrial protein occurred on a per mitochondrion level or if there was a widespread loss of the organelle. There was a moderate but significant reduction in COX I protein expression in the isolated mitochondria from the IRV rats which was restored in the IRS rats (Fig 2B); however, the reduction was not as substantial as was observed in the whole tissue lysates (Fig 2A), and there was no change in the nuclear-encoded proteins ATP synthase β or NDUFB8.
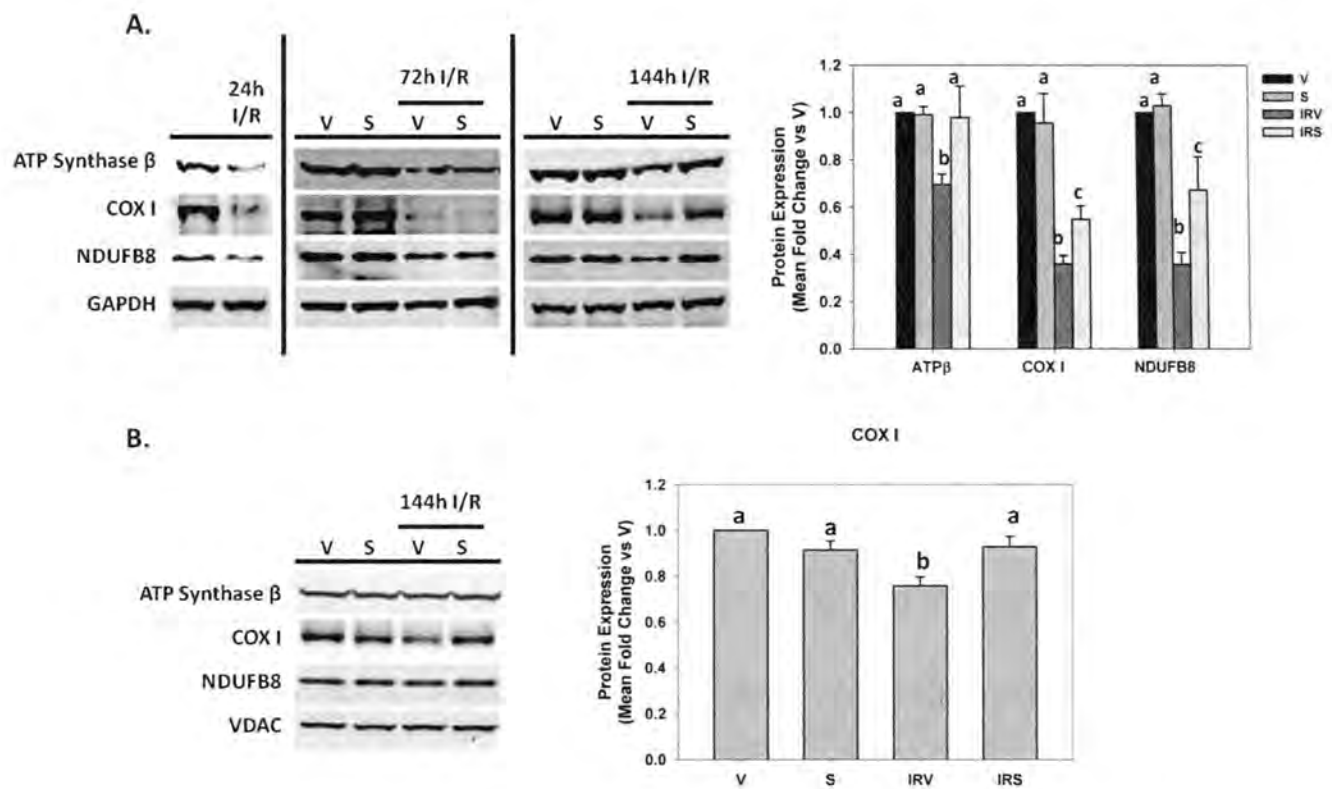
Figure 4-2. Mitochondrial protein expression is restored with SRT1720 treatment after I/R. (A) Expression of ATP synthase β, COX I, and NDUFB8 were examined by immunoblot analysis in renal cortical lysates at 24h, 72h, and 144h. Densitometric quantification of bands at 144h is shown in the graph to the right of the representative blots. (B) Mitochondrial protein expression in isolated mitochondria from the renal cortex at 144h with densitometric quantification depicted in the graph to the right of representative blots.

Proteins associated with mitochondrial fusion/fission are altered after I/R. Drp1 mediates mitochondrial fission and was persistently up-regulated after I/R, and Mfn2, which is involved in fusion of mitochondria, showed sustained down-regulation after injury. Examination of cortical tissue lysates revealed that both of these proteins were similarly altered as previously reported (Fig 4-3). Mfn2 expression was decreased at 24h, prior to initial dosing, and was still reduced in both IRV and IRS rats at 72h and 144h after injury (Fig 4-3A). Drp1 expression was not changed at 24h, but was elevated at both 72h and 144h in IRV and IRS rats (Fig 4-3A). Drp1 is expressed in the cytosol and is recruited to mitochondria undergoing fragmentation by the outer membrane protein Fis1. Therefore, examination of renal cortical expression may not reflect the level of protein actually associated with mitochondrial fission. When we examined isolated mitochondria for Drp1 expression, we observed an increase in mitochondrial-associated Drp1 in IRV rats, and this increase was attenuated in the IRS rats (Fig 4-3B). Mfn2 was still down-regulated in mitochondria from IRV rats and was not restored with SRT1720 treatment.
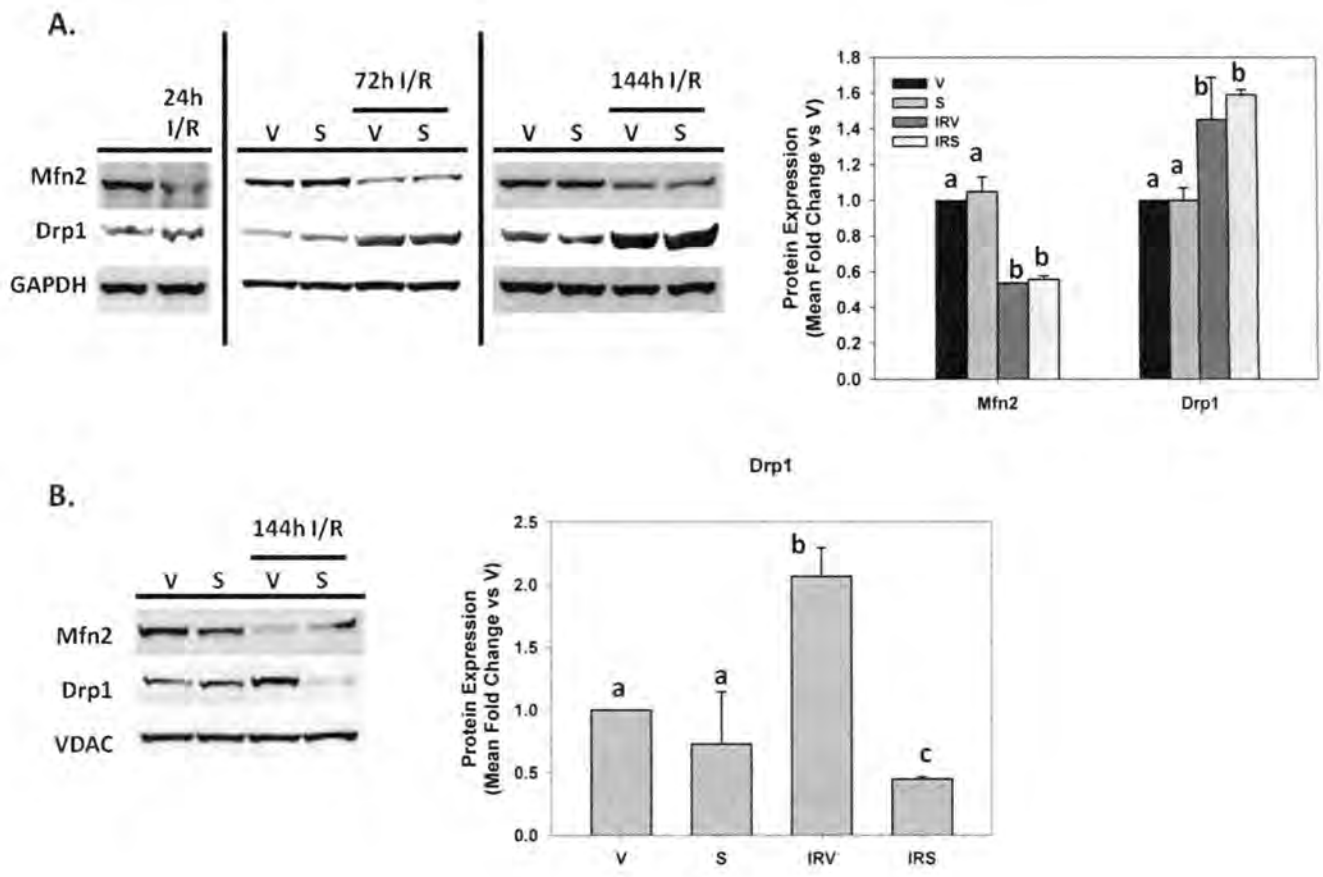
Figure 4-3. Mitochondrial-associated Drp1 is attenuated with SRT1720 treatment after I/R. (A) Mfn2 and Drp1 expression are examined by immunoblot analysis in renal cortical samples at 24h, 72h, and 144h. Densitometric quantification of 144h expression is shown in the graph to the right of the representative blots. (B) Mfn2 and Drp1 expression in mitochondria isolated from the renal cortex at 144h with densitometric quantification of Drp1 expression in the graph to the right of representative blots.

Because reduced expression of oxidative phosphorylation proteins and altered mitochondrial fission/fusion can have significant effects on mitochondrial function, we next examined mitochondrial respiratory capacity in each of the groups at 144h. Mitochondria isolated from the renal cortex of the rats were examined for state 2 and uncoupled oxygen consumption (QO_2) (Fig 4-4). Correlating with the observed decrease oxidative phosphorylation protein expression, state 2 respiration of mitochondria from IRV was down approximately 20% compared to V rats, and FCCP-uncoupled respiration was reduced approximately 40% compared to V rats (Fig 4-4). SRT1720 treatment restored both state 2 and uncoupled respiratory capacity at 144h after I/R compared to IRV rats.
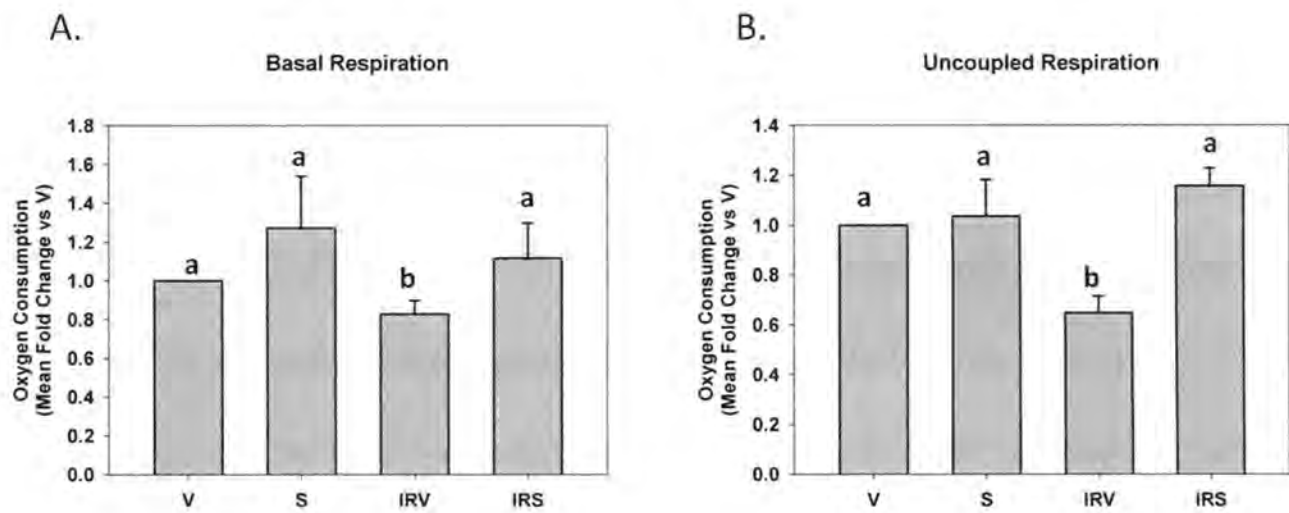
Figure 4-4. Mitochondrial QO₂ is restored in SRT1720-treated rats. (A) State 2 or basal QO_2 was examined in mitochondria isolated from the renal cortex at 144h. (B) Uncoupled QO_2 was examined in mitochondria isolated from the renal cortex at 144h by adding 1µM FCCP after state 2 QO_2 was recorded. Rates were calculated at nmol O_2/min/mg protein and expressed at mean fold change compared to the V group. Different superscripts indicate data are significant different each other ($p < 0.05$), n=4.

We next examined the effect of restoration of mitochondrial function on recovery of renal function in rats after AKI. Serum creatinine (SCr) measurements indicated that maximal organ dysfunction occurred at 24h after reperfusion, similar to our previous results in mice (Fig 4-5). In both IRV and IRS rats, there was a slow, equal and consistent recovery of SCr to control levels over the course of the 144h study period (Fig 4-5). These results suggest there was complete recovery of glomerular filtration in both SRT1720- and vehicle-treated rats after injury.
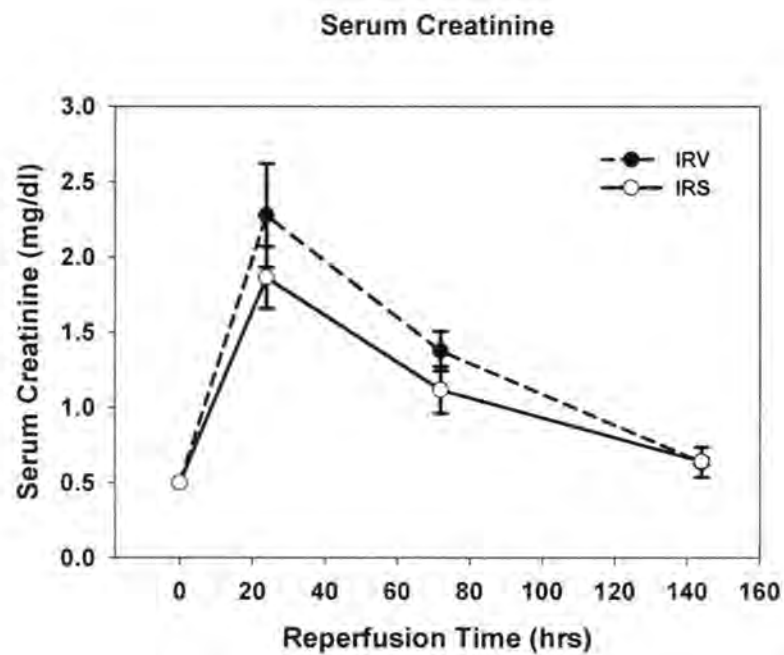
Figure 4-5. Glomerular filtration recovered in rats after I/R. Serum Creatinine (SCr) was monitored in rats after I/R to gauge recovery of renal function.

Kim-1 is a specific marker of kidney injury with tubular damage (117). It is upregulated early after injury, and continues to be expressed until the tubular epithelium has recovered (131). Kim-1 is a transmembrane protein with a large ectodomain that is cleaved and excreted into the urine, and it has been substantiated as a promising biomarker for AKI (30). Urinary Kim-1 increased to maximal levels after I/R but did not decrease in either group during the 144h study period (Fig 4-6A), suggesting that persistent tubular damage is occurring in the rats after injury even though glomerular filtration has recovered. Kim-1 protein was not expressed in kidneys of uninjured rats; however, it was robustly expressed in the renal cortex of IRV rats (Fig 4-6B). Although it was still expressed in the IRS rats, Kim-1 was attenuated with SRT1720 treatment at 144h. Examination of Kim-1 expression by immunohistochemistry (IHC) showed that it was only expressed in the I/R rats, and was localized to the apical membrane of the renal cortical tubules (Fig 4-6C). Most of the tubules expressing apical Kim-1 were dilated with flattened morphology (Fig 6Biii). There were also Kim-1 positive cells and cellular debris inside the tubular lumen, indicative of cell sloughing, a pattern that was previously reported (132). Some of the tubules showed diffuse Kim-1 cytoplasmic staining, particularly evident in the sections from IRS rats (Fig 6Civ). Overall, Kim-1 expression in cortical proximal tubules was reduced with SRT1720 treatment (Fig 4-6C).
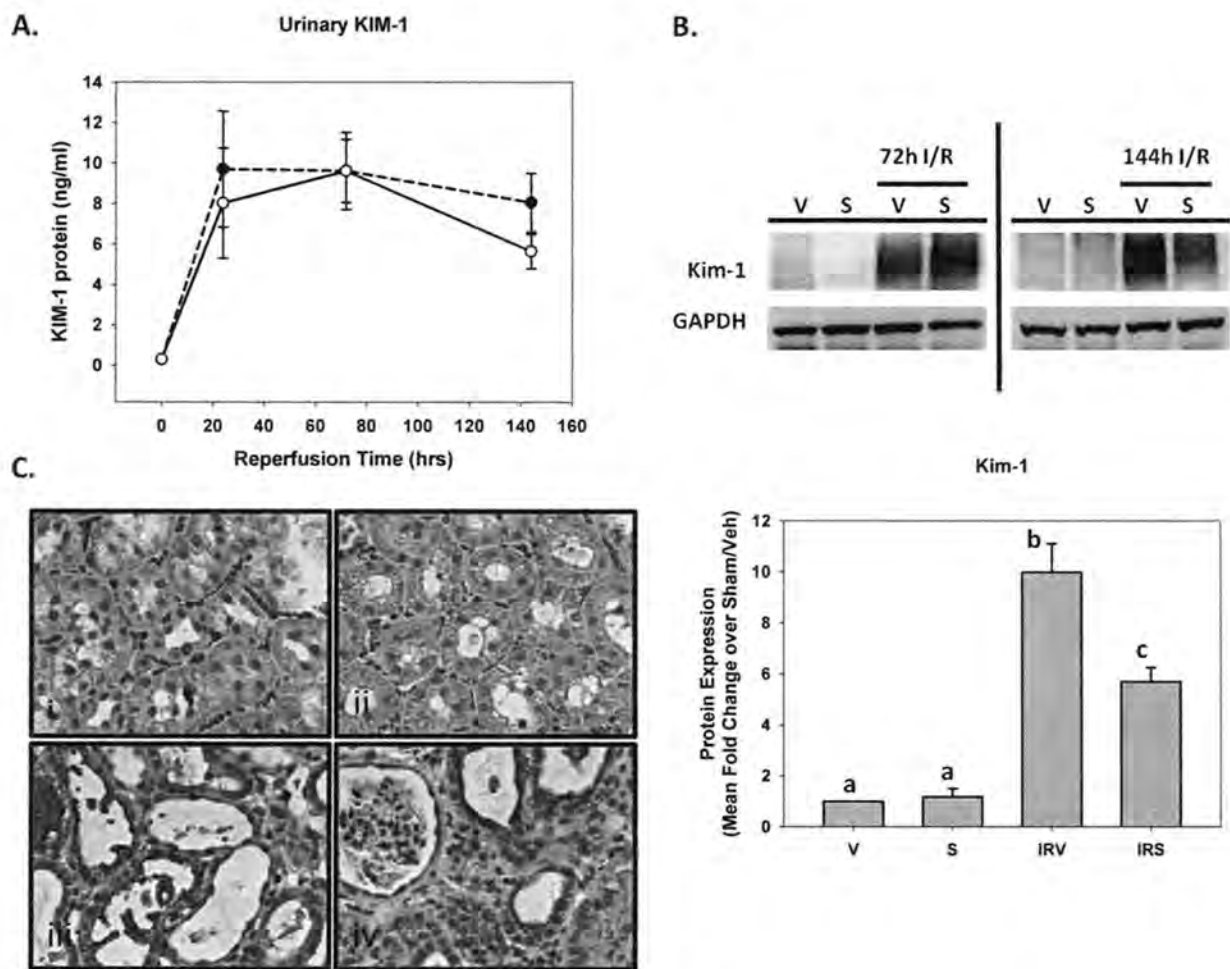
Figure 4-6. Kim-1 expression in renal cortex reduced in SRT1720-treated rats after I/R. (A) Urinary Kim-1 was measured at 24h, 72h, and 144h after I/R in SRT1720- and vehicle-treated rats by ELISA. (B) Kim-1 expression in renal cortical lysates was examined by immunoblot analysis at 72h and 144h. Densitometric quantification of 144h expression is shown in graph under the representative blots. (C) Kim-1 expression was examined by immunohistochemistry in the renal cortex of (i) V, (ii) S, (iii) IRV, and (iv) IRS rats. Brown stain indicates areas of Kim-1 immunoreactivity visualized by DAB development and hematoxylin counterstain.

Following injury, depolarized and dedifferentiated proximal tubule cells undergo numerous morphological and biochemical changes, which can be evident by alterations in the expression of various epithelial and mesenchymal markers (185, 302). One such alteration is the redistribution and loss of Na^+,K^+-ATPase expression early after injury in conjunction with loss of apical-basolateral polarity (4, 184-185). Additionally, the developmental marker vimentin, which is not typically expressed in the normal differentiated tubular epithelium, is increased after injury in proliferating cells (302). In our renal I/R model, Na^+,K^+-ATPase expression was reduced in IRV rats at 72 and 144h (Fig 4-7A). Expression of Na^+,K^+-ATPase was restored in rats treated with SRT1720at 144h after injury (Fig 4-7A). When evaluated by IHC, Na^+,K^+-ATPase was robustly expressed throughout the renal cortex, and localized to the basolateral membrane of proximal tubules (Fig 4-7Ci, Fig 4-7Cii and insets). In IRV rats, Na^+,K^+-ATPase expression was delocalized from the basolateral membrane and there was a generalized loss of expression throughout the renal cortex (Fig 4-7Ciii). With SRT1720 treatment, not only was expression restored (Fig 4-7A, Fig 4-7Civ), but also expression was localized to the basolateral membrane similar to what was observed in uninjured rats (Fig 4-7Civ inset). Vimentin was minimally expressed in uninjured rats, but was markedly elevated in IRV rats at 72h and 144h after injury (Fig 4-7B). Although it was still elevated compared to uninjured rats, vimentin expression was attenuated in IRS rats compared to the IRV rats at 144h (Fig 4-7B).
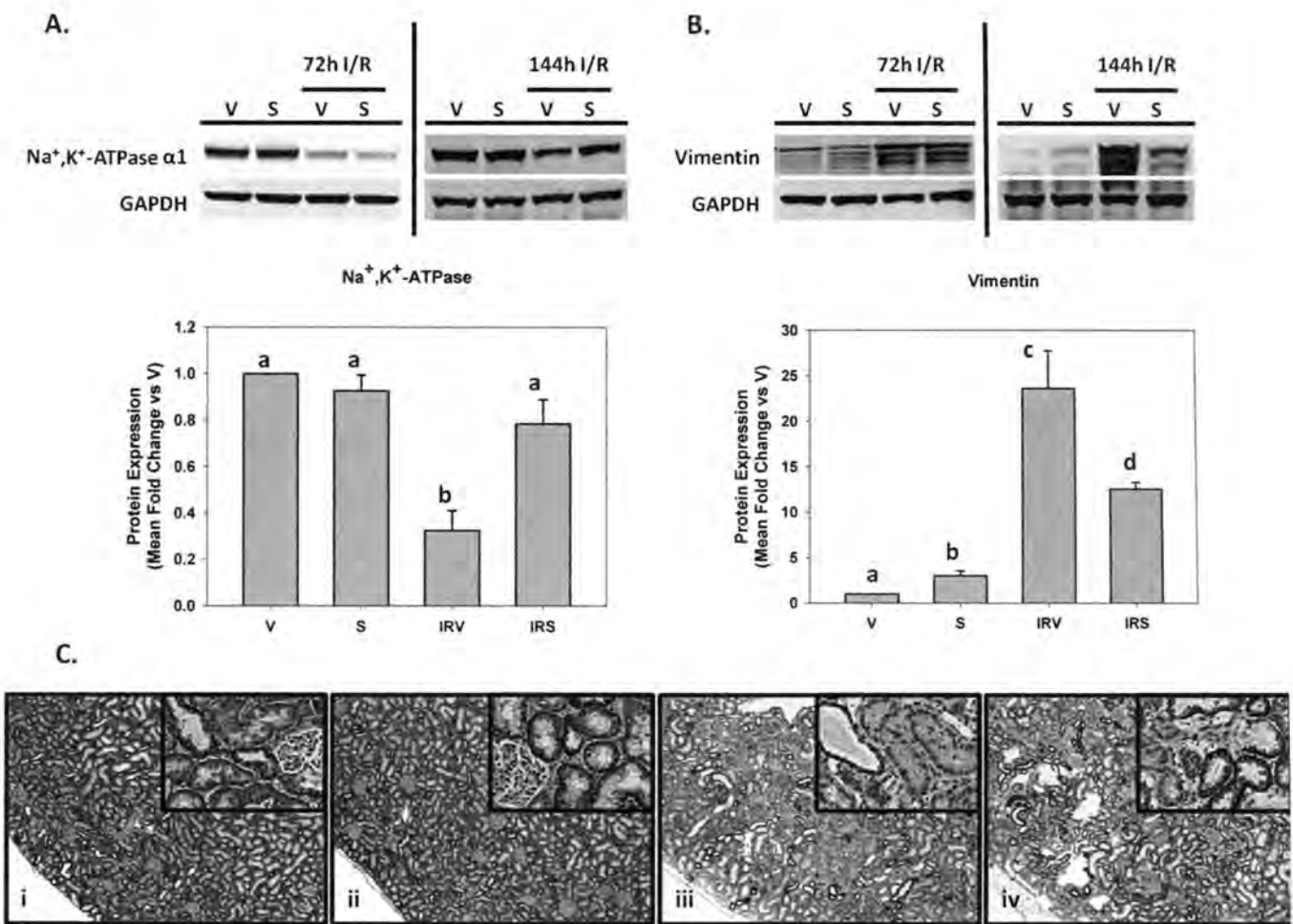
Figure 4-7. SRT1720 treatment restores polarized, differentiated proximal tubule after I/R. (A) Na$^+$,K$^+$-ATPase expression was examined in the renal cortex by immunoblot analysis at 72h and 144h. Densitometric quantification of expression at 144h is shown in the graph below the representative blots. (B) Vimentin expression was examined in the renal cortex by immunoblot analysis at 72h and 144h. Densitometric quantification of expression at 144h is shown in the graph below the representative blots. (C) Immunohistochemical localization of Na$^+$,K$^+$-ATPase expression was analyzed at 144h in (i) V, (ii) S, (iii) IRV, and (iv) IRS rats. Brown staining indicates Na$^+$,K$^+$-ATPase immunoreactivity visualized by DAB development and hematoxylin counterstain. Lower magnification images are at 10X and higher magnification insets are at 40X.

Histological examination by Periodic acid Schiff (PAS) staining showed that uninjured rats treated with SRT1720 or vehicle had normal tubule structure consistent with normal proximal tubule cell morphology and an intact brush border (Fig 4-8, Veh and SRT panels). 144h after I/R, rats give vehicle treatment displayed evidence of proximal tubule disruption, including tubule dilation, loss of brush border integrity, and flattened epithelial cell morphology (IRV, arrowheads).
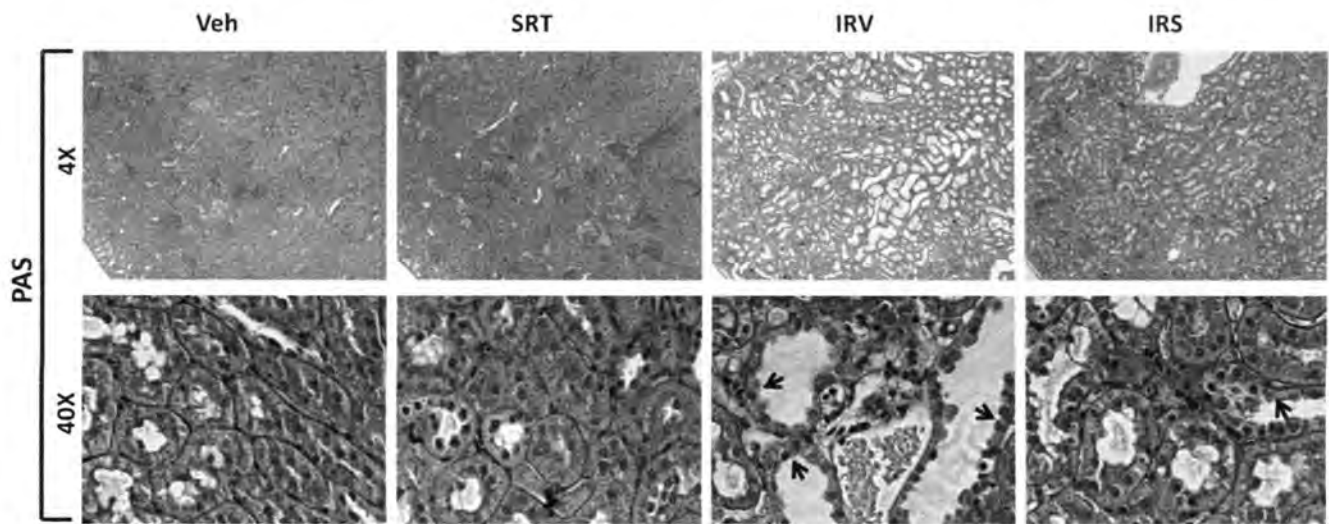
Figure 4-8. Improved tubule histology with SRT1720 treatment after AKI.
Uninjured rats displayed normal proximal tubule morphology when examined by PAS
staining. Histological evidence of tubule disruption was observed 144h after I/R plus
vehicle treatment (IRV) was characterized by tubule dilation, loss of brush border, and
flattened cell morphology (arrowheads). Although still observed in SRT1720-treated
rats after I/R (IRS), tubule disruption appeared to be less extensive compared to IRV
rats.

DISCUSSION

In this study we have shown that SRT1720 stimulates renal mitochondrial biogenesis *in vivo*, and by treating rats with SRT1720 after renal ischemia-reperfusion (I/R), recovery of mitochondrial and tubular function was expedited. The effects of SRT1720 were also associated with PGC-1α deacetylation, suggesting the mechanism of action is through a SIRT1-mediated pathway. Overall, we think that using agents that improve mitochondrial function after AKI may offer unique therapeutic benefits to aid in restoration of kidney function. These agents may also offer new therapeutic strategies for treating injuries and/or diseases of other organs which are plagued by mitochondrial dysfunction.

Mitochondrial protein expression was restored in kidneys from rats treated with SRT1720. We have previously shown that proteins such as ATPB, NDUFB8, and COX I are depleted early after AKI (either I/R-mediated or glycerol-induced myoglobinuric AKI) and are not restored within at least 144h after injury (91). Not only did we observe restored protein expression, but also we observed reduced mitochondrial-associated Drp1, suggesting that mitochondrial fragmentation was diminished in SRT1720-treated rats after I/R. The influence of Drp1, Mfn, and mitochondrial fragmentation on apoptosis and exacerbation of injury has been well documented in several studies from Zheng Dong's group (38-40), and inhibiting this response protects the kidney from further injury after I/R. Additionally, we were able to demonstrate recovery of mitochondrial respiratory capacity following SRT1720 treatment, indicating that restoration of the protein markers correlated with rescued mitochondrial function. The significance of

recovery of mitochondrial function after AKI is not completely understood yet. However, we have previously shown that persistent loss of mitochondrial protein expression correlates with persistent tubule dysfunction after injury (91). The current study further supports other studies which have demonstrated the beneficial effects of SRT1720, and other SIRT1 activators, in models of mitochondrial deficiency (85, 178, 180). This is the first study, however, to demonstrate that SRT1720 can rescue mitochondrial function following an acute organ injury with mitochondrial damage. Our results are also in agreement with previous reports that SRT1720 treatment results in SIRT1 activation and deacetylation of PGC-1α (85, 180).

As expected, serum creatinine was significantly elevated 24h after injury and recovered over the course of 144h. SRT1720 treatment did not alter recovery of SCr compared to vehicle treatment after injury. This was not unexpected as SCr recovered fairly fast without intervention. Additionally, SCr is not specific for the type of injury present and thus is not the best marker for diagnostic differentiation between prerenal, intrinsic, or postrenal AKI, and to determine whether acute tubular necrosis is present or not. We examined Kim-1 in the urine and tissue from the rats in our study and found that cortical proximal tubule Kim-1 expression was persistently elevated after I/R. In both tissue lysates as well as within the urine, Kim-1 was robustly elevated and did not recover over the 144h study period, suggesting that there was persistent tubule damage present. Rats treated with SRT1720 after injury had reduced Kim-1 expression in kidney lysates compared to vehicle-treated rats, suggesting that at least some of the injury was reversed with treatment. Kim-1 has emerged as specific marker proximal tubule damage

associated with kidney injury, and there is evidence that it is more effective as a diagnostic and prognostic indicator of kidney injury compared to traditional markers such as SCr and BUN (31). Human KIM-1 is also up-regulated in dedifferentiated proximal tubules in human renal disease (282). KIM-1 was elevated in biopsy and urine samples, and co-localized with α-smooth muscle actin (α-SMA), aquaporin, and vimentin indicating KIM-1 was expressed in undifferentiated proximal tubule cells, and was associated with interstitial macrophages and fibrosis (282). Our Kim-1 results are consistent with the vimentin results indicating that SRT1720 treatment expedites recovery of a normal, differentiated tubule epithelium. Additionally, our results are consistent with reports from human disease models, which suggest that the models and therapeutic interventions have potential clinical relevance.

Na^+,K^+-ATPase expression was lost in the renal cortex of rats after I/R and expression was not restored within 144h, indicating a prolonged state of depolarization. Additionally, vimentin expression was robustly up-regulated at 72h and 144h after injury, suggesting a dedifferentiated state as the epithelium was still undergoing repair processes. SRT1720 treatment restored Na^+,K^+-ATPase expression and normalized vimentin expression in I/R rats, suggesting that restoration of a polarized, differentiated tubular epithelium was expedited in rats treated with SRT1720 after injury compared to vehicle-treated rats. The observation that markers of cell polarity and differentiation were restored within approximately 6 days may have significant clinical significance, especially in context with our unpublished observations in mouse I/R studies that these markers are not normalized until approximately two weeks after injury in untreated

animals. The connection between rescue of mitochondrial function and restoration of cell polarity and differentiation is not completely understood yet, but the results are consistent with previous studies in our lab which have correlated restoration of mitochondrial function with RPTC redifferentiation, polarization, and repair after oxidant injury (115, 220).

Seo-Mayer, et al., demonstrated that basolateral expression of the Na^+,K^+-ATPase may be preserved by activating AMPK prior to I/R (247). The authors suggest that, in the face of energy-deprivation, stimulation of AMPK may alleviate some of the epithelial cell damage by activating energy-conserving pathways. Indeed, Na^+,K^+-ATPase expression and function may be regulated by AMPK and AMPK family members, such as the salt-inducible kinases (268). It is possible that similar energy-salvaging mechanisms are activated upon SIRT1 activation which are restoring Na^+,K^+-ATPase expression and localization after I/R, although this has yet to be shown. Several reports have also indicated that SRT1720, and other reported SIRT1 activators, in fact activate AMPK, but we have not observed this effect in the current study or previously (90), so we assume its effects are through SIRT1 and not AMPK. AMPK and SIRT1 pathways seem to converge quite often and have been suggested to even work synergistically on PGC-1α activation (47-49). In muscle, it has been shown that AMPK and PGC-1α regulate Na^+,K^+-ATPase expression and function (134), as AMPK regulated phosphorylation of the PLM subunit, an important regulatory subunit of the Na^+,K^+-ATPase, and expression of the α1 and α2 subunits was significantly reduced in PGC-1α KO. As a modulator of PGC-1α activity/expression after injury, SRT1720 treatment may be manipulating one or

a combination of these pathways to preserve Na$^+$,K$^+$-ATPase expression after I/R. Although we did not observe any direct evidence of AMPK activation with SRT1720 treatment in our model, it is possible that the combined effects of AMPK activation after injury with SRT1720-induced SIRT1 activation modulated Na$^+$,K$^+$-ATPase expression via PGC-1α or some other mechanism.

SIRT1 regulates many functions in the cell and it is possible that SRT1720 treatment activated recovery mechanisms not related to its effects on mitochondrial function. Mice overexpressing SIRT1 specifically within the kidney were protected against cisplatin-induced nephrotoxicity (119). Although they observed sufficient protection of mitochondrial function, but not mitochondrial numbers, in the SIRT1 transgenic mice (Tg), the authors attributed the protection to a preservation of peroxisome function after injury. Retaining peroxisome numbers increased levels of catalase, thus reducing ROS and apoptosis and retaining kidney function (119). The authors also examined I/R injury in the Tg mice, but did not see any protection in this model. We did not examine peroxisome numbers or function in the current study, so it is possible that SRT1720 treatment had a similar effect that we are not reporting. However, it should be noted that in our model, SIRT1 stimulation does not commence until 24h after reperfusion when tissue injury is extensive and when functional markers such as SCr have reached peak levels. In the SIRT1 Tg mice, there was significant protection from tissue damage, thus there are inherent differences in how the injured cells may respond to SIRT1 activation under different conditions. It is conceivable that a cell with severely depleted mitochondrial numbers and function may respond quite differently to a SIRT1/PGC-1α

activator compared to a cell with largely retained function. It must also be pointed out that there are different conclusions which can be drawn from various renal biomarkers and may reflect specific (or non-specific) functional implications. Whereas Hasegawa, et al., reported protection of kidney function based on attenuated SCr and BUN levels, we did not see any changes in SCr, but instead observed recovery of markers associated with proximal tubule polarity and function (Kim-1, Na^+,K^+-ATPase, vimentin).

In conclusion, treatment with the SIRT1 activator SRT1720 improved renal cortical mitochondrial function following I/R within 6 days after injury. Restoration of mitochondrial function correlated with normalization of proximal tubule polarization and differentiation. Recovery of mitochondrial function following AKI appears to be an essential component of the recovery process, in particular for recovery of normal proximal tubule function. SIRT1 activation and other compounds which target PGC-1α activity and/or expression offer unique therapeutic options to improve tubule repair after injury.

Chapter 5:

Conclusions and Future Directions

Conclusions

Lethal and sublethal injury to the proximal tubule epithelium contributes to tubule and overt organ dysfunction after acute kidney injury. Repair of the tubule epithelium is essential for proper functional recovery. Mitochondrial dysfunction is a primary mechanism of subcellular injury during AKI, and restoration of mitochondrial function may offer unique therapeutic targets to improve renal repair after injury.

In cell models of reperfusion injury using the oxidant tertbutyl hyrdroperoxide (TBHP), mitochondrial biogenesis is induced during recovery of mitochondrial function (220). Additionally, promoting mitochondrial biogenesis through PGC-1α overexpression expedites recovery of mitochondrial and cellular functions in renal proximal tubule cells (RPTC) after TBHP injury (221).

Initially, it was essential to identify compounds that induce mitochondrial biogenesis in renal cells. Our laboratory had identified several compounds which increase mitochondrial protein expression and function in RPTC, including several compounds identified as SIRT1 activators and the 5-hydroxytryptamine IIB receptor agonist DOI (223-224). SIRT1 activation was a promising target to induce mitochondrial biogenesis,

and a report identifying potent SIRT1 activators identified the compound SRT1720 as a potent SIRT1 agonst (178).

SRT1720 was a potent SIRT1 activator when tested in an in vitro assay for SIRT1-mediated deacetylase activity, induced PGC-1 deacetylation , and stimulated mitochondrial biogenesis in RPTC. Although it was indirect evidence of mitochondrial biogenesis, we observed increased mitochondrial protein expression, increased mitochondrial DNA, increased basal and FCCP-uncoupled mitochondrial oxygen consumption, and elevated total cellular ATP levels with only 24h exposure of 1-10μM SRT1720. The results suggested that we had identified a potent activator of mitochondrial biogenesis, and this was the first report to show SRT1720 effects in primary renal cells. Prior to our report, SRT1720 had been examined in skeletal muscle cell lines and with chronic treatment (weeks to months) in animals (85, 178, 251). SRT1720 stimulated pathways consistent with mitochondrial biogenesis and effectively reversed conditions associated with metabolic deficiencies primarily eliciting its effects in the skeletal muscle and liver. According to our results, SRT1720 was also effective in renal cells with a short exposure.

Studies from our laboratory have previously characterized an in vitro reperfusion injury model in primary RPTC (205). RPTC exposed to TBHP undergo significant cell death, and the surviving cells are sublethally injured. Mitochondrial function is disrupted early after oxidant exposure and remains interrupted for 96h to 144h. Mitochondrial function spontaneously recovers by 144h due to induction of PGC-1α mitochondrial biogenesis

(205, 220). When we treated injured cells with SRT1720, mitochondrial function was restored within 24h as opposed to the previously characterized 6 days. Uncoupled mitochondrial respiration and total cellular ATP levels were restored after 24h treatment with SRT1720. The results from this study were consistent with our recently published results examining serotonergic-regulated mitochondrial biogenesis following oxidant exposure (224). These studies were important because we were able to identify pharmacological agents that induced mitochondrial biogenesis in renal cells, and because we demonstrated that activating mitochondrial biogenesis after oxidant injury expedited recovery of mitochondrial function. Although the targeted mechanism appeared to work well in a cell model of renal injury, we still did not have evidence that it would work *in vivo* or if restoring mitochondrial function would affect recovery of renal function after acute kidney injury.

Since we had identified a compound that induced mitochondrial biogenesis in primary renal cells and expedited recovery of mitochondrial function in cells after oxidant injury, we sought to move the studies into an *in vivo* acute kidney injury model. One model, an ischemia-reperfusion injury model in the mouse, induces renal dysfunction within 24h after reperfusion. Mitochondrial dysfunction was a well-known consequence of I/R injury, but a full characterization of recovery of mitochondrial function after injury had not been described. Additionally, we sought to characterize mitochondrial dysfunction and recovery in a glycerol-induced myoglobinuric AKI model. Similar to the I/R model, the glycerol model induced renal dysfunction within 24h after injection. Mitochondrial dysfunction was also known to occur in the glycerol-mediated AKI model, but a

characterization of the mechanisms involved in recovery of mitochondrial function after injury had not been described.

Before we could test our biogenic compounds *in vivo* we needed to fully understand the consequences of AKI on mitochondrial function, as well as the mechanisms and time line for mitochondrial and organ repair. Therefore, we initially examined the endogenous dysfunction and repair associated with AKI. Because of the results we obtained in the RPTC injury model, we hypothesized that mitochondrial dysfunction would be reversed after the initial injury. We also hypothesized that mitochondrial biogenesis would be activated to restore mitochondrial function, and that restoration of mitochondrial function would correlate with recovery of organ function. We had evidence from preliminary studies that kidney function is maximally impaired at 24h after AKI (based on SCr), and function recovers over the course of approximately 144h. With that in mind, we decided to examine the extent of mitochondrial injury and recovery at various time points between onset of injury and until recovery of organ function at 144h. In both injury models, we observed persistent loss of mitochondrial electron transport chain proteins, disruption of fusion and fission proteins, and up-regulation of proteins associated with mitochondrial biogenesis. The persistent disruption in mitochondrial homeostasis was associated with sustained tubule pathology, even in the presence of recovered glomerular filtration. The results from this study revealed that there is persistent mitochondrial dysfunction after AKI, and induction of mitochondrial biogenesis later in the recovery period (72h – 144h) was not sufficient to restore mitochondrial protein expression. Therefore, our initial findings did not fit with our hypothesis because we did not see any

163

recovery of mitochondrial function at any time between 24h and 144h after injury. Probing further revealed the persistent tubule injury, and this was the site of mitochondrial dysfunction. Therefore, basing our studies on the time course of SCr recovery was not the best way to design the study because SCr levels do not represent tubule dysfunction. Results we have obtained since the study was published indicate that restoration of mitochondrial proteins, and normalization of fusion/fission proteins, takes approximately two weeks to return to normal levels. This was also the time it took for markers of tubule injury (e.g. kidney injury molecule-1) to return to normal in ischemic and nephrotoxic injury models (132), and for functional tubule proteins (e.g. Na^+,K^+-ATPase expression) to restore suggesting that recovery of mitochondrial function does in fact correlate with recovery of tubule function after injury.

Because mitochondrial proteins were disrupted for an extended period after AKI, we hypothesized that treating animals with an activator of mitochondrial biogenesis would expedite recovery of mitochondrial function and subsequently renal function. We had identified SRT1720 as an activator of mitochondrial biogenesis in renal cells in culture, and we sought to examine its effects in vivo after AKI. From preliminary studies in naïve mice, we determined that a dose of 5 mg/kg body weight effectively induced mitochondrial gene expression 24h after just one dose of SRT1720.

To test the effects of SRT1720 in an AKI model, we decided to test it in a rat I/R model. The rat I/R model was chosen for a couple of reasons: 1) although they reach a similar level of kidney dysfunction after I/R (based on SCr), the rats do not appear as sick as the

mice, so there are less compounding variables to consider in the model. 2) The majority of functional and injury biomarkers are analyzed in the urine, and the rat model consistently produces sufficient urine after injury to monitor function/injury. The mice, however, often become anuric after injury, thus limiting the number of markers which can be measured after injury. 3) Kidney injury molecule-1 (Kim-1) is a promising biomarker which is specifically up-regulated after tubule damage, and is expressed in the urine after injury. Currently, there are ELISAs available to measure Kim-1 in rat urine, but they are not yet available for mouse samples.

Rats were treated with a once-daily dose of SRT1720 (5 mg/kg) or vehicle starting 24h after I/R and markers of kidney and mitochondrial function were monitored after injury. SRT1720 did not restore mitochondrial protein expression at 72h after injury, but ATP synthase β, NDUFB8, and COX I were at least partially restored at 144h in SRT1720-treated rats after injury, whereas these proteins were still significantly depleted in vehicle-treated rats. Additionally, both state 2 and uncoupled mitochondrial respiration were depressed in I/R rats at 144h, but both of these functional parameters were completely restored in rats treated with SRT1720 rats after injury. These data were consistent with what we had previously reported in oxidant-injured RPTC, and demonstrated that *in vivo* treatment with SRT1720 after injury restores mitochondrial function, albeit within 144h as opposed to 24h observed in cells.

We had previously demonstrated that tubule disruption persists in our I/R model, even as glomerular filtration and SCr levels recover (91). Because we had correlated persistent

mitochondrial dysfunction with sustained tubule pathology, we hypothesized that by restoring mitochondrial function, we would restore tubule function. Kidney injury molecule-1 (Kim-1), a protein which is expressed after tubule damage, was robustly and persistently up-regulated after I/R. Treatment with SRT1720 after ischemia diminished Kim-1 expression in renal cortical tissue. Expression of Kim-1 is also associated with undifferentiated, depolarized tubule epithelial cells. Loss of Na^+,K^+-ATPase expression occurs early after ischemic injury and is characteristic of transition to mesenchymal-type cells and loss of basolateral-apical polarity. Additionally, vimentin is a developmental intermediate filament expressed in dedifferentiated cells and is a marker of epithelial-mesenchymal transition. Loss of Na^+,K^+-ATPase expression was evident in both immunoblot analyses and by immunohistochemistry. SRT1720 treatment restored expression of Na^+,K^+-ATPase after injury. Vimentin expression was markedly increased after injury, and treatment with SRT1720 attenuated expression by 144h. These results suggest that the proximal tubule epithelium undergoes prolonged dedifferentiation and depolarization as surviving cells repair the damaged tubule. SRT1720 restored expression of Na^+,K^+-ATPase and normalized vimentin expression suggesting that treatment expedited recovery of the polarized, functional proximal tubule.

Taken together, these results indicate that recovery of mitochondrial function is associated with restoration of a normal, differentiated proximal tubule epithelium. Mitochondrial biogenesis is a component of recovery of mitochondrial function after AKI, but it is a delayed process that takes several weeks to restore mitochondrial protein expression and function without intervention. SRT1720 enhances mitochondrial

biogenesis by activating the master regulator PGC-1α via SIRT1-mediated deacetylation. We have demonstrated in both the RPTC oxidant injury model as well as an *in vivo* AKI model that stimulating mitochondrial biogenesis with SRT1720 expedites recovery of mitochondrial function after injury. Restoration of mitochondrial function was associated with recovery of cell and organ function, suggesting that PGC-1α and mitochondrial biogenesis is a viable target that warrants further attention as a potential therapeutic intervention for AKI.

Future Directions

Mitochondrial biogenesis was initiated after I/R or glycerol-mediated AKI. When we examined alterations in gene expression associated with AKI, we observed increased expression of the nuclear co-activator PGC-1α. However, we also observed a robust increase in the PGC-1 family member PGC-1 related co-activator (PRC) (Fig 5-1). In addition to its elevation after glycerol-induced AKI, PRC was also robustly increased after I/R AKI as well. PRC is a ubiquitously expressed protein, and has also been associated with mitochondrial biogenesis, although the information on it is much scarcer than it is for PGC-1α or PGC-1β. We did not see PGC-1β increase after injury, suggesting that it does not contribute to recovery of mitochondrial function. It would be interesting to distinguish the roles of each PGC-1 family member after AKI, and to verify that induction of PGC-1 was essential for recovery from AKI. To accomplish this, we would need to take advantage of either conditional knockouts or siRNA in vivo to knock down expression of each family member to see how it affects recovery of mitochondrial and organ function after AKI. We attempted to use siRNA to reduce PGC-1α expression in vivo; however, due to either a dosing/timing issue or other technicality, we were not able to successfully knock down expression. Further studies distinguishing the potential roles of different mediators of mitochondrial biogenesis may be of interest to help identify novel targets to pursue to rescue mitochondrial function after injury.
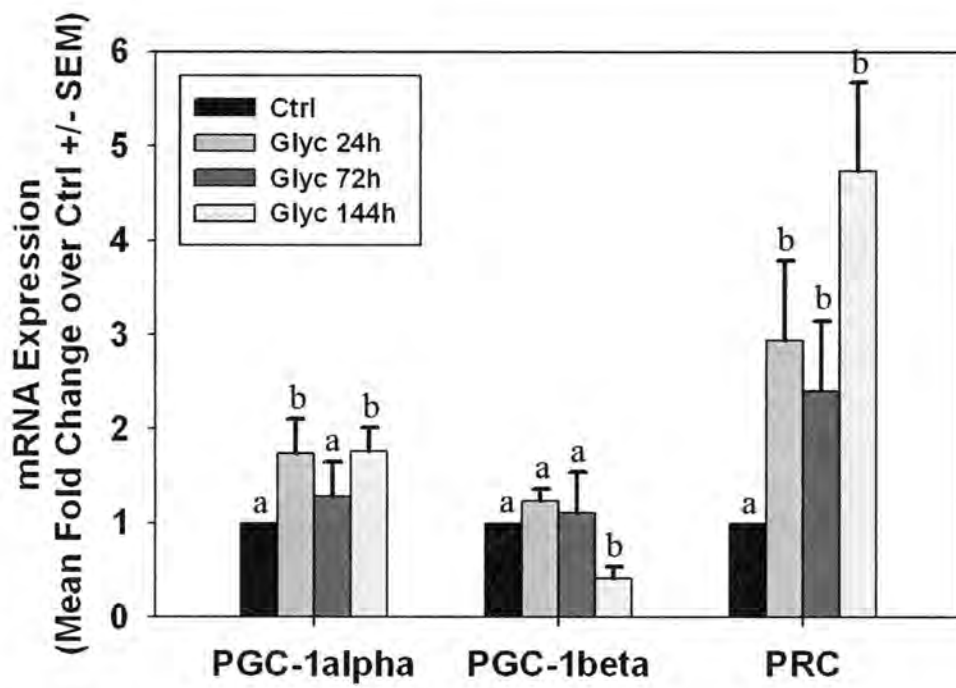
Figure 5-1. Increased PGC-1 mRNA after AKI. mRNA expression of PGC-1 family members PGC-1α, PGC-β, and PRC were examined by qRT-PCR at 24h, 72h, and 144h after glycerol-induced AKI.

Our laboratory is currently testing a number of compounds that increase PGC-1α activity and/or expression. A recent publication by Wills L, et al., demonstrated that the β2 adrenergic receptor agonist formoterol increases PGC-1α expression in RPTC and induces mitochondrial biogenesis in cell cultures and in the mouse kidney *in vivo* (300). We have tested this compound in the mouse I/R model. Treatment with formoterol partially restored mitochondrial gene expression that is depleted after injury (Fig 5-2). Mice were administered either formoterol (0.1 mg/kg) or vehicle starting at 24h after I/R, and were euthanized at 72h after injury. Illustrated below, expression of PGC-1α, NRF-1, ATP synthase β, ND1, and COX I were depleted after injury, but were partially recovered in mice treated with formoterol.
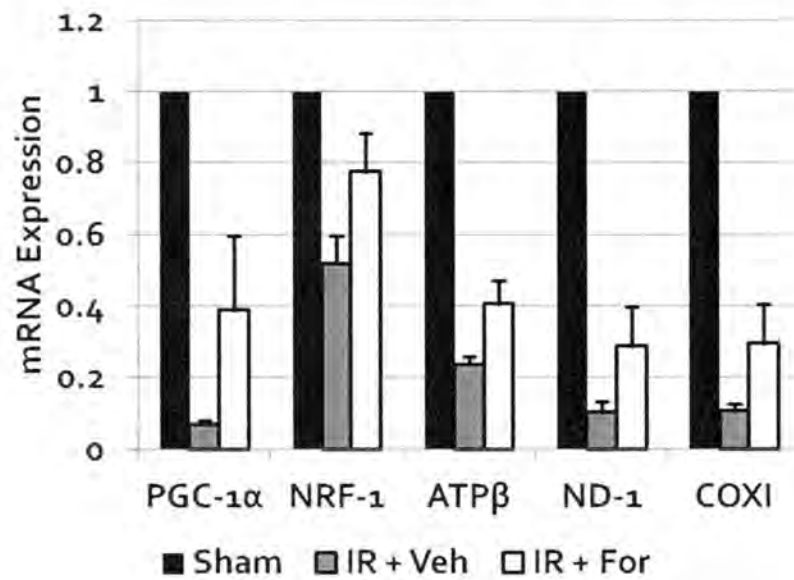
Figure 5-2. Formoterol treatment after I/R partially restores mitochondrial gene expression. mRNA expression of genes associated with mitochondrial function and mitochondrial biogenesis were examined by qRT-PCR in mice treated with formoterol (IR + For) or vehicle (IR + Veh) after I/R. Expression of PGC-1α, NRF-1, ATP synthase β, ND-1, and COX I were examined at 72h after ischemic injury.

Additionally, restoration of mitochondrial gene expression was associated with recovery of kidney function, including SCr and urinary glucose levels (Fig 5-3). Further studies need to be pursued using formoterol (and possibly other β2 adrenergic agonists) after injury to determine the effect on recovery of tubule function. Because we observed recovery of Kim-1 expression, Na,K-ATPase expression, and normalization of vimentin expression with SRT1720 treatment, using another drug to promote mitochondrial biogenesis after injury may help validate PGC-1 and restoration of mitochondrial function as a common prerequisite for recovery of normal tubule function.
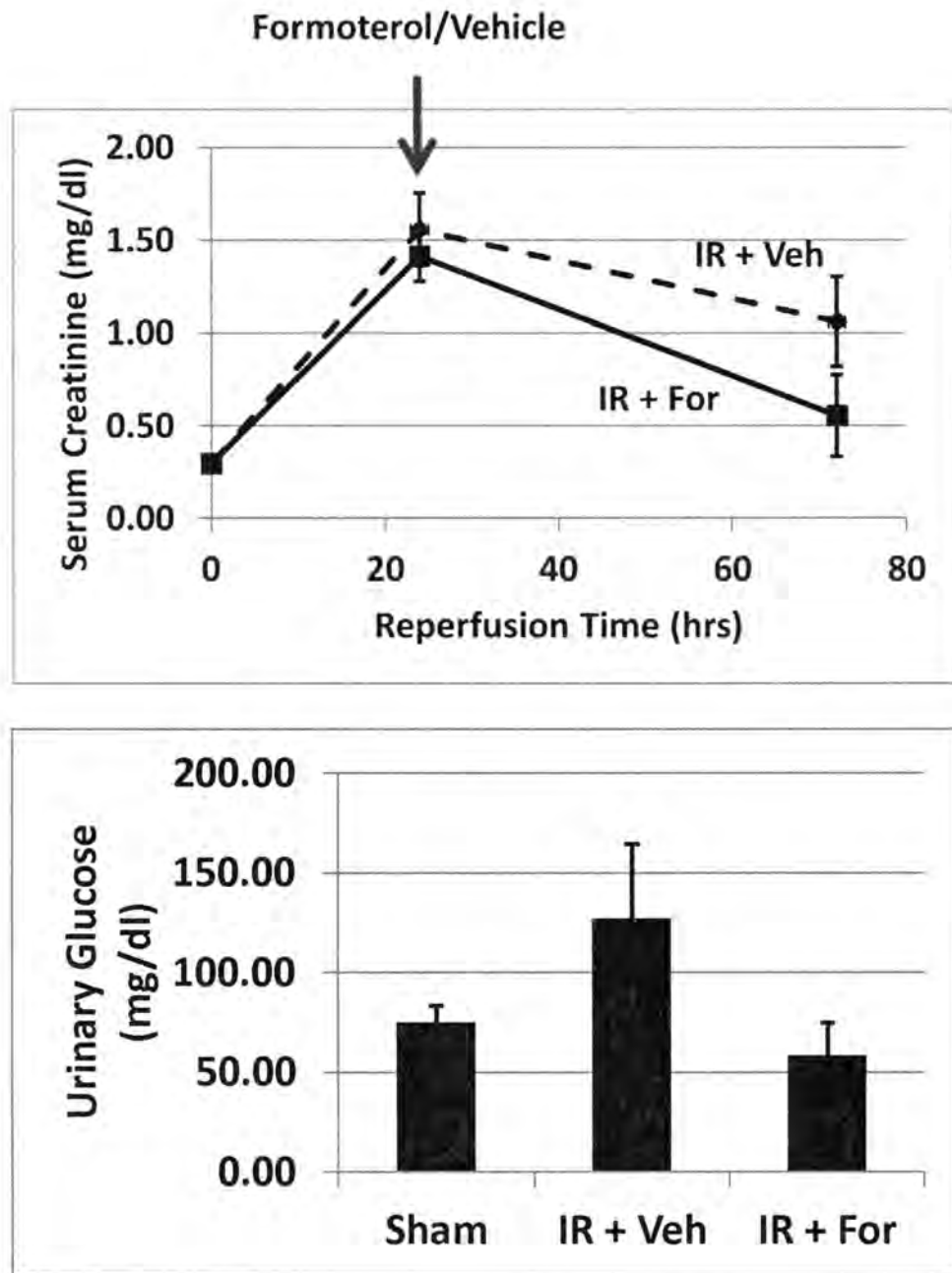
Figure 5-3. Formoterol promotes recovery of SCr and urinary glucose levels after I/R. Mice were administered formoterol (0.1 mg/kg) or vehicle 24h after I/R until they were euthanized at 72h. SCr was monitored during recovery, and urinary glucose levels were examined at 72h to assess kidney function.

SRT1720 induces mitochondrial biogenesis in kidneys of mice within 24h after a single injection (5 mg/kg, i.p.). Mitochondrial biogenesis is also activated in other organs, including the skeletal muscle (Fig 5-4), and the liver, heart, and brain (not shown). Chronic treatment with SRT1720 in diabetic and obesity models improves glucose tolerance, insulin sensitivity, and reduces cholesterol, triglyceride levels, and weight gain while promoting a number of other improvements in overall health, such as improved locomoter activity and reduced liver inflammation and steatosis (178, 180). It would be interesting to examine the potential benefits of SRT1720 treatment in models of acute organ injuries to organs outside of the kidney. Enhancing mitochondrial biogenesis after acute injuries to other organs which result in mitochondrial dysfunction may offer unique therapeutic targets for treating these disorders.
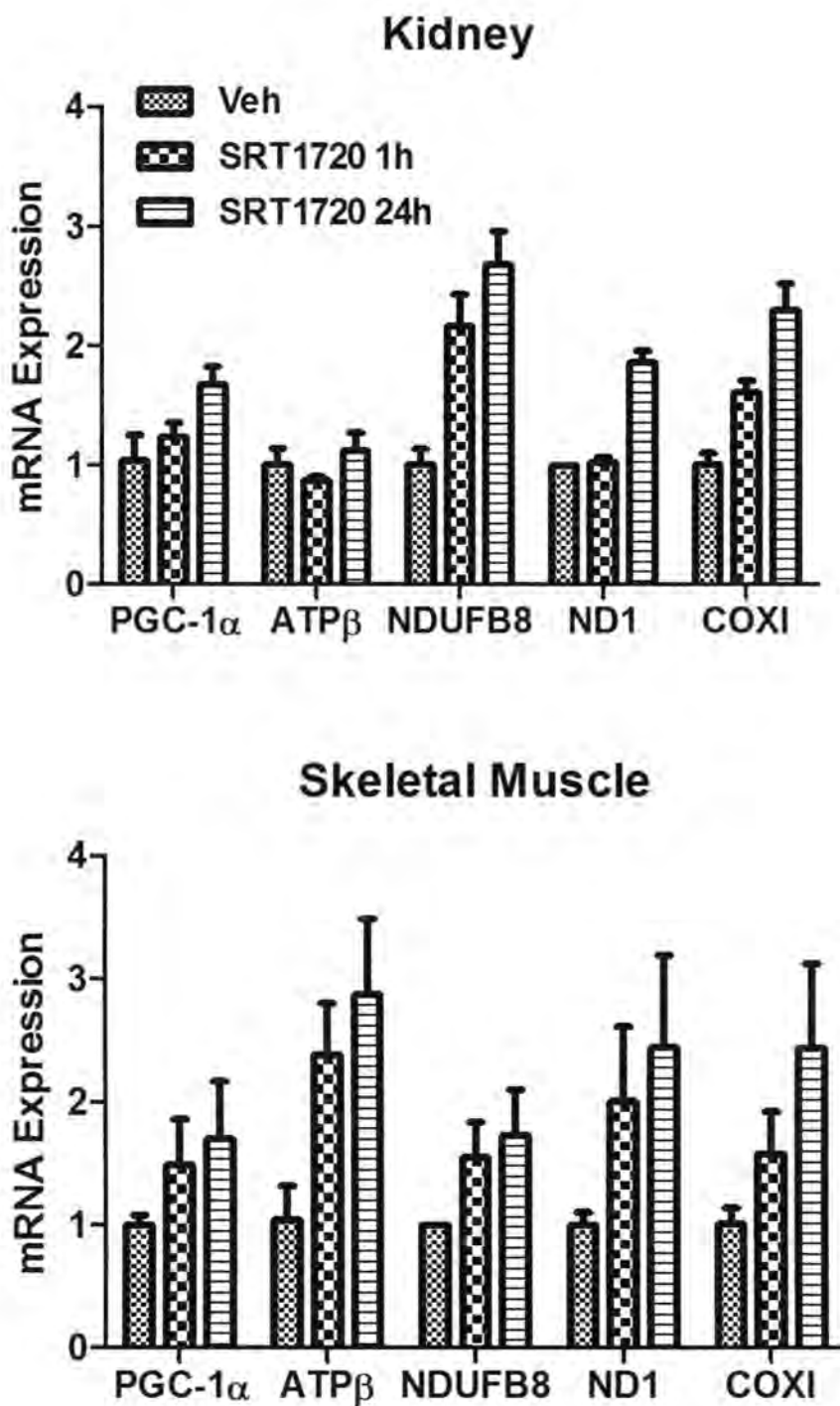
Figure 5-4. SRT1720 increases mitochondrial biogenesis in mouse kidney and skeletal muscle. mRNA expression of genes associated with mitochondrial function and biogenesis was examined in the kidney and skeletal muscle of mice at one hour and 24h after a single injection (5 mg/kg, i.p.).

The experiments in my studies were carried out in approximately 8-week old mice or rats, representing an age group in humans that does not typically have a high incidence of AKI. AKI incidence is generally higher in older and diabetic populations. These populations also tend to have lower rates of mitochondrial biogenesis and diminished mitochondrial function compared to healthy, younger groups. Additionally, we have performed I/R in diabetic rats, and have observed an increased susceptibility to I/R injury (Fig 5-5). It would be interesting to characterize the mitochondrial injury associated with I/R in a diabetic rat model, or aged mouse model, and the influence of mitochondrial biogenesis on restoration of mitochondrial function. Additionally, it would be interesting to examine the effects of SRT1720 treatment, or another agent which promotes mitochondrial biogenesis, in the more susceptible animal model to determine whether biogenesis is a viable target for populations which are more at risk to develop AKI.
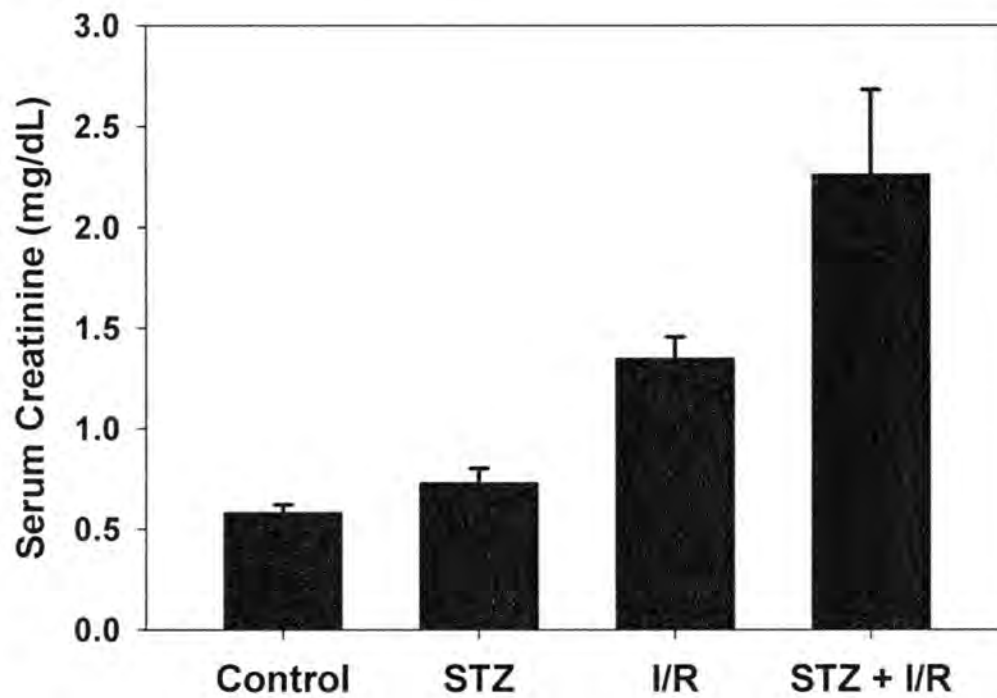
Figure 5-5. Diabetic rats are more susceptible to the effects of I/R. Four weeks after streptozotocin (STZ) treatment, a model to induce diabetes, rats were subjected to 22m I/R. Weight-matched controls were also subjected to I/R to compare development of AKI. Twenty-four hours after I/R, SCr was examined to assess renal function.

REFERENCES

1. Abdel-Zaher, A.O., R.H. Abdel-Hady, M.M. Mahmoud, and M.M. Farrag. The potential protective role of alpha-lipoic acid against acetaminophen-induced hepatic and renal damage. *Toxicology* 243(3): 261-70, 2008.

2. Abul-Ezz, S.R., P.D. Walker, and S.V. Shah. Role of glutathione in an animal model of myoglobinuric acute renal failure. *Proc Natl Acad Sci U S A* 88(21): 9833-7, 1991.

3. Adelstein, R.S. and E. Eisenberg. Regulation and kinetics of the actin-myosin-ATP interaction. *Annu Rev Biochem* 49: 921-56, 1980.

4. Alejandro, V.S., W.J. Nelson, P. Huie, R.K. Sibley, D. Dafoe, P. Kuo, J.D. Scandling, Jr., and B.D. Myers. Postischemic injury, delayed function and Na+/K(+)-ATPase distribution in the transplanted kidney. *Kidney Int* 48(4): 1308-15, 1995.

5. Arany, I. and R.L. Safirstein. Cisplatin nephrotoxicity. *Semin Nephrol* 23(5): 460-4, 2003.

6. Asif, A., G. Garces, R.A. Preston, and D. Roth. Current trials of interventions to prevent radiocontrast-induced nephropathy. *Am J Ther* 12(2): 127-32, 2005.

7. Attardi, G. and G. Schatz. Biogenesis of mitochondria. *Annu Rev Cell Biol* 4: 289-333, 1988.

8. Aust, S.D., L.A. Morehouse, and C.E. Thomas. Role of metals in oxygen radical reactions. *J Free Radic Biol Med* 1(1): 3-25, 1985.

9. Bach, D., S. Pich, F.X. Soriano, N. Vega, B. Baumgartner, J. Oriola, J.R. Daugaard, J. Lloberas, M. Camps, J.R. Zierath, R. Rabasa-Lhoret, H. Wallberg-Henriksson, M. Laville, M. Palacin, H. Vidal, F. Rivera, M. Brand, and A. Zorzano. Mitofusin-2 determines mitochondrial network architecture and mitochondrial metabolism. A novel regulatory mechanism altered in obesity. *J Biol Chem* 278(19): 17190-7, 2003.

10. Bach, D., D. Naon, S. Pich, F.X. Soriano, N. Vega, J. Rieusset, M. Laville, C. Guillet, Y. Boirie, H. Wallberg-Henriksson, M. Manco, M. Calvani, M. Castagneto, M. Palacin, G. Mingrone, J.R. Zierath, H. Vidal, and A. Zorzano. Expression of Mfn2, the Charcot-Marie-Tooth neuropathy type 2A gene, in human skeletal muscle: effects of type 2 diabetes, obesity, weight loss, and the regulatory role of tumor necrosis factor alpha and interleukin-6. *Diabetes* 54(9): 2685-93, 2005.

11. Badr, K.F., V.E. Kelley, H.G. Rennke, and B.M. Brenner. Roles for thromboxane A2 and leukotrienes in endotoxin-induced acute renal failure. *Kidney Int* 30(4): 474-80, 1986.

12. Barger, P.M., A.C. Browning, A.N. Garner, and D.P. Kelly. p38 mitogen-activated protein kinase activates peroxisome proliferator-activated receptor alpha: a potential role in the cardiac metabolic stress response. *J Biol Chem* 276(48): 44495-501, 2001.

13. Basma, A.N., R.E. Heikkila, M.S. Saporito, M. Philbert, H.M. Geller, and W.J. Nicklas. 1-Methyl-4-(2'-ethylphenyl)-1,2,3,6-tetrahydropyridine-induced toxicity in PC12 cells is enhanced by preventing glycolysis. *J Neurochem* 58(3): 1052-9, 1992.

14.   Bastin, J., F. Aubey, A. Rotig, A. Munnich, and F. Djouadi. Activation of peroxisome proliferator-activated receptor pathway stimulates the mitochondrial respiratory chain and can correct deficiencies in patients' cells lacking its components. *J Clin Endocrinol Metab* 93(4): 1433-41, 2008.

15.   Baur, J.A., K.J. Pearson, N.L. Price, H.A. Jamieson, C. Lerin, A. Kalra, V.V. Prabhu, J.S. Allard, G. Lopez-Lluch, K. Lewis, P.J. Pistell, S. Poosala, K.G. Becker, O. Boss, D. Gwinn, M. Wang, S. Ramaswamy, K.W. Fishbein, R.G. Spencer, E.G. Lakatta, D. Le Couteur, R.J. Shaw, P. Navas, P. Puigserver, D.K. Ingram, R. de Cabo, and D.A. Sinclair. Resveratrol improves health and survival of mice on a high-calorie diet. *Nature* 444(7117): 337-42, 2006.

16.   Baur, J.A. and D.A. Sinclair. Therapeutic potential of resveratrol: the in vivo evidence. *Nat Rev Drug Discov* 5(6): 493-506, 2006.

17.   Beeson, C.C., G.C. Beeson, and R.G. Schnellmann. A high-throughput respirometric assay for mitochondrial biogenesis and toxicity. *Anal Biochem* 404(1): 75-81, 2010.

18.   Bergeron, R., J.M. Ren, K.S. Cadman, I.K. Moore, P. Perret, M. Pypaert, L.H. Young, C.F. Semenkovich, and G.I. Shulman. Chronic activation of AMP kinase results in NRF-1 activation and mitochondrial biogenesis. *Am J Physiol Endocrinol Metab* 281(6): E1340-6, 2001.

19.   Bershadsky, A.D. and V.I. Gelfand. ATP-dependent regulation of cytoplasmic microtubule disassembly. *Proc Natl Acad Sci U S A* 78(6): 3610-3, 1981.

20.   Bershadsky, A.D. and V.I. Gelfand. Role of ATP in the regulation of stability of cytoskeletal structures. *Cell Biol Int Rep* 7(3): 173-87, 1983.

21.   Bessems, J.G. and N.P. Vermeulen. Paracetamol (acetaminophen)-induced toxicity: molecular and biochemical mechanisms, analogues and protective approaches. *Crit Rev Toxicol* 31(1): 55-138, 2001.

22.   Better, O.S. The crush syndrome revisited (1940-1990). *Nephron* 55(2): 97-103, 1990.

23.   Bhalodia, Y., N. Kanzariya, R. Patel, N. Patel, J. Vaghasiya, N. Jivani, and H. Raval. Renoprotective activity of benincasa cerifera fruit extract on ischemia/reperfusion-induced renal damage in rat. *Iran J Kidney Dis* 3(2): 80-5, 2009.

24.   Biswas, G., O.A. Adebanjo, B.D. Freedman, H.K. Anandatheerthavarada, C. Vijayasarathy, M. Zaidi, M. Kotlikoff, and N.G. Avadhani. Retrograde Ca2+ signaling in C2C12 skeletal myocytes in response to mitochondrial genetic and metabolic stress: a novel mode of inter-organelle crosstalk. *EMBO J* 18(3): 522-33, 1999.

25.   Blesa, J.R., J.A. Prieto-Ruiz, J.M. Hernandez, and J. Hernandez-Yago. NRF-2 transcription factor is required for human TOMM20 gene expression. *Gene* 391(1-2): 198-208, 2007.

26.   Bogacka, I., H. Xie, G.A. Bray, and S.R. Smith. Pioglitazone induces mitochondrial biogenesis in human subcutaneous adipose tissue in vivo. *Diabetes* 54(5): 1392-9, 2005.

27.   Boily, G., E.L. Seifert, L. Bevilacqua, X.H. He, G. Sabourin, C. Estey, C. Moffat, S. Crawford, S. Saliba, K. Jardine, J. Xuan, M. Evans, M.E. Harper, and M.W.

McBurney. SirT1 regulates energy metabolism and response to caloric restriction in mice. *PLoS One* 3(3): e1759, 2008.

28. Bonventre, J.V. Mechanisms of ischemic acute renal failure. *Kidney Int* 43(5): 1160-78, 1993.

29. Bonventre, J.V. and J.M. Weinberg. Recent advances in the pathophysiology of ischemic acute renal failure. *J Am Soc Nephrol* 14(8): 2199-210, 2003.

30. Bonventre, J.V. Kidney injury molecule-1 (KIM-1): a urinary biomarker and much more. *Nephrol Dial Transplant* 24(11): 3265-8, 2009.

31. Bonventre, J.V. and L. Yang. Cellular pathophysiology of ischemic acute kidney injury. *J Clin Invest* 121(11): 4210-21, 2011.

32. Bordone, L. and L. Guarente. Calorie restriction, SIRT1 and metabolism: understanding longevity. *Nat Rev Mol Cell Biol* 6(4): 298-305, 2005.

33. Bordone, L., D. Cohen, A. Robinson, M.C. Motta, E. van Veen, A. Czopik, A.D. Steele, H. Crowe, S. Marmor, J. Luo, W. Gu, and L. Guarente. SIRT1 transgenic mice show phenotypes resembling calorie restriction. *Aging Cell* 6(6): 759-67, 2007.

34. Borniquel, S., I. Valle, S. Cadenas, S. Lamas, and M. Monsalve. Nitric oxide regulates mitochondrial oxidative stress protection via the transcriptional coactivator PGC-1alpha. *FASEB J* 20(11): 1889-91, 2006.

35. Borra, M.T., F.J. O'Neill, M.D. Jackson, B. Marshall, E. Verdin, K.R. Foltz, and J.M. Denu. Conserved enzymatic production and biological effect of O-acetyl-ADP-ribose by silent information regulator 2-like NAD+-dependent deacetylases. *J Biol Chem* 277(15): 12632-41, 2002.

36. Bosch, X., E. Poch, and J.M. Grau. Rhabdomyolysis and acute kidney injury. *N Engl J Med* 361(1): 62-72, 2009.

37. Brenner, B.M. Functional and structural determinants of glomerular filtration. A brief historical perspective. *Fed Proc* 36(12): 2599-601, 1977.

38. Brooks, C., Q. Wei, L. Feng, G. Dong, Y. Tao, L. Mei, Z.J. Xie, and Z. Dong. Bak regulates mitochondrial morphology and pathology during apoptosis by interacting with mitofusins. *Proc Natl Acad Sci U S A* 104(28): 11649-54, 2007.

39. Brooks, C., Q. Wei, S.G. Cho, and Z. Dong. Regulation of mitochondrial dynamics in acute kidney injury in cell culture and rodent models. *J Clin Invest* 119(5): 1275-85, 2009.

40. Brooks, C., S.G. Cho, C.Y. Wang, T. Yang, and Z. Dong. Fragmented mitochondria are sensitized to Bax insertion and activation during apoptosis. *Am J Physiol Cell Physiol* 300(3): C447-55, 2011.

41. Brown, J.R. and C.A. Thompson. Contrast-induced acute kidney injury: the at-risk patient and protective measures. *Curr Cardiol Rep* 12(5): 440-5, 2010.

42. Bunn, H.F., W.T. Esham, and R.W. Bull. The renal handling of hemoglobin. I. Glomerular filtration. *J Exp Med* 129(5): 909-23, 1969.

43. Bunn, H.F. and J.H. Jandl. The renal handling of hemoglobin. II. Catabolism. *J Exp Med* 129(5): 925-34, 1969.

44. Burns, A.T., D.R. Davies, A.J. McLaren, L. Cerundolo, P.J. Morris, and S.V. Fuggle. Apoptosis in ischemia/reperfusion injury of human renal allografts. *Transplantation* 66(7): 872-6, 1998.

45.   Buzzi Fde, C., M. Fracasso, V.C. Filho, R. Escarcena, E. del Olmo, and A. San Feliciano. New antinociceptive agents related to dihydrosphingosine. *Pharmacol Rep* 62(5): 849-57, 2010.

46.   Cameron, J.S. Allergic interstitial nephritis: clinical features and pathogenesis. *Q J Med* 66(250): 97-115, 1988.

47.   Canto, C. and J. Auwerx. PGC-1alpha, SIRT1 and AMPK, an energy sensing network that controls energy expenditure. *Curr Opin Lipidol* 20(2): 98-105, 2009.

48.   Canto, C., Z. Gerhart-Hines, J.N. Feige, M. Lagouge, L. Noriega, J.C. Milne, P.J. Elliott, P. Puigserver, and J. Auwerx. AMPK regulates energy expenditure by modulating NAD+ metabolism and SIRT1 activity. *Nature* 458(7241): 1056-60, 2009.

49.   Canto, C., L.Q. Jiang, A.S. Deshmukh, C. Mataki, A. Coste, M. Lagouge, J.R. Zierath, and J. Auwerx. Interdependence of AMPK and SIRT1 for metabolic adaptation to fasting and exercise in skeletal muscle. *Cell Metab* 11(3): 213-9, 2010.

50.   Cao, W., K.W. Daniel, J. Robidoux, P. Puigserver, A.V. Medvedev, X. Bai, L.M. Floering, B.M. Spiegelman, and S. Collins. p38 mitogen-activated protein kinase is the central regulator of cyclic AMP-dependent transcription of the brown fat uncoupling protein 1 gene. *Mol Cell Biol* 24(7): 3057-67, 2004.

51.   Cartoni, R., B. Leger, M.B. Hock, M. Praz, A. Crettenand, S. Pich, J.L. Ziltener, F. Luthi, O. Deriaz, A. Zorzano, C. Gobelet, A. Kralli, and A.P. Russell. Mitofusins 1/2 and ERRalpha expression are increased in human skeletal muscle after physical exercise. *J Physiol* 567(Pt 1): 349-58, 2005.

52.   Chau, C.M., M.J. Evans, and R.C. Scarpulla. Nuclear respiratory factor 1 activation sites in genes encoding the gamma-subunit of ATP synthase, eukaryotic initiation factor 2 alpha, and tyrosine aminotransferase. Specific interaction of purified NRF-1 with multiple target genes. *J Biol Chem* 267(10): 6999-7006, 1992.

53.   Cheng, Z., Y. Tseng, and M.F. White. Insulin signaling meets mitochondria in metabolism. *Trends Endocrinol Metab* 21(10): 589-98, 2010.

54.   Chertow, G.M., E. Burdick, M. Honour, J.V. Bonventre, and D.W. Bates. Acute kidney injury, mortality, length of stay, and costs in hospitalized patients. *J Am Soc Nephrol* 16(11): 3365-70, 2005.

55.   Choo, H.J., J.H. Kim, O.B. Kwon, C.S. Lee, J.Y. Mun, S.S. Han, Y.S. Yoon, G. Yoon, K.M. Choi, and Y.G. Ko. Mitochondria are impaired in the adipocytes of type 2 diabetic mice. *Diabetologia* 49(4): 784-91, 2006.

56.   Chow, L.S., L.J. Greenlund, Y.W. Asmann, K.R. Short, S.K. McCrady, J.A. Levine, and K.S. Nair. Impact of endurance training on murine spontaneous activity, muscle mitochondrial DNA abundance, gene transcripts, and function. *J Appl Physiol* 102(3): 1078-89, 2007.

57.   Civitarese, A.E., S. Carling, L.K. Heilbronn, M.H. Hulver, B. Ukropcova, W.A. Deutsch, S.R. Smith, and E. Ravussin. Calorie restriction increases muscle mitochondrial biogenesis in healthy humans. *PLoS Med* 4(3): e76, 2007.

58.   Cohen, H.Y., C. Miller, K.J. Bitterman, N.R. Wall, B. Hekking, B. Kessler, K.T. Howitz, M. Gorospe, R. de Cabo, and D.A. Sinclair. Calorie restriction promotes

mammalian cell survival by inducing the SIRT1 deacetylase. *Science* 305(5682): 390-2, 2004.

59.   Conger, J.D. and J.V. Weil. Abnormal vascular function following ischemia-reperfusion injury. *J Investig Med* 43(5): 431-42, 1995.

60.   Cooper, K. and W.M. Bennett. Nephrotoxicity of common drugs used in clinical practice. *Arch Intern Med* 147(7): 1213-8, 1987.

61.   Corcoran, A.C. and I.H. Page. Renal damage from ferroheme pigments myoglobin, hemoglobin, hematin. *Tex Rep Biol Med* 3(4): 528-44, 1945.

62.   Coste, A., J.F. Louet, M. Lagouge, C. Lerin, M.C. Antal, H. Meziane, K. Schoonjans, P. Puigserver, B.W. O'Malley, and J. Auwerx. The genetic ablation of SRC-3 protects against obesity and improves insulin sensitivity by reducing the acetylation of PGC-1{alpha}. *Proc Natl Acad Sci U S A* 105(44): 17187-92, 2008.

63.   Coudrier, E., D. Kerjaschki, and D. Louvard. Cytoskeleton organization and submembranous interactions in intestinal and renal brush borders. *Kidney Int* 34(3): 309-20, 1988.

64.   Covington, M.D. and R.G. Schnellmann. Chronic high glucose downregulates mitochondrial calpain 10 and contributes to renal cell death and diabetes-induced renal injury. *Kidney Int* 81(4): 391-400, 2012.

65.   Crompton, M. The mitochondrial permeability transition pore and its role in cell death. *Biochem J* 341 (Pt 2): 233-49, 1999.

66.   Cross, C.E., B. Halliwell, E.T. Borish, W.A. Pryor, B.N. Ames, R.L. Saul, J.M. McCord, and D. Harman. Oxygen radicals and human disease. *Ann Intern Med* 107(4): 526-45, 1987.

67.   Csiszar, A., N. Labinskyy, J.T. Pinto, P. Ballabh, H. Zhang, G. Losonczy, K. Pearson, R. de Cabo, P. Pacher, C. Zhang, and Z. Ungvari. Resveratrol induces mitochondrial biogenesis in endothelial cells. *Am J Physiol Heart Circ Physiol* 297(1): H13-20, 2009.

68.   Czubryt, M.P., J. McAnally, G.I. Fishman, and E.N. Olson. Regulation of peroxisome proliferator-activated receptor gamma coactivator 1 alpha (PGC-1 alpha) and mitochondrial function by MEF2 and HDAC5. *Proc Natl Acad Sci U S A* 100(4): 1711-6, 2003.

69.   da Silva, L.B., P.V. Palma, P.M. Cury, and V. Bueno. Evaluation of stem cell administration in a model of kidney ischemia-reperfusion injury. *Int Immunopharmacol* 7(13): 1609-16, 2007.

70.   Daitoku, H., K. Yamagata, H. Matsuzaki, M. Hatta, and A. Fukamizu. Regulation of PGC-1 promoter activity by protein kinase B and the forkhead transcription factor FKHR. *Diabetes* 52(3): 642-9, 2003.

71.   Damianovich, M., I. Ziv, S.N. Heyman, S. Rosen, A. Shina, D. Kidron, T. Aloya, H. Grimberg, G. Levin, A. Reshef, A. Bentolila, A. Cohen, and A. Shirvan. ApoSense: a novel technology for functional molecular imaging of cell death in models of acute renal tubular necrosis. *Eur J Nucl Med Mol Imaging* 33(3): 281-91, 2006.

72.   Damman, K., D.J. Van Veldhuisen, G. Navis, V.S. Vaidya, T.D. Smilde, B.D. Westenbrink, J.V. Bonventre, A.A. Voors, and H.L. Hillege. Tubular damage in chronic systolic heart failure is associated with reduced survival independent of glomerular filtration rate. *Heart* 96(16): 1297-302, 2010.

73.	Dasgupta, B. and J. Milbrandt. Resveratrol stimulates AMP kinase activity in neurons. *Proc Natl Acad Sci U S A* 104(17): 7217-22, 2007.

74.	de Mendonca, A., J.L. Vincent, P.M. Suter, R. Moreno, N.M. Dearden, M. Antonelli, J. Takala, C. Sprung, and F. Cantraine. Acute renal failure in the ICU: risk factors and outcome evaluated by the SOFA score. *Intensive Care Med* 26(7): 915-21, 2000.

75.	Dean, B.M., M. Sensi, and D. Perrett. Elevation of rat erythrocyte nucleotide levels following acute renal failure induced by glycerol or mercuric chloride. *Nephron* 22(4-6): 538-43, 1978.

76.	Devarajan, P. Update on mechanisms of ischemic acute kidney injury. *J Am Soc Nephrol* 17(6): 1503-20, 2006.

77.	Dittenhafer-Reed, K.E., J.L. Feldman, and J.M. Denu. Catalysis and mechanistic insights into sirtuin activation. *Chembiochem* 12(2): 281-9, 2011.

78.	Dong, Z., Y. Patel, P. Saikumar, J.M. Weinberg, and M.A. Venkatachalam. Development of porous defects in plasma membranes of adenosine triphosphate-depleted Madin-Darby canine kidney cells and its inhibition by glycine. *Lab Invest* 78(6): 657-68, 1998.

79.	Duffield, J.S., P.G. Tipping, T. Kipari, J.F. Cailhier, S. Clay, R. Lang, J.V. Bonventre, and J. Hughes. Conditional ablation of macrophages halts progression of crescentic glomerulonephritis. *Am J Pathol* 167(5): 1207-19, 2005.

80.	Dufour, C.R., B.J. Wilson, J.M. Huss, D.P. Kelly, W.A. Alaynick, M. Downes, R.M. Evans, M. Blanchette, and V. Giguere. Genome-wide orchestration of cardiac functions by the orphan nuclear receptors ERRalpha and gamma. *Cell Metab* 5(5): 345-56, 2007.

81.	Dykens, J.A. and Y. Will. The significance of mitochondrial toxicity testing in drug development. *Drug Discov Today* 12(17-18): 777-85, 2007.

82.	Epstein, F.H., M. Brezis, P. Silva, and S. Rosen. Physiological and clinical implications of medullary hypoxia. *Artif Organs* 11(6): 463-7, 1987.

83.	Evans, M.J. and R.C. Scarpulla. Interaction of nuclear factors with multiple sites in the somatic cytochrome c promoter. Characterization of upstream NRF-1, ATF, and intron Sp1 recognition sequences. *J Biol Chem* 264(24): 14361-8, 1989.

84.	Feige, J.N. and J. Auwerx. Transcriptional targets of sirtuins in the coordination of mammalian physiology. *Curr Opin Cell Biol* 20(3): 303-9, 2008.

85.	Feige, J.N., M. Lagouge, C. Canto, A. Strehle, S.M. Houten, J.C. Milne, P.D. Lambert, C. Mataki, P.J. Elliott, and J. Auwerx. Specific SIRT1 activation mimics low energy levels and protects against diet-induced metabolic disorders by enhancing fat oxidation. *Cell Metab* 8(5): 347-58, 2008.

86.	Feldkamp, T., A. Kribben, and J.M. Weinberg. Assessment of mitochondrial membrane potential in proximal tubules after hypoxia-reoxygenation. *Am J Physiol Renal Physiol* 288(6): F1092-102, 2005.

87.	Fischer, M.J., B.B. Brimhall, D.C. Lezotte, J.E. Glazner, and C.R. Parikh. Uncomplicated acute renal failure and hospital resource utilization: a retrospective multicenter analysis. *Am J Kidney Dis* 46(6): 1049-57, 2005.

88.	Fligiel, S.E., E.C. Lee, J.P. McCoy, K.J. Johnson, and J. Varani. Protein degradation following treatment with hydrogen peroxide. *Am J Pathol* 115(3): 418-25, 1984.

89.   Frank, S., B. Gaume, E.S. Bergmann-Leitner, W.W. Leitner, E.G. Robert, F. Catez, C.L. Smith, and R.J. Youle. The role of dynamin-related protein 1, a mediator of mitochondrial fission, in apoptosis. *Dev Cell* 1(4): 515-25, 2001.

90.   Funk, J.A., S. Odejinmi, and R.G. Schnellmann. SRT1720 induces mitochondrial biogenesis and rescues mitochondrial function after oxidant injury in renal proximal tubule cells. *J Pharmacol Exp Ther* 333(2): 593-601, 2010.

91.   Funk, J.A. and R.G. Schnellmann. Persistent disruption of mitochondrial homeostasis after acute kidney injury. *Am J Physiol Renal Physiol* 302(7): F853-64, 2012.

92.   Gao, C.L., C. Zhu, Y.P. Zhao, X.H. Chen, C.B. Ji, C.M. Zhang, J.G. Zhu, Z.K. Xia, M.L. Tong, and X.R. Guo. Mitochondrial dysfunction is induced by high levels of glucose and free fatty acids in 3T3-L1 adipocytes. *Mol Cell Endocrinol* 320(1-2): 25-33, 2010.

93.   Gerhart-Hines, Z., J.T. Rodgers, O. Bare, C. Lerin, S.H. Kim, R. Mostoslavsky, F.W. Alt, Z. Wu, and P. Puigserver. Metabolic control of muscle mitochondrial function and fatty acid oxidation through SIRT1/PGC-1alpha. *EMBO J* 26(7): 1913-23, 2007.

94.   Giguere, V. Transcriptional control of energy homeostasis by the estrogen-related receptors. *Endocr Rev* 29(6): 677-96, 2008.

95.   Glaumann, B. Effect of mannitol, dextran (macrodex), allopurinol, and methylprednisolone on the morphology of the proximal tubule of the rat kidney made ischemic in vivo. *Virchows Arch B Cell Pathol* 23(4): 297-323, 1977.

96.   Glaumann, B., H. Glaumann, I.K. Berezesky, and B.F. Trump. Studies on cellular recovery from injury. II. Ultrastructural studies on the recovery of the pars convoluta of the proximal tubule of the rate kidney from temporary ischemia. *Virchows Arch B Cell Pathol* 24(1): 1-18, 1977.

97.   Gleyzer, N., K. Vercauteren, and R.C. Scarpulla. Control of mitochondrial transcription specificity factors (TFB1M and TFB2M) by nuclear respiratory factors (NRF-1 and NRF-2) and PGC-1 family coactivators. *Mol Cell Biol* 25(4): 1354-66, 2005.

98.   Gobe, G., X.J. Zhang, D.A. Willgoss, E. Schoch, N.A. Hogg, and Z.H. Endre. Relationship between expression of Bcl-2 genes and growth factors in ischemic acute renal failure in the rat. *J Am Soc Nephrol* 11(3): 454-67, 2000.

99.   Gohil, V.M., J. Gvozdenovic-Jeremic, M. Schlame, and M.L. Greenberg. Binding of 10-N-nonyl acridine orange to cardiolipin-deficient yeast cells: implications for assay of cardiolipin. *Anal Biochem* 343(2): 350-2, 2005.

100.   Goligorsky, M.S., W. Lieberthal, L. Racusen, and E.E. Simon. Integrin receptors in renal tubular epithelium: new insights into pathophysiology of acute renal failure. *Am J Physiol* 264(1 Pt 2): F1-8, 1993.

101.   Gonzalez-Flecha, B. and A. Boveris. Mitochondrial sites of hydrogen peroxide production in reperfused rat kidney cortex. *Biochim Biophys Acta* 1243(3): 361-6, 1995.

102.   Goormaghtigh, E., P. Chatelain, J. Caspers, and J.M. Ruysschaert. Evidence of a complex between adriamycin derivatives and cardiolipin: possible role in cardiotoxicity. *Biochem Pharmacol* 29(21): 3003-10, 1980.

103. Goormaghtigh, E., P. Huart, M. Praet, R. Brasseur, and J.M. Ruysschaert. Structure of the adriamycin-cardiolipin complex. Role in mitochondrial toxicity. *Biophys Chem* 35(2-3): 247-57, 1990.

104. Greschik, H., J.M. Wurtz, S. Sanglier, W. Bourguet, A. van Dorsselaer, D. Moras, and J.P. Renaud. Structural and functional evidence for ligand-independent transcriptional activation by the estrogen-related receptor 3. *Mol Cell* 9(2): 303-13, 2002.

105. Guarente, L. Sir2 links chromatin silencing, metabolism, and aging. *Genes Dev* 14(9): 1021-6, 2000.

106. Guarente, L. Sirtuins in aging and disease. *Cold Spring Harb Symp Quant Biol* 72: 483-8, 2007.

107. Guidet, B. and S.V. Shah. Enhanced in vivo H2O2 generation by rat kidney in glycerol-induced renal failure. *Am J Physiol* 257(3 Pt 2): F440-5, 1989.

108. Gumbiner, B. Structure, biochemistry, and assembly of epithelial tight junctions. *Am J Physiol* 253(6 Pt 1): C749-58, 1987.

109. Haase, M., A. Haase-Fielitz, S.M. Bagshaw, M.C. Reade, S. Morgera, S. Seevenayagam, G. Matalanis, B. Buxton, L. Doolan, and R. Bellomo. Phase II, randomized, controlled trial of high-dose N-acetylcysteine in high-risk cardiac surgery patients. *Crit Care Med* 35(5): 1324-31, 2007.

110. Haase, M., R. Bellomo, P. Devarajan, P. Schlattmann, and A. Haase-Fielitz. Accuracy of neutrophil gelatinase-associated lipocalin (NGAL) in diagnosis and prognosis in acute kidney injury: a systematic review and meta-analysis. *Am J Kidney Dis* 54(6): 1012-24, 2009.

111. Haase, M., A. Haase-Fielitz, R. Bellomo, P. Devarajan, D. Story, G. Matalanis, M.C. Reade, S.M. Bagshaw, N. Seevanayagam, S. Seevanayagam, L. Doolan, B. Buxton, and D. Dragun. Sodium bicarbonate to prevent increases in serum creatinine after cardiac surgery: a pilot double-blind, randomized controlled trial. *Crit Care Med* 37(1): 39-47, 2009.

112. Hall, A.M. and R.J. Unwin. The not so 'mighty chondrion': emergence of renal diseases due to mitochondrial dysfunction. *Nephron Physiol* 105(1): p1-10, 2007.

113. Halliwell, B. and J.M. Gutteridge. Oxygen free radicals and iron in relation to biology and medicine: some problems and concepts. *Arch Biochem Biophys* 246(2): 501-14, 1986.

114. Halliwell, B. and J.M. Gutteridge. Role of free radicals and catalytic metal ions in human disease: an overview. *Methods Enzymol* 186: 1-85, 1990.

115. Hallman, M.A., S. Zhuang, and R.G. Schnellmann. Regulation of dedifferentiation and redifferentiation in renal proximal tubular cells by the epidermal growth factor receptor. *J Pharmacol Exp Ther* 325(2): 520-8, 2008.

116. Hamel, M.B., R.S. Phillips, R.B. Davis, N. Desbiens, A.F. Connors, Jr., J.M. Teno, N. Wenger, J. Lynn, A.W. Wu, W. Fulkerson, and J. Tsevat. Outcomes and cost-effectiveness of initiating dialysis and continuing aggressive care in seriously ill hospitalized adults. SUPPORT Investigators. Study to Understand Prognoses and Preferences for Outcomes and Risks of Treatments. *Ann Intern Med* 127(3): 195-202, 1997.

117. Han, W.K., G. Wagener, Y. Zhu, S. Wang, and H.T. Lee. Urinary biomarkers in the early detection of acute kidney injury after cardiac surgery. *Clin J Am Soc Nephrol* 4(5): 873-82, 2009.

118. Hardie, D.G., J.W. Scott, D.A. Pan, and E.R. Hudson. Management of cellular energy by the AMP-activated protein kinase system. *FEBS Lett* 546(1): 113-20, 2003.

119. Hasegawa, K., S. Wakino, K. Yoshioka, S. Tatematsu, Y. Hara, H. Minakuchi, K. Sueyasu, N. Washida, H. Tokuyama, M. Tzukerman, K. Skorecki, K. Hayashi, and H. Itoh. Kidney-specific overexpression of Sirt1 protects against acute kidney injury by retaining peroxisome function. *J Biol Chem* 285(17): 13045-56, 2010.

120. Hatefi, Y. and W.G. Hanstein. Interactions of reduced and oxidized triphosphopyridine nucleotides with the electron-transport system of bovine heart mitochondria. *Biochemistry* 12(18): 3515-22, 1973.

121. Hatefi, Y. The mitochondrial electron transport and oxidative phosphorylation system. *Annu Rev Biochem* 54: 1015-69, 1985.

122. Heyman, S.N., W. Lieberthal, P. Rogiers, and J.V. Bonventre. Animal models of acute tubular necrosis. *Curr Opin Crit Care* 8(6): 526-34, 2002.

123. Hock, M.B. and A. Kralli. Transcriptional control of mitochondrial biogenesis and function. *Annu Rev Physiol* 71: 177-203, 2009.

124. Hondares, E., O. Mora, P. Yubero, M. Rodriguez de la Concepcion, R. Iglesias, M. Giralt, and F. Villarroya. Thiazolidinediones and rexinoids induce peroxisome proliferator-activated receptor-coactivator (PGC)-1alpha gene transcription: an autoregulatory loop controls PGC-1alpha expression in adipocytes via peroxisome proliferator-activated receptor-gamma coactivation. *Endocrinology* 147(6): 2829-38, 2006.

125. Howitz, K.T., K.J. Bitterman, H.Y. Cohen, D.W. Lamming, S. Lavu, J.G. Wood, R.E. Zipkin, P. Chung, A. Kisielewski, L.L. Zhang, B. Scherer, and D.A. Sinclair. Small molecule activators of sirtuins extend Saccharomyces cerevisiae lifespan. *Nature* 425(6954): 191-6, 2003.

126. Humphreys, B.D. and J.V. Bonventre. The contribution of adult stem cells to renal repair. *Nephrol Ther* 3(1): 3-10, 2007.

127. Humphreys, B.D. and J.V. Bonventre. Mesenchymal stem cells in acute kidney injury. *Annu Rev Med* 59: 311-25, 2008.

128. Humphreys, B.D., M.T. Valerius, A. Kobayashi, J.W. Mugford, S. Soeung, J.S. Duffield, A.P. McMahon, and J.V. Bonventre. Intrinsic epithelial cells repair the kidney after injury. *Cell Stem Cell* 2(3): 284-91, 2008.

129. Humphreys, B.D., S.L. Lin, A. Kobayashi, T.E. Hudson, B.T. Nowlin, J.V. Bonventre, M.T. Valerius, A.P. McMahon, and J.S. Duffield. Fate tracing reveals the pericyte and not epithelial origin of myofibroblasts in kidney fibrosis. *Am J Pathol* 176(1): 85-97, 2010.

130. Huss, J.M., R.P. Kopp, and D.P. Kelly. Peroxisome proliferator-activated receptor coactivator-1alpha (PGC-1alpha) coactivates the cardiac-enriched nuclear receptors estrogen-related receptor-alpha and -gamma. Identification of novel leucine-rich interaction motif within PGC-1alpha. *J Biol Chem* 277(43): 40265-74, 2002.

131. Ichimura, T., J.V. Bonventre, V. Bailly, H. Wei, C.A. Hession, R.L. Cate, and M. Sanicola. Kidney injury molecule-1 (KIM-1), a putative epithelial cell adhesion molecule containing a novel immunoglobulin domain, is up-regulated in renal cells after injury. *J Biol Chem* 273(7): 4135-42, 1998.

132. Ichimura, T., C.C. Hung, S.A. Yang, J.L. Stevens, and J.V. Bonventre. Kidney injury molecule-1: a tissue and urinary biomarker for nephrotoxicant-induced renal injury. *Am J Physiol Renal Physiol* 286(3): F552-63, 2004.

133. Imai, S., C.M. Armstrong, M. Kaeberlein, and L. Guarente. Transcriptional silencing and longevity protein Sir2 is an NAD-dependent histone deacetylase. *Nature* 403(6771): 795-800, 2000.

134. Ingwersen, M.S., M. Kristensen, H. Pilegaard, J.F. Wojtaszewski, E.A. Richter, and C. Juel. Na,K-ATPase activity in mouse muscle is regulated by AMPK and PGC-1alpha. *J Membr Biol* 242(1): 1-10, 2011.

135. Irazu, C.E., E. Ruidera, I. Singh, J.K. Orak, C.T. Fitts, and P.R. Rajagopalan. Effect of ischemia and 24 hour reperfusion on ATP synthesis in the rat kidney. *J Exp Pathol* 4(1): 29-36, 1989.

136. Ishani, A., J.L. Xue, J. Himmelfarb, P.W. Eggers, P.L. Kimmel, B.A. Molitoris, and A.J. Collins. Acute kidney injury increases risk of ESRD among elderly. *J Am Soc Nephrol* 20(1): 223-8, 2009.

137. Iwano, M., D. Plieth, T.M. Danoff, C. Xue, H. Okada, and E.G. Neilson. Evidence that fibroblasts derive from epithelium during tissue fibrosis. *J Clin Invest* 110(3): 341-50, 2002.

138. Jager, S., C. Handschin, J. St-Pierre, and B.M. Spiegelman. AMP-activated protein kinase (AMPK) action in skeletal muscle via direct phosphorylation of PGC-1alpha. *Proc Natl Acad Sci U S A* 104(29): 12017-22, 2007.

139. Jassem, W., S.V. Fuggle, M. Rela, D.D. Koo, and N.D. Heaton. The role of mitochondria in ischemia/reperfusion injury. *Transplantation* 73(4): 493-9, 2002.

140. Jassem, W. and N.D. Heaton. The role of mitochondria in ischemia/reperfusion injury in organ transplantation. *Kidney Int* 66(2): 514-7, 2004.

141. Jenkins, B.G., E. Brouillet, Y.C. Chen, E. Storey, J.B. Schulz, P. Kirschner, M.F. Beal, and B.R. Rosen. Non-invasive neurochemical analysis of focal excitotoxic lesions in models of neurodegenerative illness using spectroscopic imaging. *J Cereb Blood Flow Metab* 16(3): 450-61, 1996.

142. Johnson, K.J., P.A. Ward, R.G. Kunkel, and B.S. Wilson. Mediation of IgA induced lung injury in the rat. Role of macrophages and reactive oxygen products. *Lab Invest* 54(5): 499-506, 1986.

143. Kale, S., A. Karihaloo, P.R. Clark, M. Kashgarian, D.S. Krause, and L.G. Cantley. Bone marrow stem cells contribute to repair of the ischemically injured renal tubule. *J Clin Invest* 112(1): 42-9, 2003.

144. Kamei, Y., H. Ohizumi, Y. Fujitani, T. Nemoto, T. Tanaka, N. Takahashi, T. Kawada, M. Miyoshi, O. Ezaki, and A. Kakizuka. PPARgamma coactivator 1beta/ERR ligand 1 is an ERR protein ligand, whose expression induces a high-energy expenditure and antagonizes obesity. *Proc Natl Acad Sci U S A* 100(21): 12378-83, 2003.

145. Karam, H., P. Bruneval, J.P. Clozel, B.M. Loffler, J. Bariety, and M. Clozel. Role of endothelin in acute renal failure due to rhabdomyolysis in rats. *J Pharmacol Exp Ther* 274(1): 481-6, 1995.

146. Kaushal, G.P., A.B. Singh, and S.V. Shah. Identification of gene family of caspases in rat kidney and altered expression in ischemia-reperfusion injury. *Am J Physiol* 274(3 Pt 2): F587-95, 1998.

147. Kaushal, G.P., A.G. Basnakian, and S.V. Shah. Apoptotic pathways in ischemic acute renal failure. *Kidney Int* 66(2): 500-6, 2004.

148. Kawai, Y., T. Nakao, N. Kunimura, Y. Kohda, and M. Gemba. Relationship of intracellular calcium and oxygen radicals to Cisplatin-related renal cell injury. *J Pharmacol Sci* 100(1): 65-72, 2006.

149. Kaya, K., M. Oguz, A.R. Akar, S. Durdu, A. Aslan, S. Erturk, R. Tasoz, and U. Ozyurda. The effect of sodium nitroprusside infusion on renal function during reperfusion period in patients undergoing coronary artery bypass grafting: a prospective randomized clinical trial. *Eur J Cardiothorac Surg* 31(2): 290-7, 2007.

150. Kelley, D.E., J. He, E.V. Menshikova, and V.B. Ritov. Dysfunction of mitochondria in human skeletal muscle in type 2 diabetes. *Diabetes* 51(10): 2944-50, 2002.

151. Kelly, D.P. and R.C. Scarpulla. Transcriptional regulatory circuits controlling mitochondrial biogenesis and function. *Genes Dev* 18(4): 357-68, 2004.

152. Kimura, T., Y. Takabatake, A. Takahashi, J.Y. Kaimori, I. Matsui, T. Namba, H. Kitamura, F. Niimura, T. Matsusaka, T. Soga, H. Rakugi, and Y. Isaka. Autophagy protects the proximal tubule from degeneration and acute ischemic injury. *J Am Soc Nephrol* 22(5): 902-13, 2011.

153. Kobryn, C.E. and L.J. Mandel. Decreased protein phosphorylation induced by anoxia in proximal renal tubules. *Am J Physiol* 267(4 Pt 1): C1073-9, 1994.

154. Kondou, I., J. Nakada, H. Hishinuma, F. Masuda, T. Machida, and H. Endou. Alterations of gluconeogenesis by ischemic renal injury in rats. *Ren Fail* 14(4): 479-83, 1992.

155. Koves, T.R., P. Li, J. An, T. Akimoto, D. Slentz, O. Ilkayeva, G.L. Dohm, Z. Yan, C.B. Newgard, and D.M. Muoio. Peroxisome proliferator-activated receptor-gamma co-activator 1alpha-mediated metabolic remodeling of skeletal myocytes mimics exercise training and reverses lipid-induced mitochondrial inefficiency. *J Biol Chem* 280(39): 33588-98, 2005.

156. Kramer, B.K., J. Preuner, A. Ebenburger, M. Kaiser, U. Bergner, C. Eilles, M.C. Kammerl, G.A. Riegger, and D.E. Birnbaum. Lack of renoprotective effect of theophylline during aortocoronary bypass surgery. *Nephrol Dial Transplant* 17(5): 910-5, 2002.

157. Kriz, W., B. Kaissling, and M. Le Hir. Epithelial-mesenchymal transition (EMT) in kidney fibrosis: fact or fantasy? *J Clin Invest* 121(2): 468-74, 2011.

158. Kulka, P.J., M. Tryba, and M. Zenz. Preoperative alpha2-adrenergic receptor agonists prevent the deterioration of renal function after cardiac surgery: results of a randomized, controlled trial. *Crit Care Med* 24(6): 947-52, 1996.

159. Kunzendorf, U., M. Haase, L. Rolver, and A. Haase-Fielitz. Novel aspects of pharmacological therapies for acute renal failure. *Drugs* 70(9): 1099-114, 2010.

160. Lagouge, M., C. Argmann, Z. Gerhart-Hines, H. Meziane, C. Lerin, F. Daussin, N. Messadeq, J. Milne, P. Lambert, P. Elliott, B. Geny, M. Laakso, P. Puigserver, and J. Auwerx. Resveratrol improves mitochondrial function and protects against metabolic disease by activating SIRT1 and PGC-1alpha. *Cell* 127(6): 1109-22, 2006.

161. Landry, J., A. Sutton, S.T. Tafrov, R.C. Heller, J. Stebbins, L. Pillus, and R. Sternglanz. The silencing protein SIR2 and its homologs are NAD-dependent protein deacetylases. *Proc Natl Acad Sci U S A* 97(11): 5807-11, 2000.

162. Lane, M.A., A. Black, A. Handy, E.M. Tilmont, D.K. Ingram, and G.S. Roth. Caloric restriction in primates. *Ann N Y Acad Sci* 928: 287-95, 2001.

163. Lassnigg, A., E. Donner, G. Grubhofer, E. Presterl, W. Druml, and M. Hiesmayr. Lack of renoprotective effects of dopamine and furosemide during cardiac surgery. *J Am Soc Nephrol* 11(1): 97-104, 2000.

164. Lee, Y.J., S.Y. Jeong, M. Karbowski, C.L. Smith, and R.J. Youle. Roles of the mammalian mitochondrial fission and fusion mediators Fis1, Drp1, and Opa1 in apoptosis. *Mol Biol Cell* 15(11): 5001-11, 2004.

165. Liano, F., E. Junco, J. Pascual, R. Madero, and E. Verde. The spectrum of acute renal failure in the intensive care unit compared with that seen in other settings. The Madrid Acute Renal Failure Study Group. *Kidney Int Suppl* 66: S16-24, 1998.

166. Lieberthal, W. and J.S. Levine. Mechanisms of apoptosis and its potential role in renal tubular epithelial cell injury. *Am J Physiol* 271(3 Pt 2): F477-88, 1996.

167. Lin, F., K. Cordes, L. Li, L. Hood, W.G. Couser, S.J. Shankland, and P. Igarashi. Hematopoietic stem cells contribute to the regeneration of renal tubules after renal ischemia-reperfusion injury in mice. *J Am Soc Nephrol* 14(5): 1188-99, 2003.

168. Lin, J., C. Handschin, and B.M. Spiegelman. Metabolic control through the PGC-1 family of transcription coactivators. *Cell Metab* 1(6): 361-70, 2005.

169. Lin, S.J., P.A. Defossez, and L. Guarente. Requirement of NAD and SIR2 for life-span extension by calorie restriction in Saccharomyces cerevisiae. *Science* 289(5487): 2126-8, 2000.

170. Linford, N.J., R.P. Beyer, K. Gollahon, R.A. Krajcik, V.L. Malloy, V. Demas, G.C. Burmer, and P.S. Rabinovitch. Transcriptional response to aging and caloric restriction in heart and adipose tissue. *Aging Cell* 6(5): 673-88, 2007.

171. Loef, B.G., R.H. Henning, A.H. Epema, G.W. Rietman, W. van Oeveren, G.J. Navis, and T. Ebels. Effect of dexamethasone on perioperative renal function impairment during cardiac surgery with cardiopulmonary bypass. *Br J Anaesth* 93(6): 793-8, 2004.

172. Lopez-Lluch, G., N. Hunt, B. Jones, M. Zhu, H. Jamieson, S. Hilmer, M.V. Cascajo, J. Allard, D.K. Ingram, P. Navas, and R. de Cabo. Calorie restriction induces mitochondrial biogenesis and bioenergetic efficiency. *Proc Natl Acad Sci U S A* 103(6): 1768-73, 2006.

173. Lu, T., Y. Pan, S.Y. Kao, C. Li, I. Kohane, J. Chan, and B.A. Yankner. Gene regulation and DNA damage in the ageing human brain. *Nature* 429(6994): 883-91, 2004.

174. Mathew, T.H. Drug-induced renal disease. *Med J Aust* 156(10): 724-8, 1992.

175. Matsuno-Yagi, A. and Y. Hatefi. Studies on the mechanism of oxidative phosphorylation. Flow-force relationships in mitochondrial energy-linked reactions. *J Biol Chem* 262(29): 14158-63, 1987.

176. McClelland, G.B., P.M. Craig, K. Dhekney, and S. Dipardo. Temperature- and exercise-induced gene expression and metabolic enzyme changes in skeletal muscle of adult zebrafish (Danio rerio). *J Physiol* 577(Pt 2): 739-51, 2006.

177. Melov, S., M.A. Tarnopolsky, K. Beckman, K. Felkey, and A. Hubbard. Resistance exercise reverses aging in human skeletal muscle. *PLoS One* 2(5): e465, 2007.

178. Milne, J.C., P.D. Lambert, S. Schenk, D.P. Carney, J.J. Smith, D.J. Gagne, L. Jin, O. Boss, R.B. Perni, C.B. Vu, J.E. Bemis, R. Xie, J.S. Disch, P.Y. Ng, J.J. Nunes, A.V. Lynch, H. Yang, H. Galonek, K. Israelian, W. Choy, A. Iffland, S. Lavu, O. Medvedik, D.A. Sinclair, J.M. Olefsky, M.R. Jirousek, P.J. Elliott, and C.H. Westphal. Small molecule activators of SIRT1 as therapeutics for the treatment of type 2 diabetes. *Nature* 450(7170): 712-6, 2007.

179. Milne, J.C. and J.M. Denu. The Sirtuin family: therapeutic targets to treat diseases of aging. *Curr Opin Chem Biol* 12(1): 11-7, 2008.

180. Minor, R.K., J.A. Baur, A.P. Gomes, T.M. Ward, A. Csiszar, E.M. Mercken, K. Abdelmohsen, Y.K. Shin, C. Canto, M. Scheibye-Knudsen, M. Krawczyk, P.M. Irusta, A. Martin-Montalvo, B.P. Hubbard, Y. Zhang, E. Lehrmann, A.A. White, N.L. Price, W.R. Swindell, K.J. Pearson, K.G. Becker, V.A. Bohr, M. Gorospe, J.M. Egan, M.I. Talan, J. Auwerx, C.H. Westphal, J.L. Ellis, Z. Ungvari, G.P. Vlasuk, P.J. Elliott, D.A. Sinclair, and R. de Cabo. SRT1720 improves survival and healthspan of obese mice. *Sci Rep* 1: 70, 2011.

181. Mirabelli, F., A. Salis, M. Vairetti, G. Bellomo, H. Thor, and S. Orrenius. Cytoskeletal alterations in human platelets exposed to oxidative stress are mediated by oxidative and Ca2+-dependent mechanisms. *Arch Biochem Biophys* 270(2): 478-88, 1989.

182. Mishra, J., Q. Ma, A. Prada, M. Mitsnefes, K. Zahedi, J. Yang, J. Barasch, and P. Devarajan. Identification of neutrophil gelatinase-associated lipocalin as a novel early urinary biomarker for ischemic renal injury. *J Am Soc Nephrol* 14(10): 2534-43, 2003.

183. Mitsos, S.E., D. Kim, B.R. Lucchesi, and J.C. Fantone. Modulation of myoglobin-H2O2-mediated peroxidation reactions by sulfhydryl compounds. *Lab Invest* 59(6): 824-30, 1988.

184. Molitoris, B.A., L.K. Chan, J.I. Shapiro, J.D. Conger, and S.A. Falk. Loss of epithelial polarity: a novel hypothesis for reduced proximal tubule Na+ transport following ischemic injury. *J Membr Biol* 107(2): 119-27, 1989.

185. Molitoris, B.A. Ischemia-induced loss of epithelial polarity: potential role of the actin cytoskeleton. *Am J Physiol* 260(6 Pt 2): F769-78, 1991.

186. Molitoris, B.A. Na(+)-K(+)-ATPase that redistributes to apical membrane during ATP depletion remains functional. *Am J Physiol* 265(5 Pt 2): F693-7, 1993.

187. Molitoris, B.A. and R.M. Sandoval. Intravital multiphoton microscopy of dynamic renal processes. *Am J Physiol Renal Physiol* 288(6): F1084-9, 2005.

188. Mootha, V.K., C.M. Lindgren, K.F. Eriksson, A. Subramanian, S. Sihag, J. Lehar, P. Puigserver, E. Carlsson, M. Ridderstrale, E. Laurila, N. Houstis, M.J. Daly, N.

Patterson, J.P. Mesirov, T.R. Golub, P. Tamayo, B. Spiegelman, E.S. Lander, J.N. Hirschhorn, D. Altshuler, and L.C. Groop. PGC-1alpha-responsive genes involved in oxidative phosphorylation are coordinately downregulated in human diabetes. *Nat Genet* 34(3): 267-73, 2003.

189. Mootha, V.K., C. Handschin, D. Arlow, X. Xie, J. St Pierre, S. Sihag, W. Yang, D. Altshuler, P. Puigserver, N. Patterson, P.J. Willy, I.G. Schulman, R.A. Heyman, E.S. Lander, and B.M. Spiegelman. Erralpha and Gabpa/b specify PGC-1alpha-dependent oxidative phosphorylation gene expression that is altered in diabetic muscle. *Proc Natl Acad Sci U S A* 101(17): 6570-5, 2004.

190. Morelli, A., Z. Ricci, R. Bellomo, C. Ronco, M. Rocco, G. Conti, A. De Gaetano, U. Picchini, A. Orecchioni, M. Portieri, F. Coluzzi, P. Porzi, P. Serio, A. Bruno, and P. Pietropaoli. Prophylactic fenoldopam for renal protection in sepsis: a randomized, double-blind, placebo-controlled pilot trial. *Crit Care Med* 33(11): 2451-6, 2005.

191. Morikawa, S., T. Sone, H. Tsuboi, H. Mukawa, I. Morishima, M. Uesugi, Y. Morita, Y. Numaguchi, K. Okumura, and T. Murohara. Renal protective effects and the prevention of contrast-induced nephropathy by atrial natriuretic peptide. *J Am Coll Cardiol* 53(12): 1040-6, 2009.

192. Moss, A.H., C.C. Solomons, and A.C. Alfrey. Elevated plasma adenine nucleotide levels in chronic renal failure and their possible significance. *Proc Clin Dial Transplant Forum* 9: 184-8, 1979.

193. Nadasdy, T., Z. Laszik, K.E. Blick, L.D. Johnson, and F.G. Silva. Proliferative activity of intrinsic cell populations in the normal human kidney. *J Am Soc Nephrol* 4(12): 2032-9, 1994.

194. Nash, K., A. Hafeez, and S. Hou. Hospital-acquired renal insufficiency. *Am J Kidney Dis* 39(5): 930-6, 2002.

195. Nath, K.A., G. Balla, G.M. Vercellotti, J. Balla, H.S. Jacob, M.D. Levitt, and M.E. Rosenberg. Induction of heme oxygenase is a rapid, protective response in rhabdomyolysis in the rat. *J Clin Invest* 90(1): 267-70, 1992.

196. Nemoto, S., M.M. Fergusson, and T. Finkel. SIRT1 functionally interacts with the metabolic regulator and transcriptional coactivator PGC-1{alpha}. *J Biol Chem* 280(16): 16456-60, 2005.

197. Niggli, V. and M.M. Burger. Interaction of the cytoskeleton with the plasma membrane. *J Membr Biol* 100(2): 97-121, 1987.

198. Nisoli, E., E. Clementi, S. Moncada, and M.O. Carruba. Mitochondrial biogenesis as a cellular signaling framework. *Biochem Pharmacol* 67(1): 1-15, 2004.

199. Nisoli, E., C. Tonello, A. Cardile, V. Cozzi, R. Bracale, L. Tedesco, S. Falcone, A. Valerio, O. Cantoni, E. Clementi, S. Moncada, and M.O. Carruba. Calorie restriction promotes mitochondrial biogenesis by inducing the expression of eNOS. *Science* 310(5746): 314-7, 2005.

200. Nolan, J.P., R.C. Venuto, and G.S. Goldmann. Role of endotoxin in glycerol-induced renal failure in the rat. *Clin Sci Mol Med* 54(6): 615-20, 1978.

201. Nony, P.A., G. Nowak, and R.G. Schnellmann. Collagen IV promotes repair of renal cell physiological functions after toxicant injury. *Am J Physiol Renal Physiol* 281(3): F443-53, 2001.

202. Nony, P.A. and R.G. Schnellmann. Interactions between collagen IV and collagen-binding integrins in renal cell repair after sublethal injury. *Mol Pharmacol* 60(6): 1226-34, 2001.

203. Nony, P.A. and R.G. Schnellmann. Mechanisms of renal cell repair and regeneration after acute renal failure. *J Pharmacol Exp Ther* 304(3): 905-12, 2003.

204. Nowak, G. and R.G. Schnellmann. Autocrine production and TGF-beta 1-mediated effects on metabolism and viability in renal cells. *Am J Physiol* 271(3 Pt 2): F689-97, 1996.

205. Nowak, G., M.D. Aleo, J.A. Morgan, and R.G. Schnellmann. Recovery of cellular functions following oxidant injury. *Am J Physiol* 274(3 Pt 2): F509-15, 1998.

206. Oberbauer, R., M. Rohrmoser, H. Regele, F. Muhlbacher, and G. Mayer. Apoptosis of tubular epithelial cells in donor kidney biopsies predicts early renal allograft function. *J Am Soc Nephrol* 10(9): 2006-13, 1999.

207. Ongwijitwat, S., H.L. Liang, E.M. Graboyes, and M.T. Wong-Riley. Nuclear respiratory factor 2 senses changing cellular energy demands and its silencing down-regulates cytochrome oxidase and other target gene mRNAs. *Gene* 374: 39-49, 2006.

208. Pacholec, M., J.E. Bleasdale, B. Chrunyk, D. Cunningham, D. Flynn, R.S. Garofalo, D. Griffith, M. Griffor, P. Loulakis, B. Pabst, X. Qiu, B. Stockman, V. Thanabal, A. Varghese, J. Ward, J. Withka, and K. Ahn. SRT1720, SRT2183, SRT1460, and resveratrol are not direct activators of SIRT1. *J Biol Chem* 285(11): 8340-51, 2010.

209. Pagel-Langenickel, I., J. Bao, J.J. Joseph, D.R. Schwartz, B.S. Mantell, X. Xu, N. Raghavachari, and M.N. Sack. PGC-1alpha integrates insulin signaling, mitochondrial regulation, and bioenergetic function in skeletal muscle. *J Biol Chem* 283(33): 22464-72, 2008.

210. Paller, M.S., J.R. Hoidal, and T.F. Ferris. Oxygen free radicals in ischemic acute renal failure in the rat. *J Clin Invest* 74(4): 1156-64, 1984.

211. Paller, M.S. Hemoglobin- and myoglobin-induced acute renal failure in rats: role of iron in nephrotoxicity. *Am J Physiol* 255(3 Pt 2): F539-44, 1988.

212. Parikh, C.R. and P. Devarajan. New biomarkers of acute kidney injury. *Crit Care Med* 36(4 Suppl): S159-65, 2008.

213. Patti, M.E., A.J. Butte, S. Crunkhorn, K. Cusi, R. Berria, S. Kashyap, Y. Miyazaki, I. Kohane, M. Costello, R. Saccone, E.J. Landaker, A.B. Goldfine, E. Mun, R. DeFronzo, J. Finlayson, C.R. Kahn, and L.J. Mandarino. Coordinated reduction of genes of oxidative metabolism in humans with insulin resistance and diabetes: Potential role of PGC1 and NRF1. *Proc Natl Acad Sci U S A* 100(14): 8466-71, 2003.

214. Pilegaard, H., B. Saltin, and P.D. Neufer. Exercise induces transient transcriptional activation of the PGC-1alpha gene in human skeletal muscle. *J Physiol* 546(Pt 3): 851-8, 2003.

215. Plotnikov, E.Y., A.V. Kazachenko, M.Y. Vyssokikh, A.K. Vasileva, D.V. Tcvirkun, N.K. Isaev, V.I. Kirpatovsky, and D.B. Zorov. The role of mitochondria in oxidative and nitrosative stress during ischemia/reperfusion in the rat kidney. *Kidney Int* 72(12): 1493-502, 2007.

216. Plotnikov, E.Y., A.A. Chupyrkina, I.B. Pevzner, N.K. Isaev, and D.B. Zorov. Myoglobin causes oxidative stress, increase of NO production and dysfunction of kidney's mitochondria. *Biochim Biophys Acta* 1792(8): 796-803, 2009.

217. Puigserver, P., Z. Wu, C.W. Park, R. Graves, M. Wright, and B.M. Spiegelman. A cold-inducible coactivator of nuclear receptors linked to adaptive thermogenesis. *Cell* 92(6): 829-39, 1998.

218. Puigserver, P., J. Rhee, J. Lin, Z. Wu, J.C. Yoon, C.Y. Zhang, S. Krauss, V.K. Mootha, B.B. Lowell, and B.M. Spiegelman. Cytokine stimulation of energy expenditure through p38 MAP kinase activation of PPARgamma coactivator-1. *Mol Cell* 8(5): 971-82, 2001.

219. Puigserver, P. and B.M. Spiegelman. Peroxisome proliferator-activated receptor-gamma coactivator 1 alpha (PGC-1 alpha): transcriptional coactivator and metabolic regulator. *Endocr Rev* 24(1): 78-90, 2003.

220. Rasbach, K.A. and R.G. Schnellmann. Signaling of mitochondrial biogenesis following oxidant injury. *J Biol Chem* 282(4): 2355-62, 2007.

221. Rasbach, K.A. and R.G. Schnellmann. PGC-1alpha over-expression promotes recovery from mitochondrial dysfunction and cell injury. *Biochem Biophys Res Commun* 355(3): 734-9, 2007.

222. Rasbach, K.A., P.T. Green, and R.G. Schnellmann. Oxidants and Ca+2 induce PGC-1alpha degradation through calpain. *Arch Biochem Biophys* 478(2): 130-5, 2008.

223. Rasbach, K.A. and R.G. Schnellmann. Isoflavones promote mitochondrial biogenesis. *J Pharmacol Exp Ther* 325(2): 536-43, 2008.

224. Rasbach, K.A., J.A. Funk, T. Jayavelu, P.T. Green, and R.G. Schnellmann. 5-hydroxytryptamine receptor stimulation of mitochondrial biogenesis. *J Pharmacol Exp Ther* 332(2): 632-9, 2010.

225. Reis, N.D. and M. Michaelson. Crush injury to the lower limbs. Treatment of the local injury. *J Bone Joint Surg Am* 68(3): 414-8, 1986.

226. Richardson, D.K., S. Kashyap, M. Bajaj, K. Cusi, S.J. Mandarino, J. Finlayson, R.A. DeFronzo, C.P. Jenkinson, and L.J. Mandarino. Lipid infusion decreases the expression of nuclear encoded mitochondrial genes and increases the expression of extracellular matrix genes in human skeletal muscle. *J Biol Chem* 280(11): 10290-7, 2005.

227. Rimbaud, S., A. Garnier, and R. Ventura-Clapier. Mitochondrial biogenesis in cardiac pathophysiology. *Pharmacol Rep* 61(1): 131-8, 2009.

228. Rockl, K.S., C.A. Witczak, and L.J. Goodyear. Signaling mechanisms in skeletal muscle: acute responses and chronic adaptations to exercise. *IUBMB Life* 60(3): 145-53, 2008.

229. Rodgers, J.T., C. Lerin, W. Haas, S.P. Gygi, B.M. Spiegelman, and P. Puigserver. Nutrient control of glucose homeostasis through a complex of PGC-1alpha and SIRT1. *Nature* 434(7029): 113-8, 2005.

230. Rogina, B. and S.L. Helfand. Sir2 mediates longevity in the fly through a pathway related to calorie restriction. *Proc Natl Acad Sci U S A* 101(45): 15998-6003, 2004.

231. Ron, D., U. Taitelman, M. Michaelson, G. Bar-Joseph, S. Bursztein, and O.S. Better. Prevention of acute renal failure in traumatic rhabdomyolysis. *Arch Intern Med* 144(2): 277-80, 1984.

232. Rong, J.X., Y. Qiu, M.K. Hansen, L. Zhu, V. Zhang, M. Xie, Y. Okamoto, M.D. Mattie, H. Higashiyama, S. Asano, J.C. Strum, and T.E. Ryan. Adipose mitochondrial biogenesis is suppressed in db/db and high-fat diet-fed mice and improved by rosiglitazone. *Diabetes* 56(7): 1751-60, 2007.

233. Roth, G.S., D.K. Ingram, and M.A. Lane. Caloric restriction in primates and relevance to humans. *Ann N Y Acad Sci* 928: 305-15, 2001.

234. Russell, A.P., M.K. Hesselink, S.K. Lo, and P. Schrauwen. Regulation of metabolic transcriptional co-activators and transcription factors with acute exercise. *FASEB J* 19(8): 986-8, 2005.

235. Saikumar, P. and M.A. Venkatachalam. Role of apoptosis in hypoxic/ischemic damage in the kidney. *Semin Nephrol* 23(6): 511-21, 2003.

236. Sano, M., S. Tokudome, N. Shimizu, N. Yoshikawa, C. Ogawa, K. Shirakawa, J. Endo, T. Katayama, S. Yuasa, M. Ieda, S. Makino, F. Hattori, H. Tanaka, and K. Fukuda. Intramolecular control of protein stability, subnuclear compartmentalization, and coactivator function of peroxisome proliferator-activated receptor gamma coactivator 1alpha. *J Biol Chem* 282(35): 25970-80, 2007.

237. Sauriyal, D.S., A.S. Jaggi, N. Singh, and A. Muthuraman. Investigating the role of endogenous opioids and K(ATP) channels in glycerol-induced acute renal failure. *Fundam Clin Pharmacol* 26(3): 347-55, 2012.

238. Savic, V., P. Vlahovic, V. Djordjevic, M. Mitic-Zlatkovic, V. Avramovic, and V. Stefanovic. Nephroprotective effects of pentoxifylline in experimental myoglobinuric acute renal failure. *Pathol Biol (Paris)* 50(10): 599-607, 2002.

239. Scarpulla, R.C. Nuclear control of respiratory chain expression in mammalian cells. *J Bioenerg Biomembr* 29(2): 109-19, 1997.

240. Scarpulla, R.C. Transcriptional activators and coactivators in the nuclear control of mitochondrial function in mammalian cells. *Gene* 286(1): 81-9, 2002.

241. Scarpulla, R.C. Nuclear activators and coactivators in mammalian mitochondrial biogenesis. *Biochim Biophys Acta* 1576(1-2): 1-14, 2002.

242. Schreiber, S.N., D. Knutti, K. Brogli, T. Uhlmann, and A. Kralli. The transcriptional coactivator PGC-1 regulates the expression and activity of the orphan nuclear receptor estrogen-related receptor alpha (ERRalpha). *J Biol Chem* 278(11): 9013-8, 2003.

243. Schrier, R.W., W. Wang, B. Poole, and A. Mitra. Acute renal failure: definitions, diagnosis, pathogenesis, and therapy. *J Clin Invest* 114(1): 5-14, 2004.

244. Schwarz, C., P. Hauser, R. Steininger, H. Regele, G. Heinze, G. Mayer, and R. Oberbauer. Failure of BCL-2 up-regulation in proximal tubular epithelial cells of donor kidney biopsy specimens is associated with apoptosis and delayed graft function. *Lab Invest* 82(7): 941-8, 2002.

245. Semedo, P., P.M. Wang, T.H. Andreucci, M.A. Cenedeze, V.P. Teixeira, M.A. Reis, A. Pacheco-Silva, and N.O. Camara. Mesenchymal stem cells ameliorate tissue damages triggered by renal ischemia and reperfusion injury. *Transplant Proc* 39(2): 421-3, 2007.

246. Semple, R.K., V.C. Crowley, C.P. Sewter, M. Laudes, C. Christodoulides, R.V. Considine, A. Vidal-Puig, and S. O'Rahilly. Expression of the thermogenic nuclear hormone receptor coactivator PGC-1alpha is reduced in the adipose tissue of morbidly obese subjects. *Int J Obes Relat Metab Disord* 28(1): 176-9, 2004.

247. Seo-Mayer, P.W., G. Thulin, L. Zhang, D.S. Alves, T. Ardito, M. Kashgarian, and M.J. Caplan. Preactivation of AMPK by metformin may ameliorate the epithelial cell damage caused by renal ischemia. *Am J Physiol Renal Physiol* 301(6): F1346-57, 2011.

248. Shah, S.V. Evidence suggesting a role for hydroxyl radical in passive Heymann nephritis in rats. *Am J Physiol* 254(3 Pt 2): F337-44, 1988.

249. Shah, S.V. and P.D. Walker. Evidence suggesting a role for hydroxyl radical in glycerol-induced acute renal failure. *Am J Physiol* 255(3 Pt 2): F438-43, 1988.

250. Shulman, L.M., Y. Yuhas, I. Frolkis, S. Gavendo, A. Knecht, and H.E. Eliahou. Glycerol induced ARF in rats is mediated by tumor necrosis factor-alpha. *Kidney Int* 43(6): 1397-401, 1993.

251. Smith, J.J., R.D. Kenney, D.J. Gagne, B.P. Frushour, W. Ladd, H.L. Galonek, K. Israelian, J. Song, G. Razvadauskaite, A.V. Lynch, D.P. Carney, R.J. Johnson, S. Lavu, A. Iffland, P.J. Elliott, P.D. Lambert, K.O. Elliston, M.R. Jirousek, J.C. Milne, and O. Boss. Small molecule activators of SIRT1 replicate signaling pathways triggered by calorie restriction in vivo. *BMC Syst Biol* 3: 31, 2009.

252. Solez, K., E.C. Kramer, J.A. Fox, and R.H. Heptinstall. Medullary plasma flow and intravascular leukocyte accumulation in acute renal failure. *Kidney Int* 6(1): 24-37, 1974.

253. Solomon, R., C. Werner, D. Mann, J. D'Elia, and P. Silva. Effects of saline, mannitol, and furosemide to prevent acute decreases in renal function induced by radiocontrast agents. *N Engl J Med* 331(21): 1416-20, 1994.

254. Song, Y.R., T. Lee, S.J. You, H.J. Chin, D.W. Chae, C. Lim, K.H. Park, S. Han, J.H. Kim, and K.Y. Na. Prevention of acute kidney injury by erythropoietin in patients undergoing coronary artery bypass grafting: a pilot study. *Am J Nephrol* 30(3): 253-60, 2009.

255. Sonoda, J., J. Laganiere, I.R. Mehl, G.D. Barish, L.W. Chong, X. Li, I.E. Scheffler, D.C. Mock, A.R. Bataille, F. Robert, C.H. Lee, V. Giguere, and R.M. Evans. Nuclear receptor ERR alpha and coactivator PGC-1 beta are effectors of IFN-gamma-induced host defense. *Genes Dev* 21(15): 1909-20, 2007.

256. Spiegel, D.M., P.D. Wilson, and B.A. Molitoris. Epithelial polarity following ischemia: a requirement for normal cell function. *Am J Physiol* 256(3 Pt 2): F430-6, 1989.

257. Stokman, G., J.C. Leemans, N. Claessen, J.J. Weening, and S. Florquin. Hematopoietic stem cell mobilization therapy accelerates recovery of renal function independent of stem cell contribution. *J Am Soc Nephrol* 16(6): 1684-92, 2005.

258. Stone, G.W., P.A. McCullough, J.A. Tumlin, N.E. Lepor, H. Madyoon, P. Murray, A. Wang, A.A. Chu, G.L. Schaer, M. Stevens, R.L. Wilensky, and W.W. O'Neill. Fenoldopam mesylate for the prevention of contrast-induced nephropathy: a randomized controlled trial. *JAMA* 290(17): 2284-91, 2003.

259. Stromski, M.E., K. Cooper, G. Thulin, K.M. Gaudio, N.J. Siegel, and R.G. Shulman. Chemical and functional correlates of postischemic renal ATP levels. *Proc Natl Acad Sci U S A* 83(16): 6142-5, 1986.

260. Supavekin, S., W. Zhang, R. Kucherlapati, F.J. Kaskel, L.C. Moore, and P. Devarajan. Differential gene expression following early renal ischemia/reperfusion. *Kidney Int* 63(5): 1714-24, 2003.

261. Susa, D., J.R. Mitchell, M. Verweij, M. van de Ven, H. Roest, S. van den Engel, I. Bajema, K. Mangundap, J.N. Ijzermans, J.H. Hoeijmakers, and R.W. de Bruin. Congenital DNA repair deficiency results in protection against renal ischemia reperfusion injury in mice. *Aging Cell* 8(2): 192-200, 2009.

262. Sutton, T.A. and B.A. Molitoris. Mechanisms of cellular injury in ischemic acute renal failure. *Semin Nephrol* 18(5): 490-7, 1998.

263. Szeto, C.C., B.C. Kwan, K.B. Lai, F.M. Lai, K.M. Chow, G. Wang, C.C. Luk, and P.K. Li. Urinary expression of kidney injury markers in renal transplant recipients. *Clin J Am Soc Nephrol* 5(12): 2329-37, 2010.

264. Takahashi, Y., K. Kako, H. Arai, T. Ohishi, Y. Inada, A. Takehara, A. Fukamizu, and E. Munekata. Characterization and identification of promoter elements in the mouse COX17 gene. *Biochim Biophys Acta* 1574(3): 359-64, 2002.

265. Tanaka, T., J. Yamamoto, S. Iwasaki, H. Asaba, H. Hamura, Y. Ikeda, M. Watanabe, K. Magoori, R.X. Ioka, K. Tachibana, Y. Watanabe, Y. Uchiyama, K. Sumi, H. Iguchi, S. Ito, T. Doi, T. Hamakubo, M. Naito, J. Auwerx, M. Yanagisawa, T. Kodama, and J. Sakai. Activation of peroxisome proliferator-activated receptor delta induces fatty acid beta-oxidation in skeletal muscle and attenuates metabolic syndrome. *Proc Natl Acad Sci U S A* 100(26): 15924-9, 2003.

266. Tanner, K.G., J. Landry, R. Sternglanz, and J.M. Denu. Silent information regulator 2 family of NAD- dependent histone/protein deacetylases generates a unique product, 1-O-acetyl-ADP-ribose. *Proc Natl Acad Sci U S A* 97(26): 14178-82, 2000.

267. Tanny, J.C. and D. Moazed. Coupling of histone deacetylation to NAD breakdown by the yeast silencing protein Sir2: Evidence for acetyl transfer from substrate to an NAD breakdown product. *Proc Natl Acad Sci U S A* 98(2): 415-20, 2001.

268. Taub, M., J.E. Springate, and F. Cutuli. Targeting of renal proximal tubule Na,K-ATPase by salt-inducible kinase. *Biochem Biophys Res Commun* 393(3): 339-44, 2010.

269. Terman, A. and U.T. Brunk. The aging myocardium: roles of mitochondrial damage and lysosomal degradation. *Heart Lung Circ* 14(2): 107-14, 2005.

270. Terman, A. Catabolic insufficiency and aging. *Ann N Y Acad Sci* 1067: 27-36, 2006.

271. Terman, A., T. Kurz, M. Navratil, E.A. Arriaga, and U.T. Brunk. Mitochondrial turnover and aging of long-lived postmitotic cells: the mitochondrial-lysosomal axis theory of aging. *Antioxid Redox Signal* 12(4): 503-35, 2010.

272. Teyssier, C., H. Ma, R. Emter, A. Kralli, and M.R. Stallcup. Activation of nuclear receptor coactivator PGC-1alpha by arginine methylation. *Genes Dev* 19(12): 1466-73, 2005.

273. Thadhani, R., M. Pascual, and J.V. Bonventre. Acute renal failure. *N Engl J Med* 334(22): 1448-60, 1996.

274. Thor, H., F. Mirabelli, A. Salis, G.M. Cohen, G. Bellomo, and S. Orrenius. Alterations in hepatocyte cytoskeleton caused by redox cycling and alkylating quinones. *Arch Biochem Biophys* 266(2): 397-407, 1988.

275. Tian, C., L.C. Murrin, and J.C. Zheng. Mitochondrial fragmentation is involved in methamphetamine-induced cell death in rat hippocampal neural progenitor cells. *PLoS One* 4(5): e5546, 2009.

276. Tissenbaum, H.A. and L. Guarente. Increased dosage of a sir-2 gene extends lifespan in Caenorhabditis elegans. *Nature* 410(6825): 227-30, 2001.

277. Toledo, F.G., S. Watkins, and D.E. Kelley. Changes induced by physical activity and weight loss in the morphology of intermyofibrillar mitochondria in obese men and women. *J Clin Endocrinol Metab* 91(8): 3224-7, 2006.

278. Trifillis, A.L., M.W. Kahng, R.A. Cowley, and B.F. Trump. Metabolic studies of postischemic acute renal failure in the rat. *Exp Mol Pathol* 40(2): 155-68, 1984.

279. Twig, G., A. Elorza, A.J. Molina, H. Mohamed, J.D. Wikstrom, G. Walzer, L. Stiles, S.E. Haigh, S. Katz, G. Las, J. Alroy, M. Wu, B.F. Py, J. Yuan, J.T. Deeney, B.E. Corkey, and O.S. Shirihai. Fission and selective fusion govern mitochondrial segregation and elimination by autophagy. *EMBO J* 27(2): 433-46, 2008.

280. Vaidya, V.S., M.A. Ferguson, and J.V. Bonventre. Biomarkers of acute kidney injury. *Annu Rev Pharmacol Toxicol* 48: 463-93, 2008.

281. Vaidya, V.S., J.S. Ozer, F. Dieterle, F.B. Collings, V. Ramirez, S. Troth, N. Muniappa, D. Thudium, D. Gerhold, D.J. Holder, N.A. Bobadilla, E. Marrer, E. Perentes, A. Cordier, J. Vonderscher, G. Maurer, P.L. Goering, F.D. Sistare, and J.V. Bonventre. Kidney injury molecule-1 outperforms traditional biomarkers of kidney injury in preclinical biomarker qualification studies. *Nat Biotechnol* 28(5): 478-85, 2010.

282. van Timmeren, M.M., M.C. van den Heuvel, V. Bailly, S.J. Bakker, H. van Goor, and C.A. Stegeman. Tubular kidney injury molecule-1 (KIM-1) in human renal disease. *J Pathol* 212(2): 209-17, 2007.

283. Vanholder, R., M.S. Sever, E. Erek, and N. Lameire. Rhabdomyolysis. *J Am Soc Nephrol* 11(8): 1553-61, 2000.

284. Vega, R.B., J.M. Huss, and D.P. Kelly. The coactivator PGC-1 cooperates with peroxisome proliferator-activated receptor alpha in transcriptional control of nuclear genes encoding mitochondrial fatty acid oxidation enzymes. *Mol Cell Biol* 20(5): 1868-76, 2000.

285. Venkatachalam, M.A., D.B. Jones, H.G. Rennke, D. Sandstrom, and Y. Patel. Mechanism of proximal tubule brush border loss and regeneration following mild renal ischemia. *Lab Invest* 45(4): 355-65, 1981.

286. Vetterlein, F., F. Hoffmann, J. Pedina, M. Neckel, and G. Schmidt. Disturbances in renal microcirculation induced by myoglobin and hemorrhagic hypotension in anesthetized rat. *Am J Physiol* 268(5 Pt 2): F839-46, 1995.

287. Villena, J.A., M.B. Hock, W.Y. Chang, J.E. Barcas, V. Giguere, and A. Kralli. Orphan nuclear receptor estrogen-related receptor alpha is essential for adaptive thermogenesis. *Proc Natl Acad Sci U S A* 104(4): 1418-23, 2007.

288. Villena, J.A. and A. Kralli. ERRalpha: a metabolic function for the oldest orphan. *Trends Endocrinol Metab* 19(8): 269-76, 2008.

289. Virbasius, J.V. and R.C. Scarpulla. Transcriptional activation through ETS domain binding sites in the cytochrome c oxidase subunit IV gene. *Mol Cell Biol* 11(11): 5631-8, 1991.

290. Vives-Bauza, C., L. Yang, and G. Manfredi. Assay of mitochondrial ATP synthesis in animal cells and tissues. *Methods Cell Biol* 80: 155-71, 2007.

291. Waanders, F., V.S. Vaidya, H. van Goor, H. Leuvenink, K. Damman, I. Hamming, J.V. Bonventre, L. Vogt, and G. Navis. Effect of renin-angiotensin-aldosterone system inhibition, dietary sodium restriction, and/or diuretics on urinary kidney injury molecule 1 excretion in nondiabetic proteinuric kidney disease: a post hoc analysis of a randomized controlled trial. *Am J Kidney Dis* 53(1): 16-25, 2009.

292. Walker, P.D. and S.V. Shah. Evidence suggesting a role for hydroxyl radical in gentamicin-induced acute renal failure in rats. *J Clin Invest* 81(2): 334-41, 1988.

293. Wallace, K.B. and A.A. Starkov. Mitochondrial targets of drug toxicity. *Annu Rev Pharmacol Toxicol* 40: 353-88, 2000.

294. Wang, H., T.H. Peiris, A. Mowery, J. Le Lay, Y. Gao, and L.E. Greenbaum. CCAAT/enhancer binding protein-beta is a transcriptional regulator of peroxisome-proliferator-activated receptor-gamma coactivator-1alpha in the regenerating liver. *Mol Endocrinol* 22(7): 1596-605, 2008.

295. Wang, Y.X., C.L. Zhang, R.T. Yu, H.K. Cho, M.C. Nelson, C.R. Bayuga-Ocampo, J. Ham, H. Kang, and R.M. Evans. Regulation of muscle fiber type and running endurance by PPARdelta. *PLoS Biol* 2(10): e294, 2004.

296. Ward, P.A., G.O. Till, J.R. Hatherill, T.M. Annesley, and R.G. Kunkel. Systemic complement activation, lung injury, and products of lipid peroxidation. *J Clin Invest* 76(2): 517-27, 1985.

297. Weinberg, J.M., M.A. Venkatachalam, N.F. Roeser, and I. Nissim. Mitochondrial dysfunction during hypoxia/reoxygenation and its correction by anaerobic metabolism of citric acid cycle intermediates. *Proc Natl Acad Sci U S A* 97(6): 2826-31, 2000.

298. Weisenberg, R.C. Microtubule formation in vitro in solutions containing low calcium concentrations. *Science* 177(4054): 1104-5, 1972.

299. Wenz, T., F. Diaz, B.M. Spiegelman, and C.T. Moraes. Activation of the PPAR/PGC-1alpha pathway prevents a bioenergetic deficit and effectively improves a mitochondrial myopathy phenotype. *Cell Metab* 8(3): 249-56, 2008.

300. Wills, L.P., R.E. Trager, G.C. Beeson, C.C. Lindsey, Y.K. Peterson, C.C. Beeson, and R.G. Schnellmann. beta2 Adrenoceptor Agonist Formoterol Stimulates Mitochondrial Biogenesis. *J Pharmacol Exp Ther* 2012.

301. Wilson-Fritch, L., S. Nicoloro, M. Chouinard, M.A. Lazar, P.C. Chui, J. Leszyk, J. Straubhaar, M.P. Czech, and S. Corvera. Mitochondrial remodeling in adipose tissue associated with obesity and treatment with rosiglitazone. *J Clin Invest* 114(9): 1281-9, 2004.

302. Witzgall, R., D. Brown, C. Schwarz, and J.V. Bonventre. Localization of proliferating cell nuclear antigen, vimentin, c-Fos, and clusterin in the postischemic kidney. Evidence for a heterogenous genetic response among

nephron segments, and a large pool of mitotically active and dedifferentiated cells. *J Clin Invest* 93(5): 2175-88, 1994.

303. Wolfert, A.I. and D.E. Oken. Glomerular hemodynamics in established glycerol-induced acute renal failure in the rat. *J Clin Invest* 84(6): 1967-73, 1989.

304. Wood, J.G., B. Rogina, S. Lavu, K. Howitz, S.L. Helfand, M. Tatar, and D. Sinclair. Sirtuin activators mimic caloric restriction and delay ageing in metazoans. *Nature* 430(7000): 686-9, 2004.

305. Wright, E.M., B.A. Hirayama, and D.F. Loo. Active sugar transport in health and disease. *J Intern Med* 261(1): 32-43, 2007.

306. Wrutniak-Cabello, C., F. Casas, and G. Cabello. Thyroid hormone action in mitochondria. *J Mol Endocrinol* 26(1): 67-77, 2001.

307. Wu, H., S.B. Kanatous, F.A. Thurmond, T. Gallardo, E. Isotani, R. Bassel-Duby, and R.S. Williams. Regulation of mitochondrial biogenesis in skeletal muscle by CaMK. *Science* 296(5566): 349-52, 2002.

308. Wu, Z., P. Puigserver, U. Andersson, C. Zhang, G. Adelmant, V. Mootha, A. Troy, S. Cinti, B. Lowell, R.C. Scarpulla, and B.M. Spiegelman. Mechanisms controlling mitochondrial biogenesis and respiration through the thermogenic coactivator PGC-1. *Cell* 98(1): 115-24, 1999.

309. Xinwei, J., F. Xianghua, Z. Jing, G. Xinshun, X. Ling, F. Weize, H. Guozhen, J. Yunfa, W. Weili, and L. Shiqiang. Comparison of usefulness of simvastatin 20 mg versus 80 mg in preventing contrast-induced nephropathy in patients with acute coronary syndrome undergoing percutaneous coronary intervention. *Am J Cardiol* 104(4): 519-24, 2009.

310. Yin, W., A.P. Signore, M. Iwai, G. Cao, Y. Gao, and J. Chen. Rapidly increased neuronal mitochondrial biogenesis after hypoxic-ischemic brain injury. *Stroke* 39(11): 3057-63, 2008.

311. Zager, R.A. and R.B. Prior. Gentamicin and gram-negative bacteremia. A synergism for the development of experimental nephrotoxic acute renal failure. *J Clin Invest* 78(1): 196-204, 1986.

312. Zager, R.A. and L.M. Gamelin. Pathogenetic mechanisms in experimental hemoglobinuric acute renal failure. *Am J Physiol* 256(3 Pt 2): F446-55, 1989.

313. Zager, R.A., C. Foerder, and C. Bredl. The influence of mannitol on myoglobinuric acute renal failure: functional, biochemical, and morphological assessments. *J Am Soc Nephrol* 2(4): 848-55, 1991.

314. Zager, R.A. Combined mannitol and deferoxamine therapy for myohemoglobinuric renal injury and oxidant tubular stress. Mechanistic and therapeutic implications. *J Clin Invest* 90(3): 711-9, 1992.

315. Zager, R.A. and C.A. Foerder. Effects of inorganic iron and myoglobin on in vitro proximal tubular lipid peroxidation and cytotoxicity. *J Clin Invest* 89(3): 989-95, 1992.

316. Zager, R.A., K.M. Burkhart, D.S. Conrad, and D.J. Gmur. Iron, heme oxygenase, and glutathione: effects on myohemoglobinuric proximal tubular injury. *Kidney Int* 48(5): 1624-34, 1995.

317. Zager, R.A. Mitochondrial free radical production induces lipid peroxidation during myohemoglobinuria. *Kidney Int* 49(3): 741-51, 1996.

318.   Zahn, J.M., R. Sonu, H. Vogel, E. Crane, K. Mazan-Mamczarz, R. Rabkin, R.W. Davis, K.G. Becker, A.B. Owen, and S.K. Kim. Transcriptional profiling of aging in human muscle reveals a common aging signature. *PLoS Genet* 2(7): e115, 2006.

319.   Zang, M., S. Xu, K.A. Maitland-Toolan, A. Zuccollo, X. Hou, B. Jiang, M. Wierzbicki, T.J. Verbeuren, and R.A. Cohen. Polyphenols stimulate AMP-activated protein kinase, lower lipids, and inhibit accelerated atherosclerosis in diabetic LDL receptor-deficient mice. *Diabetes* 55(8): 2180-91, 2006.

320.   Zeisberg, M. and J.S. Duffield. Resolved: EMT produces fibroblasts in the kidney. *J Am Soc Nephrol* 21(8): 1247-53, 2010.

321.   Zeisberg, M. and E.G. Neilson. Mechanisms of tubulointerstitial fibrosis. *J Am Soc Nephrol* 21(11): 1819-34, 2010.

322.   Zhuang, S., Y. Yan, J. Han, and R.G. Schnellmann. p38 kinase-mediated transactivation of the epidermal growth factor receptor is required for dedifferentiation of renal epithelial cells after oxidant injury. *J Biol Chem* 280(22): 21036-42, 2005.

323.   Zhuang, S., B. Lu, R.A. Daubert, K.D. Chavin, L. Wang, and R.G. Schnellmann. Suramin promotes recovery from renal ischemia/reperfusion injury in mice. *Kidney Int* 75(3): 304-11, 2009.

324.   Zuk, A., J.V. Bonventre, D. Brown, and K.S. Matlin. Polarity, integrin, and extracellular matrix dynamics in the postischemic rat kidney. *Am J Physiol* 275(3 Pt 1): C711-31, 1998.